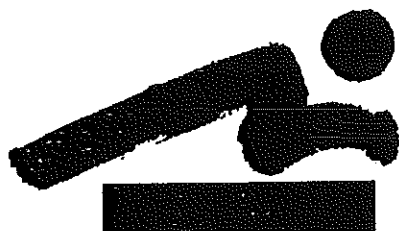


Hydrodynamic and Water Quality Modeling of Lake Champlain



**Lake Champlain
Basin Program**

Prepared by
Applied Science Associates, Inc.

for
Lake Champlain Management Conference

July 1996

Figure 1

F

1

1

1

1

1. The first part of the document is a list of references. The references are listed in a standard format, with the author's name, the title of the work, and the publisher's name. The references are as follows:

1

1

1

Trial	Control	MCI	AD
1	95	85	75
2	95	85	75
3	95	80	70
4	95	78	68
5	95	75	65

—

1.

**HYDRODYNAMIC AND WATER QUALITY
MODELING OF LAKE CHAMPLAIN**

Submitted to:

Lake Champlain Management Conference
c/o Water Management Division
U.S. Environmental Protection Agency, Region 1
JFK Building
Boston, Massachusetts 02203

Submitted by:

Daniel Mendelsohn
Tatsusaburo Isaji
Henry Rines
Applied Science Associates, Inc.
70 Dean Knauss Drive
Narragansett, Rhode Island 02882

ASA Project #92-34

This technical report is the nineteenth in a series of reports prepared under the Lake Champlain Basin Program. Those in print are listed below.

Lake Champlain Basin Program Technical Reports

1. *A Research and Monitoring Agenda for Lake Champlain.* Proceedings of a Workshop, December 17-19, 1991, Burlington, VT. Lake Champlain Research Consortium. May, 1992.
2. *Design and Initial Implementation of a Comprehensive Agricultural Monitoring and Evaluation Network for the Lake Champlain Basin.* NY-VT Strategic Core Group. February, 1993.
3. (A) *GIS Management Plan for the Lake Champlain Basin Program.* Vermont Center for Geographic Information, Inc., and Associates in Rural Development. March, 1993.

(B) *Handbook of GIS Standards and Procedures for the Lake Champlain Basin Program.* Vermont Center for Geographic Information, Inc. March, 1993.

(C) *GIS Data Inventory for the Lake Champlain Basin Program.* Vermont Center for Geographic Information, Inc. March, 1993.
4. (A) *Lake Champlain Economic Database Project. Executive Summary.* Holmes & Associates. March 1993.

(B) *Socio-Economic Profile, Database, and Description of the Tourism Economy for the Lake Champlain Basin.* Holmes & Associates. March 1993

(B) *Socio-Economic Profile, Database, and Description of the Tourism Economy for the Lake Champlain Basin. Appendices.* Holmes & Associates. March 1993

(C) *Potential Applications of Economic Instruments for Environmental Protection in the Lake Champlain Basin.* Anthony Artuso. March 1993.

(D) *Conceptual Framework for Evaluation of Pollution Control Strategies and Water Quality Standards for Lake Champlain.* Anthony Artuso. March 1993.
5. *Lake Champlain Sediment Toxics Assessment Program. An Assessment of Sediment - Associated Contaminants in Lake Champlain - Phase 1.* Alan McIntosh, Editor, UVM School of Natural Resources. February 1994.

Lake Champlain Sediment Toxics Assessment Program. An Assessment of Sediment - Associated Contaminants in Lake Champlain - Phase 1. Executive Summary. Alan McIntosh, Editor, UVM School of Natural Resources. February 1994.
6. (A) *Lake Champlain Nonpoint Source Pollution Assessment.* Lenore Budd, Associates in Rural Development Inc. and Donald Meals, UVM School of Natural Resources. February 1994.

(B) *Lake Champlain Nonpoint Source Pollution Assessment. Appendices A-J.* Lenore Budd, Associates in Rural Development Inc. and Donald Meals, UVM School of Natural Resources. February 1994.

7. *Internal Phosphorus Loading Studies of St. Albans Bay. Executive Summary.* VT Dept of Environmental Conservation. March 1994.
 - (A) *Dynamic Mass Balance Model of Internal Phosphorus Loading in St. Albans Bay, Lake Champlain.* Eric Smeltzer, Neil Kamman, Karen Hyde and John C. Drake. March 1994.
 - (B) *History of Phosphorus Loading to St. Albans Bay, 1850 - 1990.* Karen Hyde, Neil Kamman and Eric Smeltzer. March 1994.
 - (C) *Assessment of Sediment Phosphorus Distribution and Long-Term Recycling in St. Albans Bay, Lake Champlain.* Scott Martin, Youngstown State University. March 1994.
8. *Lake Champlain Wetlands Acquisition Study.* Jon Binhammer, VT Nature Conservancy. June 1994.
9. *A Study of the Feasibility of Restoring Lake Sturgeon to Lake Champlain.* Deborah A. Moreau and Donna L. Parrish, VT Cooperative Fish & Wildlife Research Unit, University of Vermont. June 1994.
10. *Population Biology and Management of Lake Champlain Walleye.* Kathleen L. Newbrough, Donna L. Parrish, and Matthew G. Mitro, Fish & Wildlife Research Unit, University of Vermont. June 1994.
11. (A) *Report on Institutional Arrangements for Watershed Management of the Lake Champlain Basin. Executive Summary.* Yellow Wood Associates, Inc. January 1995.
(B) *Report on Institutional Arrangements for Watershed Management of the Lake Champlain Basin.* Yellow Wood Associates, Inc. January 1995.
(C) *Report on Institutional Arrangements for Watershed Management of the Lake Champlain Basin. Appendices.* Yellow Wood Associates, Inc. January 1995.
12. (A) *Preliminary Economic Analysis of the Draft Plan for the Lake Champlain Basin Program. Executive Summary.* Holmes & Associates and Anthony Artuso. March 1995
(B) *Preliminary Economic Analysis of the Draft Plan for the Lake Champlain Basin Program.* Holmes & Associates and Anthony Artuso. March 1995
13. *Patterns of Harvest and Consumption of Lake Champlain Fish and Angler Awareness of Health Advisories.* Nancy A. Connelly and Barbara A. Knuth. September 1995.
14. (A) *Preliminary Economic Analysis of the Draft Plan for the Lake Champlain Basin Program. Executive Summary - Part 2.* Holmes & Associates and Anthony Artuso. November 1995
(B) *Preliminary Economic Analysis of the Draft Plan for the Lake Champlain Basin Program - Part 2.* Holmes & Associates and Anthony Artuso. November 1995
15. *Zebra Mussels and Their Impact on Historic Shipwrecks.* Lake Champlain Maritime Museum. January 1996.
16. *Background Technical Information for Opportunities for Action; An Evolving Plan for the Future of the Lake Champlain Basin.* Lake Champlain Basin Program. June 1996

17. (A) *Executive Summary. Economic Analysis of the Draft Final Plan for the Lake Champlain Management Conference.* Holmes & Associates and Anthony Artuso. July 1996

(B) *Economic Analysis of the Draft Final Plan for the Lake Champlain Basin Management Conference.* Holmes & Associates and Anthony Artuso. July 1996
18. *Catalog of Digital Spatial Data for the Lake Champlain Basin .* Vermont Center for Geographic Information, Inc. September 1996.
19. *Hydrodynamic and Water Quality Modeling of Lake Champlain.* Applied Science Associates, Inc. July 1996.

This report was funded and prepared under the authority of the Lake Champlain Special Designation Act of 1990, P.L. 101-596, through the U.S. Environmental Protection Agency (EPA grant #EPA X 001840-01). Publication of this report does not signify that the contents necessarily reflect the views of the States of New York and Vermont, the Lake Champlain Basin Program, or the U.S. Environmental Protection Agency.

TABLE OF CONTENTS

ABSTRACT	iii
LIST OF FIGURES	v
LIST OF TABLES	ix
1. INTRODUCTION	1
2. LAKE CHAMPLAIN HYDRODYNAMIC MODEL	4
2.1 Background	4
2.2 Model Development	5
2.2.1 Hydrodynamic Equations	5
2.2.2 Solution Scheme	7
2.2.3 Simple Case Runs	10
2.2.3.1 Comparison to an Analytical Solution	10
2.2.3.2 Oscillation in a Rectangular Closed Basin	14
2.3 Application to Lake Champlain	15
2.3.1 Grids of Lake Champlain	15
2.3.2 Model Simulation of Summer 1991	18
2.3.3 Model Simulation of Winter 1991	33
2.4 Discussion and Recommendations	37
3. LAKE CHAMPLAIN PHOSPHORUS MODEL	38
3.1 Background	38
3.2 Model Development	40
3.2.1 Exchange Coefficients	40
3.2.1.1 Exchange Coefficients Calculated from Data	40
3.2.1.2 Hydrodynamic Model Calculated Exchange Coefficients	46
3.2.2 Conservation of Constituent Mass	48
3.2.3 Phosphorus Cycle Kinetics	51
3.3 Application to Lake Champlain	59
3.3.1 Lake Segmentation	60
3.3.2 Exchange Rate Coefficients	70
3.3.2.1 Exchange Coefficients from Data	70
3.3.2.2 Hydrodynamic Model Calculated Exchange Coefficients	74
3.3.3 Phosphorus Cycle Kinetics Calibration	84
3.4 Discussion and Recommendations	104
4. SUMMARY AND CONCLUSIONS	105
5. REFERENCES	108

APPENDICES

- A.1 Hydrodynamics Model File Formats
- A.2 Phosphorus Model File Formats
- A.3 GIS Data File Formats

ABSTRACT

A hydrodynamic and water quality model system has been developed to simulate transport, mixing and hydrodynamic dispersion for estimation of spatial and temporal distribution and transport of water quality constituents in Lake Champlain. The hydrodynamic and water quality models were developed independently and may be applied as a system or stand-alone.

The hydrodynamic model development and analysis focussed on simulation of the wind driven response of the lake in particular to the development of large amplitude internal seiches reported in stratified conditions (Myer and Greundling, 1979). The vertically averaged layer equations for hydrodynamics in a lake presented by Lynch (1986), were used for the model development. The standard explicit, finite difference method is used for solution. A comparison to an analytical solution for a two layer system in a rectangular channel open at one end gave favorable results. A similar comparison to wind driven response in a closed basin also gave excellent results.

The hydrodynamic model application to the real geometry of Lake Champlain was performed on coarse and fine resolution grids. Simulations for the summer 1991 and winter 1991 were performed. A number of summer simulations were made which varied the depth of the thermocline and the density difference between the upper and lower layers. Results were compared to preliminary data from a concurrent field program underway at Middlebury College, Vermont which monitored current and temperature profiles in the main basin of the lake. Comparison of analyses of the predicted and observed currents at three mooring sites indicates the existence of an oscillation peak at a four day period. Transport and mixing were also estimated for the main basin of the lake based calculated current fields.

The water quality model described was developed to study the kinetics, distribution and concentration of nutrients in the lake. The development focussed on the phosphorus cycle, including phytoplankton population simulation, and the estimation of lake response to phosphorus loadings. A comprehensive water, chloride, (as a conservative tracer) and phosphorus mass balance data set, developed through the joint effort of the VTDEC and NYSDEC for the two year period between March 1990 and 1992, is used to provide flow and loading information for model input and mean *in-situ* concentration information for comparison with model calculations. A method for the direct computation of the exchange coefficients from the hydrodynamic model output is presented. Results are compared to exchange coefficients calculated from tracer data.

The model conservation of mass equations are solved using a multiply-connected control volume approach in three dimensions and in time. This is a sophisticated version of the standard segment model approach. The model incorporates a unique approach to the determination of inter-segment mixing exchange based entirely on a conservative tracer data set, chloride in this case. The WASP5 model (Ambrose et al., 1993) phosphorus cycle kinetic rate equations were also incorporated into the control volume model.

A comparison of mixing exchange calculations of the present model and those of the VTDEC model were made, for the two year average data set with consistent results. Total phosphorus concentration predictions were then made based on a "hydrologic base year" input data set and in-lake concentrations. A sensitivity study on phytoplankton and phosphorus settling rates, the fraction of organic phosphorus, phytoplankton respiration and death rates, saturating light intensity, carbon to chlorophyll ratio, phosphorus mineralization rate, chlorophyll river input and intersegment exchange was performed. Based on these sensitivity runs a best-fit parameter set was iteratively chosen.

LIST OF FIGURES

	Page
Figure 1.1 Lake Champlain drainage basin	2
Figure 2.1 Definition sketch for layered system	8
Figure 2.2 Simulation of internal standing wave in open channel	12
Figure 2.3 Closed basin dimension	13
Figure 2.4 Interface oscillation in closed basin with two layers of fluid	16
Figure 2.5 Hydrodynamic grids of Lake Champlain	17
Figure 2.6 Field observed current during summer 1991	19
Figure 2.7a Power spectral densities and coherence square Valcour Island Mooring . .	20
Figure 2.7b Power spectral densities and coherence square Juniper Island Mooring . .	21
Figure 2.7c Power spectral densities and coherence square Thompsons Point Mooring .	22
Figure 2.8 Field observed thermal structure during summer 1991	23
Figure 2.9a Hydrodynamic simulation for August 1991, with run parameters density difference = 0.5 (kg/m ³), stratification at 15 m	26
Figure 2.9b Hydrodynamic simulation for August 1991, with run parameters density difference = 1.0 (kg/m ³), stratification at 15 m	27
Figure 2.9c Hydrodynamic simulation for August 1991, with run parameters density difference = 1.5 (kg/m ³), stratification at 15 m	28
Figure 2.9d Hydrodynamic simulation for August 1991, with run parameters density difference = 0.5 (kg/m ³), stratification at 20 m	29
Figure 2.9e Hydrodynamic simulation for August 1991, with run parameters density difference = 1.0 (kg/m ³), stratification at 20 m	30
Figure 2.9f Hydrodynamic simulation for August 1991, as case 1K_AUG9, except bottom friction of 0.003	31

	Page
Figure 2.9g Hydrodynamic simulation for July-August 1991, with run parameters density difference = 1.0 (kg/m ³), stratification at 15 m	32
Figure 2.10 Field observed current during winter 1991-1992	34
Figure 2.11a Hydrodynamic simulation for November 1991, with run parameters density difference = 0.2 (kg/m ³), stratification at 25 m	35
Figure 2.11b Hydrodynamic simulation for November 1991, with one layer, the labeled 'model upper' corresponds to one layer result (vertical mean) and the label 'model lower' is null	36
Figure 3.1 Conceptual diagram of hydrodynamic exchanges in the box model	43
Figure 3.2 Conceptual diagram of non-exchange mechanisms affecting concentration .	49
Figure 3.3 Phosphorus concentration and sedimentation flux versus distance from tributary (Chapra and Reckhow, 1983)	52
Figure 3.4 Schematic of a multispecies phosphorus model (Chapra and Reckhow, 1983)	53
Figure 3.5 Actual and approximate solar radiation (Thomann and Mueller, 1983)	56
Figure 3.6 Phosphorous model segmentation geography	71
Figure 3.7 Schematic of the model segmentation, connections and net flow path . . .	72
Figure 3.8 Comparison of mixing exchange coefficient calculations (a) VTDEC calculations versus ASA calculations (b) hydrologic base year versus 2 year data	75
Figure 3.9 Flow rate by segment (a) outflow at the downstream face of each segment (b) flow input by segment for the hydrologic base year versus 2 year data	76
Figure 3.10 Predicted mean net transport rate in the upper layer for the 1K_AUG13 hydrodynamic simulation	78
Figure 3.11 Predicted mean net transport rate in the lower layer for the 1K_AUG13 hydrodynamic simulation	79

	Page
Figure 3.12 Predicted mean exchange rate in the upper layer for the 1K_AUG13 hydrodynamic simulation	80
Figure 3.13 Predicted mean exchange rate in the lower layer for the 1K_AUG13 hydrodynamic simulation	81
Figure 3.14 Lake Champlain gridded depths	83
Figure 3.15 Mean observed concentration by segment and model-predicted concentrations using the base case parameters for (a) total phosphorus and (b) chlorophyll <i>a</i>	89
Figure 3.16 Effect on model-predicted concentrations of increasing total daily insolation from 312 to 422 langleys per day for (a) total phosphorus and (b) chlorophyll <i>a</i> . Mean annual observed concentrations and base case predictions are shown for comparison	91
Figure 3.17 Effect on model-predicted concentrations of increasing saturating light intensity from 300 to 500 langleys per day for (a) total phosphorus and (b) chlorophyll <i>a</i> . Mean annual observed concentrations and base case predictions are shown for comparison	92
Figure 3.18 Effect on model-predicted concentrations of decreasing the phytoplankton carbon to chlorophyll ratio from 35 to 25 for (a) total phosphorus and (b) chlorophyll <i>a</i> . Mean annual observed concentrations and base case predictions are shown for comparison	93
Figure 3.19 Effect on model-predicted concentrations of decreasing the phytoplankton respiration rate from 0.125 to 0.05 per day for (a) total phosphorus and (b) chlorophyll <i>a</i> . Mean annual observed concentrations and base case predictions are shown for comparison	94
Figure 3.20 Effect on model-predicted concentrations of decreasing the phytoplankton death rate from 0.02 to 0.06 per day for (a) total phosphorus and (b) chlorophyll <i>a</i> . Mean annual observed concentrations and base case predictions are shown for comparison	95

Figure 3.21	Effect on model-predicted concentrations of varying the fraction of phosphorus recycled to the organic pool, F_{op} , from a base case of 0.5 to values of 0.25 or 0.75 for (a) total phosphorus and (b) chlorophyll <i>a</i> . Mean annual observed concentrations and base case predictions are shown for comparison	97
Figure 3.22	Effect on model-predicted concentrations of varying the phytoplankton settling rate from a base case of 0.25 to values of 0.05, 0.1, 0.4, or 0.5 m/day for (a) total phosphorus and (b) chlorophyll <i>a</i> . Mean annual observed concentrations and base case predictions are shown for comparison	98
Figure 3.23	Effect on model-predicted concentrations of varying the phosphorus settling rate from a base case of 0.25 to values of 0.05, 0.1, 0.4, or 0.5 m/day for (a) total phosphorus and (b) chlorophyll <i>a</i> . Mean annual observed concentrations and base case predictions are shown for comparison	99
Figure 3.24	Effect on model-predicted concentrations of adding chlorophyll loads to river inputs based on their total phosphorus concentrations for (a) total phosphorus and (b) chlorophyll <i>a</i> . Mean annual observed concentrations and base case predictions are shown for comparison	100
Figure 3.25	Effect on model-predicted concentrations using the hydrologic base year exchange values instead of the two year average for (a) total phosphorus and (b) chlorophyll <i>a</i> . Mean annual observed concentrations and base case predictions are shown for comparison	101
Figure 3.26	(a) Total phosphorus concentrations predicted by the model using the calibrated model parameters. Mean annual observed concentrations and base case predictions are shown for comparison. (b) Chlorophyll <i>a</i> concentrations predicted by the model using the calibrated model parameters. Mean annual observed concentrations and base case predictions are shown for comparison	103

LIST OF TABLES

	Page
Table 2.1 Model parameters for the case of channel with one side open	14
Table 2.2 "Base" case parameters for hydrodynamic simulations	24
Table 2.3 Description of cases for summer simulations	25
Table 2.4 Description of cases for winter simulations	33
Table 3.1 Phosphorus cycle kinetic rate equation terms (Ambrose et al., 1993)	57
Table 3.2 Lake model segment morphometric data, and listing of lake sampling stations within each segment (NYSDEC and VTDEC, 1993)	60
Table 3.3 Water, chloride, and total phosphorus budgets for Lake Champlain for the period of March 1990 to February 1992 (NYSDEC and VTDEC, 1993)	61
Table 3.4 Model input data for gaged tributaries, ungaged areas, and direct wastewater treatment facility (WWTF) discharges, for the period of March 1990 to February 1992 (NYSDEC and VTDEC, 1993)	62
Table 3.5 Model input data for gaged tributaries, ungaged areas, and direct wastewater treatment facility (WWTF) discharges for the hydrologic base year of January 1991 to December 1991 (NYSDEC and VTDEC, 1993)	64
Table 3.6 Two year survey, March - February 1992	66
Table 3.7 Hydrologic base year, January 1991 - December 1991	67
Table 3.8 Phosphorus partitioning abbreviations	68
Table 3.9 Mean chloride and total phosphorus concentrations in each lake segment, 1990-1991. C.V. = coefficient of variation of the mean (NYSDEC and VTDEC, 1993)	69
Table 3.10a Two year survey data exchange coefficient	70
Table 3.10b Hydrologic base year versus two year survey	73

	Page
Table 3.10c Hydrodynamic model calculated exchange coefficients	84
Table 3.11 Phosphorus cycle kinetic rate equations terms for the "BASE" case	86
Table 3.12 Phosphorus kinetics sensitivity study parameters	87
Table 3.13 Hydrologic base year data averaged by segment	87

1. INTRODUCTION

Lake Champlain is one of the largest bodies of freshwater in the United States, stretching almost 200 km long and 19 km wide. Its drainage basin of 10450 km² includes portions of Vermont, New York, and Quebec (Figure 1.1). It has long served the areas inhabitants in a variety of ways including recreation, transportation, and fisheries. As with many other water bodies, man's presence on and around the lake and in its drainage basin has had negative impacts. The most pressing water quality problem today is excess phosphorus loading which contributes to eutrophication and subsequent degradation of lake water quality (VTDEC/NYSDEC, 1991).

To address the water quality issues of Lake Champlain a federal act was signed into law in November 1990 adding the lake to the list of ten (10) waterbodies eligible for lake water quality demonstration programs. The goal of this program is to preserve or enhance water quality by controlling point and non-point sources of pollution with the development of appropriate methods, technologies, and strategies. The act also calls for the establishment of a Lake Champlain Management Conference (LCMC) consisting of representatives of various constituencies. The LCMC is to develop a comprehensive plan for the lake to prevent and control pollution as well as to restore and maintain the water quality, indigenous populations, and multiple uses of the lake.

An important step in the development of a comprehensive plan for lake management is to study and understand the underlying physical processes that guide the levels and distribution of pollutants in the lake. Toward that goal the management conference initiated the present study. The objective of the present study was to develop a model to simulate transport, mixing and hydrodynamic dispersion for estimation of spatial and temporal distribution and transport of water quality constituents and biological measures of importance. Applied Science Associates, Inc. was retained by the management conference and its supporting organizations, the New England Interstate Water Pollution Control Commission and US Environmental Protection Agency (EPA), to develop the model system.

The model system development has been divided into two sections, hydrodynamics and water quality, due to the great disparity in spatial and temporal scale at which relevant events occur in each. The hydrodynamic model was developed to study the circulation, mixing and transport phenomena in the lake with a particular focus on the wind driven

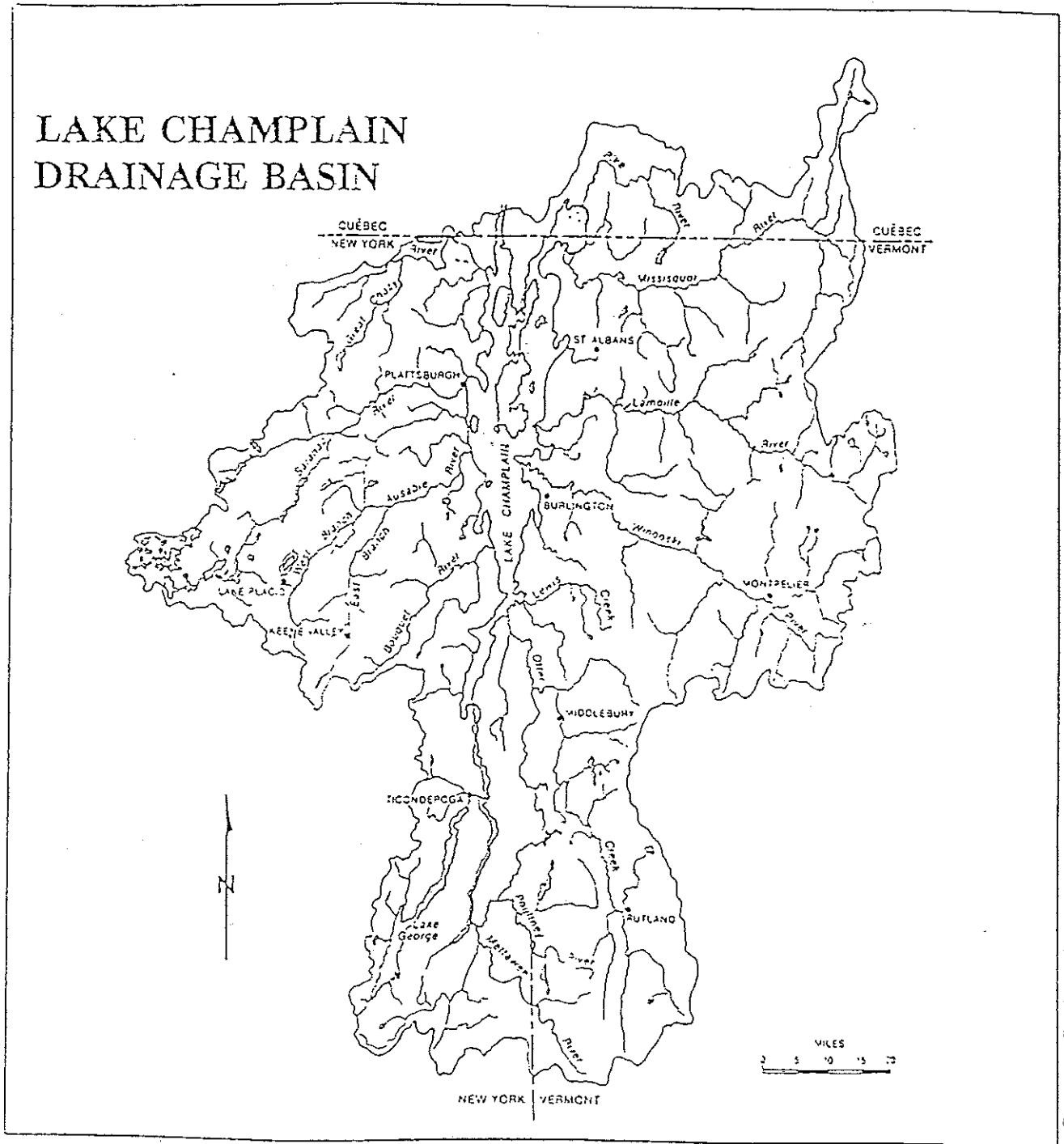


Figure 1.1 Lake Champlain drainage basin.

response of the lake and the development of large amplitude internal seiches reported during stratified conditions (Myer and Greundling, 1979). A concurrent field program at Middlebury College, Vermont, also under the auspices of the LCMC monitored current and temperature profiles in the main basin of the lake. Preliminary data from that study is used to compare with model calculations.

The water quality model was developed to study the dynamics and kinetics of the distribution and concentration of phosphorus in the lake. The development focussed on the phosphorus cycle, including phytoplankton population simulation, and the estimation of lake response to phosphorus loadings. Comprehensive water, chloride (conservative tracer) and phosphorus mass balance data sets have been developed through the joint effort of the Vermont Department of Environmental Conservation (VTDEC) and New York State Department of Environmental Conservation (NYSDEC) for the two year period between March 1990 and February 1992. Results are reported in the Lake Champlain Diagnostic - Feasibility Study, (VTDEC and NYSDEC, 1993). Data from the study is used to provide flow and loading and to "force" the water quality model and for mean *in-situ* concentration information to compare with model calculations.

This report follows the basic division of hydrodynamics and water quality. Section 2 describes the hydrodynamic model development, its application to Lake Champlain and comparison to field data. Some recommendations for additional field studies are made concerning areas and types of data not adequately represented in the existing data. Section 2 also describes how mixing and transport values are derived from the hydrodynamic data set. Section 3 documents the water quality model development, the integration of the WASP5. (Ambrose et al., 1993) phosphorus kinetics, the application of the model to the lake and its comparison with observations. Appendices contain file formats for all model input and output data sets.

2. LAKE CHAMPLAIN HYDRODYNAMIC MODEL

2.1 Background

A basic objective of this portion of study is to develop a hydrodynamic model that describes general circulation of Lake Champlain. This includes water mass balance due to river runoff, wind driven current, and internal seiching. The lake consists of several interconnected basins, some of which are fairly independent. Each basin has quite different morphology and the importance of circulation modes in each certainly varies. The most notable phenomenon is an internal seiche due to the strong thermal stratification during summer in the Main Lake (Myer and Gruending, 1979).

Myer (1977) analyzed stratification and associated currents and pointed out the internal seiche to have the most significant contribution among the various forms of circulation in the lake during the summer. The analyses were extensive but the coverage of data was limited in time and space. As a part of the water quality demonstration program of the Lake Champlain Management Conference, a field investigation has been under way (LCMC, 1993). This field study addresses direct measurement of circulation in the main lake by including long term deployments of three moorings, each with two current meters and a thermistor chain attached. Also, included are hydrographic and side-scan sonar surveys. The field study will continue into succeeding years and additional field observations and detailed analysis should become available then. The present modeling study was carried out without the formal data report and analysis.

A preliminary result of current and thermistor chain data for the summer and winter 1991 has been made available to us (Manley, 1993). Exploratory analyses on the summer period observations were carried out to estimate the thermal structure that will be used as input to the hydrodynamic model and to compare with the simulation result. All current measurements indicated the existence of oscillations, peaked at a four day period, the detail of which will be discussed in a later section.

The initial model choice for implementation was Applied Science Associates' Legendre polynomial basis function model which solves the conservation of mass, momentum and heat (temperature). Preliminary application of this model to the main basin of the lake indicated that this approach was not suited for nor computationally efficient enough to solve for wave propagation of the internal fluid interface in a timely manner. The

number of polynomials necessary to adequately resolve the vertical structure of the water column in stratified conditions (i.e. to resolve the interface) and to maintain the definition of the interface over time along with stability restraints prove excessive. For this reason, a more appropriate solution form for the inherently layered system was sought.

The following sections of this report discuss the development of a layered hydrodynamic model that deals with the stratified flow. The model will be first applied to a simple geometric basin to verify code and to learn model behavior in simulation of internal waves. The model will then be applied to Lake Champlain to simulate some portion of period observed in the field investigation. The results will be evaluated and recommendations for improvement will be made.

2.2 Model Development

Any model scheme selected to solve for the location of stratification by advecting heat must overcome several critical physical criteria: proper vertical diffusion at the interface, heat budget estimation over the course of thermal development and propagation of the internal wave that might travel rapidly through the domain (roughly 60-80 km over four days in the Main lake). Most models employ fairly simple numerical schemes to solve the internal current structure (three-dimensional baroclinic component) and are not capable of handling a rapidly progressing interfacial front.

One approach is to rely on the field observation for the initial specification of thermal structure and to eliminate the equation of heat conservation. This assumes a priori that lake water is stratified with a certain thermal structure. The propagation of the interface is then computed by solving the continuity equation for each fluid layer. This leads to the obvious selection of a layered approach for the vertical structure of the model. For this reason the vertically averaged layer equations developed by Lynch (1986) were selected as the starting point for our model development.

2.2.1 Hydrodynamic Equations

Detailed derivations of the equations and fundamental assumptions can be found in Lynch (1986). The fundamentals will be repeated here. The mass and momentum conservation equations are integrated in the vertical, to give

$$\frac{\partial}{\partial x}(H_i \bar{u}_i) + \frac{\partial}{\partial y}(H_i \bar{v}_i) + \frac{\partial H_i}{\partial t} = s_i \quad (2.1)$$

$$\frac{\partial \bar{u}_i}{\partial t} + \bar{u}_i \frac{\partial \bar{u}_i}{\partial x} + \bar{v}_i \frac{\partial \bar{u}_i}{\partial y} = f \bar{v}_i - \bar{\gamma}_i \frac{\partial P_a}{\partial x} - g(\bar{\gamma}_i \rho \zeta \frac{\partial \zeta}{\partial x} + (\bar{\gamma} I_x)_i) + \frac{\bar{\gamma}_i}{H} (\tau_{x_{i-1}} - \tau_{x_i}) \quad (2.2)$$

$$\frac{\partial \bar{v}_i}{\partial t} + \bar{u}_i \frac{\partial \bar{v}_i}{\partial x} + \bar{v}_i \frac{\partial \bar{v}_i}{\partial y} = f \bar{u}_i - \bar{\gamma}_i \frac{\partial P_a}{\partial y} - g(\bar{\gamma}_i \rho \zeta \frac{\partial \zeta}{\partial y} + (\bar{\gamma} I_y)_i) + \frac{\bar{\gamma}_i}{H} (\tau_{y_{i-1}} - \tau_{y_i}) \quad (2.3)$$

where

- x = horizontal independent variable in east/west
- y = horizontal independent variable in north/south
- t = independent variable in time
- i = layer index, 0 is surface
- ζ_i = vertical position of i-th layer surface
- H_i = $\zeta_{i-1} - \zeta_i$, layer thickness
- u_i = vertically averaged east/west velocity in i-th layer
- v_i = north/south velocity in i-th layer
- s_i = water mass or momentum source term in i-th layer
- f = Coriolis parameter $2\Omega \sin \theta$, θ is latitude
- ρ = bulk fluid density, mass/volume
- γ = $1/\rho$
- P_a = atmospheric pressure
- g = gravity
- τ_z = shear stress at layer interface

$(\bar{\gamma} I_x)_i$ is the integrated baroclinic term. For the case where the density is vertically constant in each of the layers, the term reduces to a sum of baroclinic contributions from overlying layers and interfaces.

$$\begin{aligned} (\bar{\gamma} I_x)_i &= \frac{1}{\rho_i} [H_1 \frac{\partial \rho_1}{\partial x} + H_2 \frac{\partial \rho_2}{\partial x} + \dots + H_{i-1} \frac{\partial \rho_{i-1}}{\partial x} + \frac{H_i}{2} \frac{\partial \rho_i}{\partial x}] \\ &+ \frac{1}{\rho_i} [(\rho_2 - \rho_1) \frac{\partial \zeta_1}{\partial x} + (\rho_3 - \rho_2) \frac{\partial \zeta_2}{\partial x} + \dots + (\rho_i - \rho_{i-1}) \frac{\partial \zeta_{i-1}}{\partial x}] \end{aligned} \quad (2.4)$$

The integrated barocline term in the north/south (y) direction is identical to the east/west equation, replacing x with y.

The equations are subject to the following boundary conditions; at land boundaries normal components of velocity are zero,

$$\mathbf{u} \cdot \mathbf{n} = 0$$

where \mathbf{u} denotes the total current vector and \mathbf{n} is the outward directed normal, at open boundaries, if any exist, the surface elevation must be specified through time.

Shear stresses are applied at the top and bottom of each layer interface. They are assumed to be of the quadratic stress form. At the upper face of the top layer;

$$\tau_{zx} = \rho C_w |W| W_x, \tau_{zy} = \rho C_w |W| W_y$$

where C_w is a surface wind drag coefficient and $W_x, W_y, |W|$ are the horizontal components and absolute speed of the surface wind. ρ is air density. At the interface;

$$\tau_{zx} = \rho C_i |V| V_x, \tau_{zy} = \rho C_i |V| V_y$$

where C_i is a layer interface drag coefficient and $V_x, V_y, |V|$ are the relative layer velocities. The lower face of the bottom layer uses the same form, with the bottom drag coefficient, C_d instead of C_i .

There is no mass flux across any interface. The variable, ζ , is defined as the moving material surface which separates the layers. Figure 2.1 shows a schematic for the layer system model.

2.2.2 Solution Scheme

The dependent variables to be solved for in equations 2.1 to 2.4 are the layer thickness and layer averaged horizontal velocity, both as a function of horizontal position and time over the period of the simulation.

The equations are solved by standard finite difference methods on a rectangular grid. The numerical integration is done explicitly both in space and time. Velocities and elevations are staggered in space (Arakawa's C grid), as well as in time. Linear interpolation is used to derive values of variables at points other than grid points.

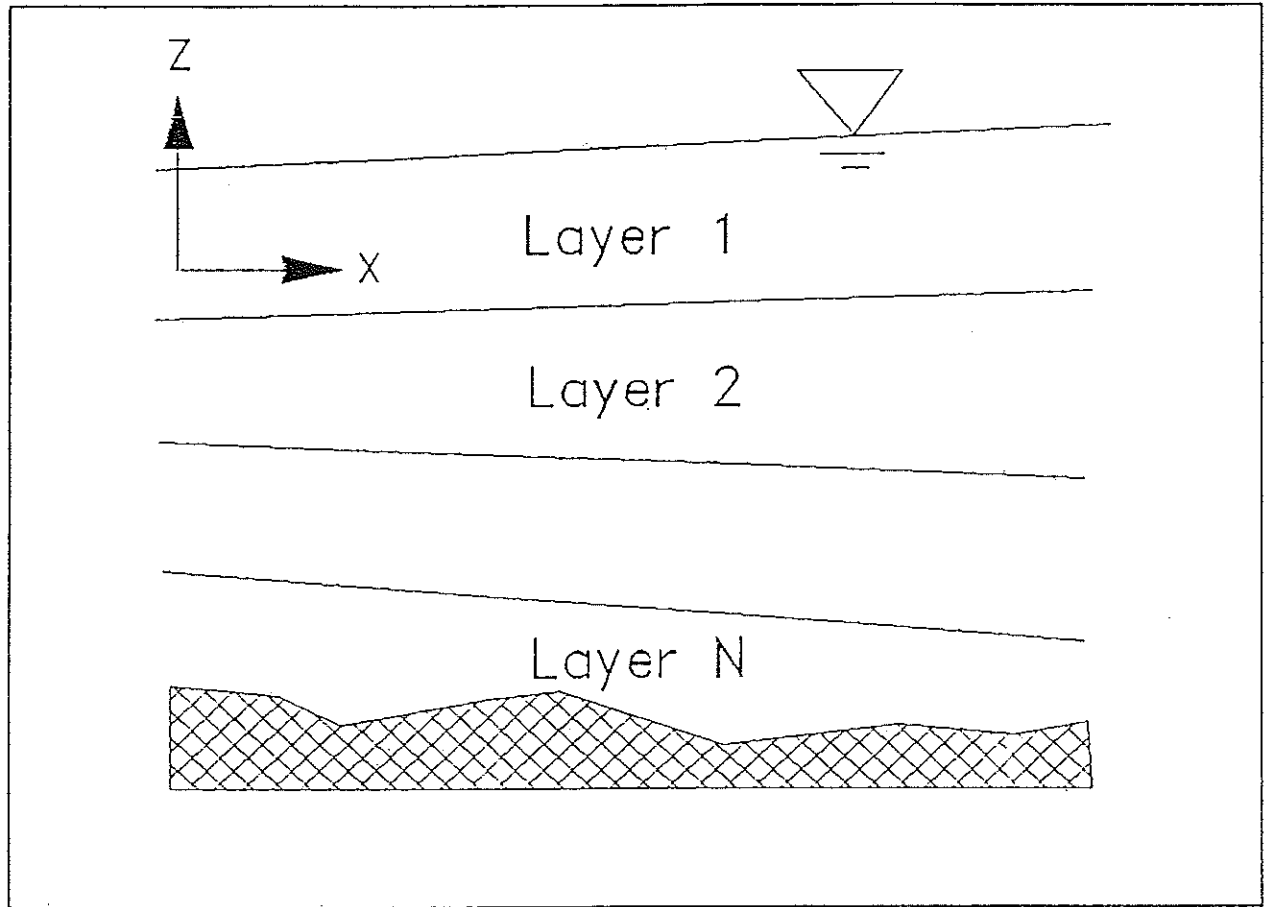


Figure 2.1 Definition sketch for layered system.

The finite difference form of the conservation of mass equation, (equation 2.1), is

$$\begin{aligned}
 H^{+dt}(ij,k) = & H(ij,k) \\
 & - dt \left[\frac{H(ij,k) u(ij,k) - H(i-1,j,k) u(i-1,j,k)}{dx} \right. \\
 & \left. + \frac{H(ij,k)v(ij,k) - H(ij-1,k)v(ij-1,k)}{dy} - s(ij,k) \right]
 \end{aligned} \quad (2.5)$$

where dt , dx , and dy are time step and horizontal grid spaces, respectively. The subscripts i,j,k are east and north grid and layer indices, respectively. The over bar expression (layer averaged) is eliminated for brevity.

The finite difference form of the east/west momentum component (equation (2.2), is given by:

$$\begin{aligned}
 u^{+dt}(ij,k) = & u(ij,k) \\
 & + dt \left[-u(ij,k) \frac{u(i+1,j,k) - u(i-1,j,k)}{2dx} - v(ij,k) \frac{u(ij+1,k) - u(ij-1,k)}{2dy} \right. \\
 & + \bar{f}v(ij,k) - \frac{Pa(ij,k) - Pa(i-1,j,k)}{\rho dx} - g \left(\frac{\zeta(ij,k) - \zeta(i-1,j,k)}{dx} + \gamma I_x(ij,k) \right) \\
 & \left. + \frac{C_i(u(ij,k) - u(ij,k-1))}{H(ij,k)} - \frac{C_i(u(ij,k) - u(ij,k+1))}{H(ij,k)} \right]
 \end{aligned} \quad (2.6)$$

where P_a is the atmospheric pressure.

For the integrated baroclinic terms, equation (2.4) becomes

$$\begin{aligned}
 \gamma I_x(ij,k) = & + \frac{1}{\rho} (ij,k) [(\rho(ij,2) - \rho(ij,1)) \frac{\zeta(ij,1) - \zeta(i-1,j,1)}{dx} \\
 & - (\rho(ij,3) - \rho(ij,2)) \frac{\zeta(ij,2) - \zeta(i-1,j,2)}{dx} \\
 & - \dots + \\
 & - (\rho(ij,k) - \rho(ij,k-1)) \frac{\zeta(ij,k-1) - \zeta(i-1,j,k-1)}{dx}]
 \end{aligned} \quad (2.7)$$

The over bar expression in the Coriolis term denotes spatial interpolation which is required due to the staggered grid point scheme. It is also assumed that $\gamma\rho_i \approx 1$ and $\partial\rho/\partial x = 0$ (i.e., constant density within a layer). Equation 2.3 for the north/south conservation of momentum is treated identically and will not be repeated here.

The explicit time step is split into two half time steps. In the first half time step, the velocities are computed. In the second half step, layer thicknesses are solved for using the newly calculated velocities. Appropriate boundary conditions are imposed in each time step; velocities normal to land boundaries are set to zero and surface elevations are specified at the open boundaries.

A problem in the layered scheme is the fact that depth varying bathymetry will intersect layer boundaries. The layer boundaries may also intersect each other when the layer thickness change is large. The problem is similar to the flooding/drying boundary condition as water recedes in shallow areas. Numerically drying or layer intersecting is not a problem with a small time step in the explicit scheme, but wetting or recovering layer thickness is the real difficulty since there is no basis for the computation of velocity without water mass. A possible method one may use to handle this is to diffuse velocity by smoothing or imposing some amount of interface stress. The excessive use of either, though, may lead to over-damping.

2.2.3 Simple Case Runs

To verify program coding and to examine model response, a series of runs were made with simplified geometry and physical conditions for a fluid system of two layers, each of constant density, in a rectangular basin. The first case simulates a standing internal wave form for comparison to a known analytical solution. The second case examines dynamic response to various density conditions in a basin with geometry similar in size to Lake Champlain.

2.2.3.1 Comparison to an Analytical Solution

The model was applied to simulate an internal wave in a rectangular basin with two layers of fluid each with a different density. The rectangular basin was a channel closed at one end and open at the other, where the surface and interface must be specified for all time

(similar to Figure 2.3 except one side open). Interface elevations can be expressed by the analytic solution of Wang (1975),

$$\zeta_2 = A(1.0 - \frac{gh_1}{\omega^2} k_1^2) \cos(k_1 x) + B(1.0 - \frac{gh_2}{\omega^2} k_2^2) \cos(k_2 x) \quad (2.8)$$

$$A = \frac{a(1.0 - \frac{gh_2}{\omega^2} k_2^2) - b}{(k_1^2 - k_2^2) \frac{gh_2}{\omega^2} \cos(k_1 L)} \quad B = \frac{a(-1.0 + \frac{gh_2}{\omega^2} k_1^2) - b}{(k_1^2 - k_2^2) \frac{gh_2}{\omega^2} \cos(k_2 L)}$$

where

ζ_2	=	interface location
$\delta\rho$	=	density difference
g	=	gravity
h_1, h_2	=	layer depth and $H = h_1 + h_2$
ω_2	=	wave frequency at interface
k_1^2	=	$(\rho_1 H \omega_2) / (\delta\rho g h_1 h_2)$
k_2^2	=	ω_2 / gH
ρ_1	=	density of upper layer
x	=	horizontal location
a	=	wave amplitude of surface
b	=	wave amplitude of interface

The basin configuration and model parameters are in Table 2.1.

Initially velocities and water elevations in the entire domain were assigned to the values given by the analytic solution. Figure 2.2 shows the interface locations for model output (stars) and the analytic solution (solid lines) at successive 1/4 periods (one period = 500 sec). The model was able to continue to simulate the interface standing wave indefinitely. Without the initial values of the analytic solution, it took several periods to approach the analytic solution.

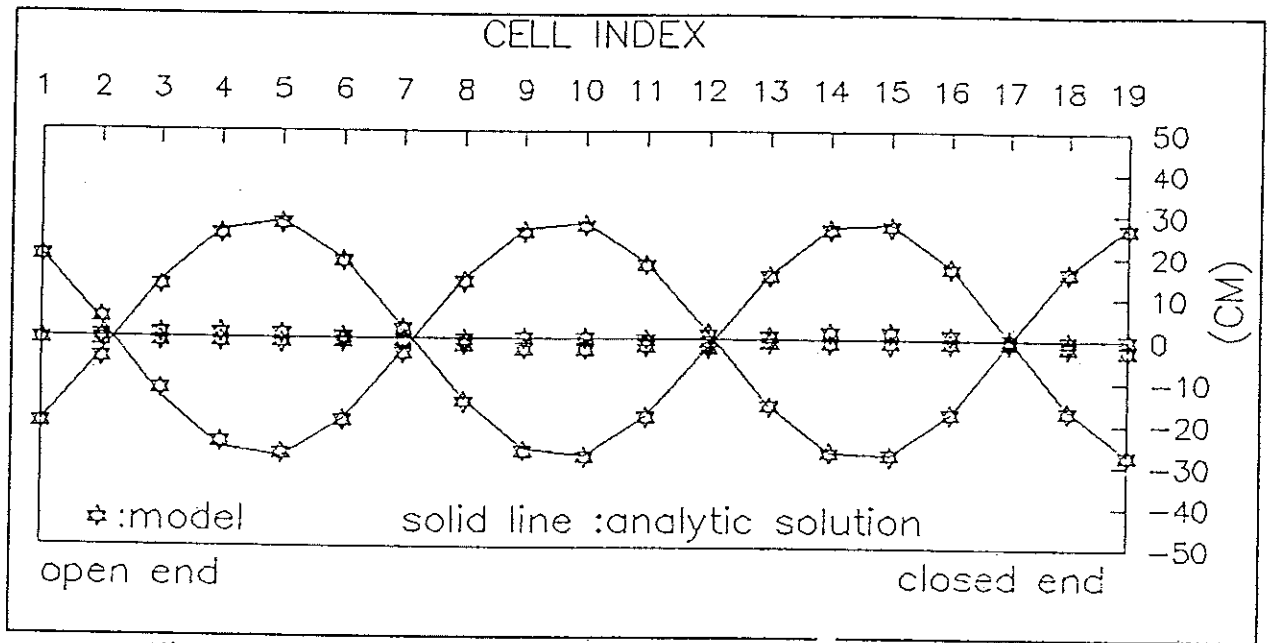


Figure 2.2 Simulation of an internal standing wave in an open channel.

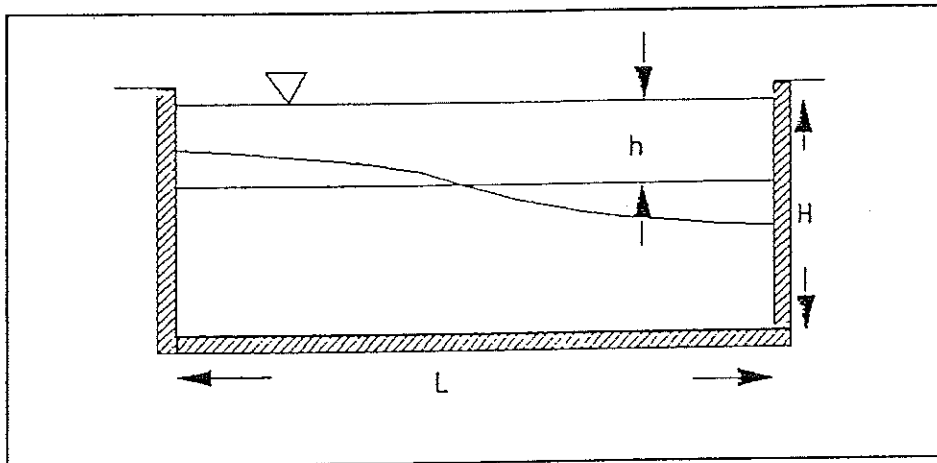


Figure 2.3 Closed basin dimension.

Table 2.1 Model parameters for the case of channel with one side open.

Channel Length	100 meters
Width	50 meters
Depth	20 meters
Layer Thickness	
Top Layer	10 meters
Bottom Layer	10 meters
Layer Density	
Top Layer	1000 kg/m ³
Bottom Layer	1005 kg/m ³
Open Boundary Wave Amplitude	
Surface	0.0 meters
Interface	0.2 meters
Open Boundary Wave	500 seconds
Model Cell Size, dx = dy	50 meters
Model Time Step, dt	1.0 seconds

2.2.3.2 Oscillation in a Rectangular Closed Basin

For the second comparison to an analytic solution a basin was configured to be compatible in size with the main basin of Lake Champlain (60 km long, 50 m deep). All sides were closed land boundaries. Given an initial wind induced surface stress which is subsequently released the model should respond with a certain internal wave frequency for a given geometry and density stratification.

The effective frequency for an internal seiche is given by Turner (1973) as:

$$N = \frac{m}{2L} \left(g \frac{\delta \rho h (H-h)}{\rho_o H} \right)^{1/2} \quad (2.9)$$

where

- N = wave frequency
- m = mode of oscillation (1)
- L = basin length (60 km)
- g = gravity
- $\delta \rho$ = excess density of lower layer
- ρ_o = density of upper layer
- h = upper layer thickness (20 meters)
- H = total depth (50 meters)

Initially all velocities and elevations were set to zero. A surface stress of 0.1 N/m^2 was then imposed for 2 days and abruptly reduced zero. Once interface waves are established they will persist. Figure 2.4 plots resultant wave periods for four runs of varying density differences ($\delta\rho = 0.5, 1, 2, 4 \text{ kg/m}^3$). The straight solid line represents Equation (2.9) above. A similar set of responses can be obtained by changing the location of interface, h . This experiment indicates an expected seiche period of approximately four days for the given basin configuration and the density difference of 1.0 kg/m^3 . A density deviation of $+0.5 \text{ kg/m}^3$ shortens the period by a half day, and -0.5 lengthens it by $1 \frac{1}{2}$ days.

It should be noted that the grid resolution with respect to wave length is a critical parameter. For a given grid unless resolution is sufficient, some short waves may degenerate if they happen to develop. Experiments have also shown that a high wind stress of short duration tends to develop an interface of sharp slope. A sharp slope consists of a number of harmonic waves, some of which may be short and is therefore also influenced by the grid resolution.

2.3 Application to Lake Champlain

2.3.1 Grids of Lake Champlain

Two grids, one coarse (1 km) and one fine (0.5 km) resolution were prepared (Figure 2.5) for Lake Champlain. The 1 km grid is adequate to solve individual basins, and practical in terms of exercising simulations with reasonable computational times (30 cpu minutes/simulation day on a 486DX2 cpu). The 0.5 km grid resolves finer detail and may better represent inter basin mass exchange. On the other hand the 0.5 km grid is not fine enough to represent interbasin passage configuration accurately in that a number of them are on the order of 100 m in width. The cpu time required to simulate the long term seiche period on the 0.5 km grid is excessive (4 cpu hours/simulation day). Grid cells were filled by an average depth value from the digital depth data base. The office of Department of Conservation, New York state provided a major portion of lake coverage which is originally based on NOAA navigational charts. Additional depth digitizing was performed by ASA in the Northeast Arm, also from the NOAA charts. Some portions of the region, such as the

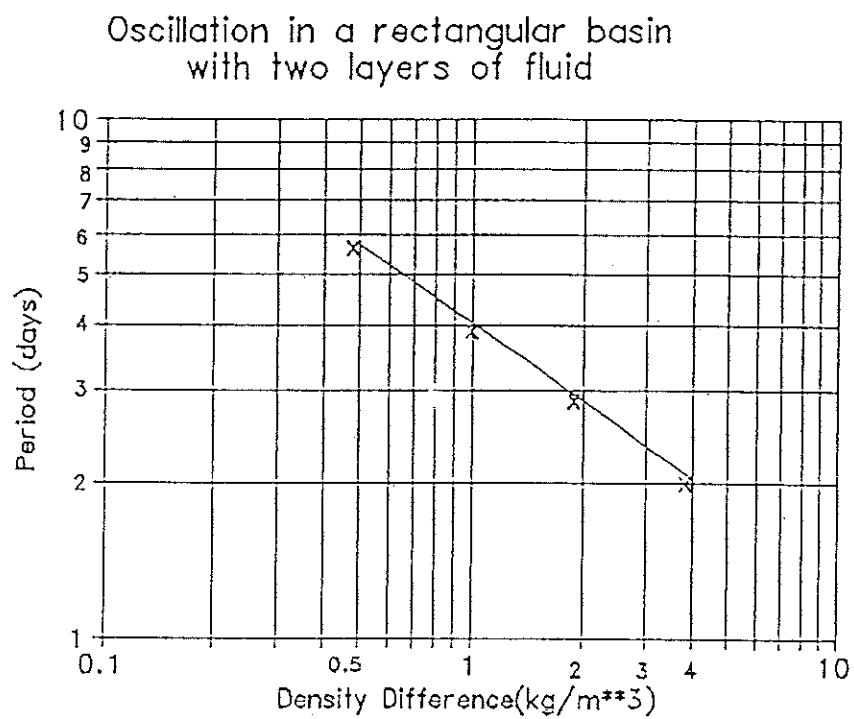


Figure 2.4 Interface oscillation in closed basin with two layers of fluid.

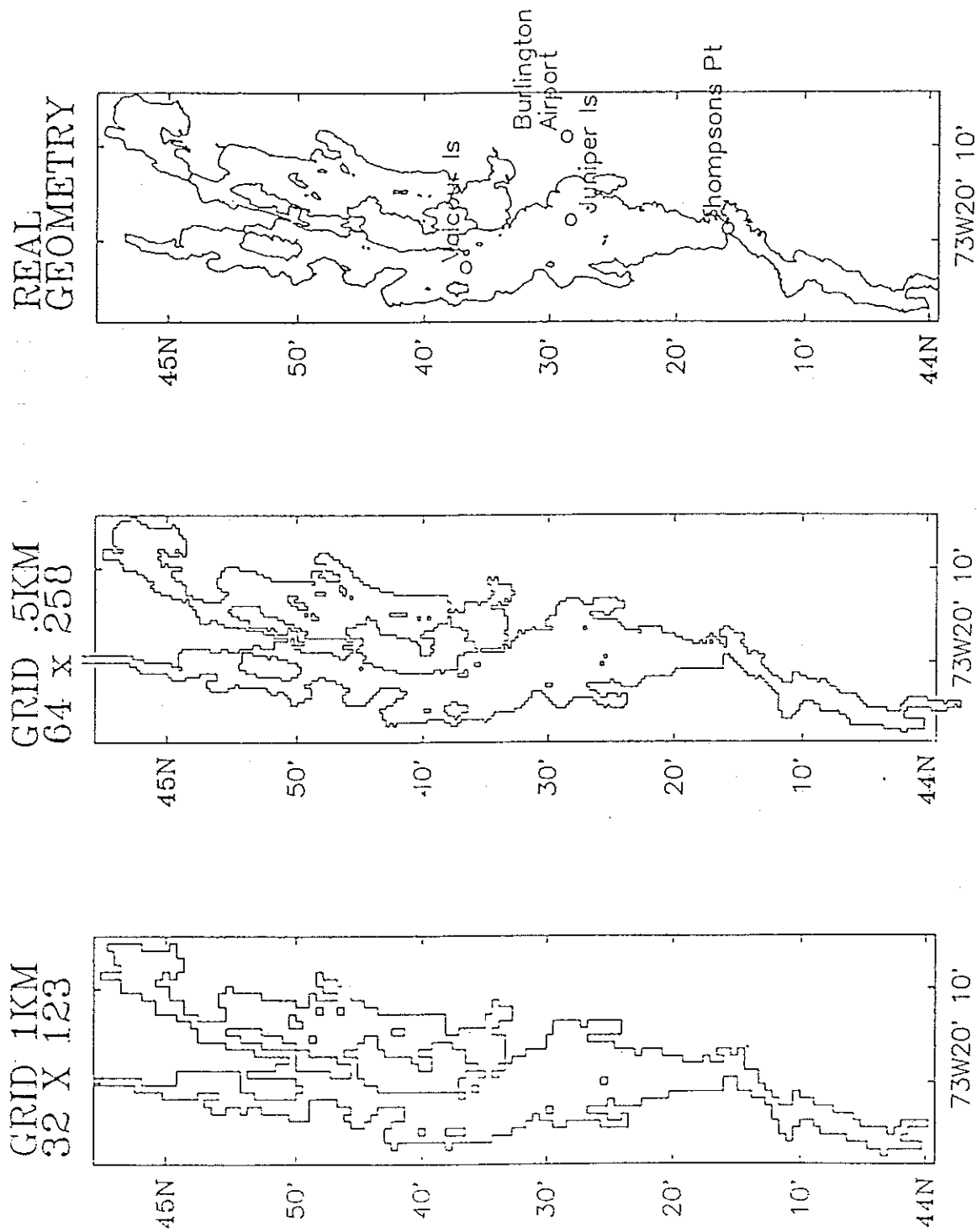


Figure 2.5 Hydrodynamic grids of Lake Champlain.

inlets that connect basins, do not have adequate data. This remains a major deficiency for the calculation of mass exchange between basins.

2.3.2 Model Simulation of Summer 1991

As mentioned above, preliminary results of current, thermistor chain and meteorological record data for summer and winter 1991 have been made available (Manley, 1993). Figure 2.6 shows upper and lower current observations denoted at three mooring locations, Valcour Island, Juniper Island and Thompsons Point, for the period between June and November, 1991 (see Figure 2.5). Figure 2.7a-c shows the power spectral density and the coherence square function between the upper and lower currents of the north-south velocity components at the Valcour Island, Juniper Island and Thompsons Point mooring, respectively. Figure 2.8 depicts changes in thermal structure as vertical location of maximum water temperature change and integrated temperature difference at these mooring locations. All figures indicated the existence of an oscillation with a four-day period. The north/south components of currents of the top and bottom meters are highly coherent at that period.

The thermal structure had two distinct features for early and later summer. The thermal stratification had already developed at the start of field observation (June 1991) and intensified until the middle of August. After that upper-lower temperature differences decreased and thermocline depth increased indicating increased mixing, possibly due to high wind events and consequent strong internal seiching (refer to Figure 2.8). The current features seemed to reflect the progress of thermal structure development; relatively weak currents in the early summer as thermal stratification was developing and strong currents (oscillation) in the late summer as the location of stratification deepened and the density difference reduced. At Valcour Island the bottom currents became stronger than those at the surface for late summer.

The entire month of August 1991 was chosen as the period to simulate hydrodynamics and to compare with the field observations. As mentioned above, the August data resides between two distinct thermal periods. For the first part of the month the wind was relatively weak and thermal stratification was developing. In the latter part of the month winds became strong with notable north/south components.

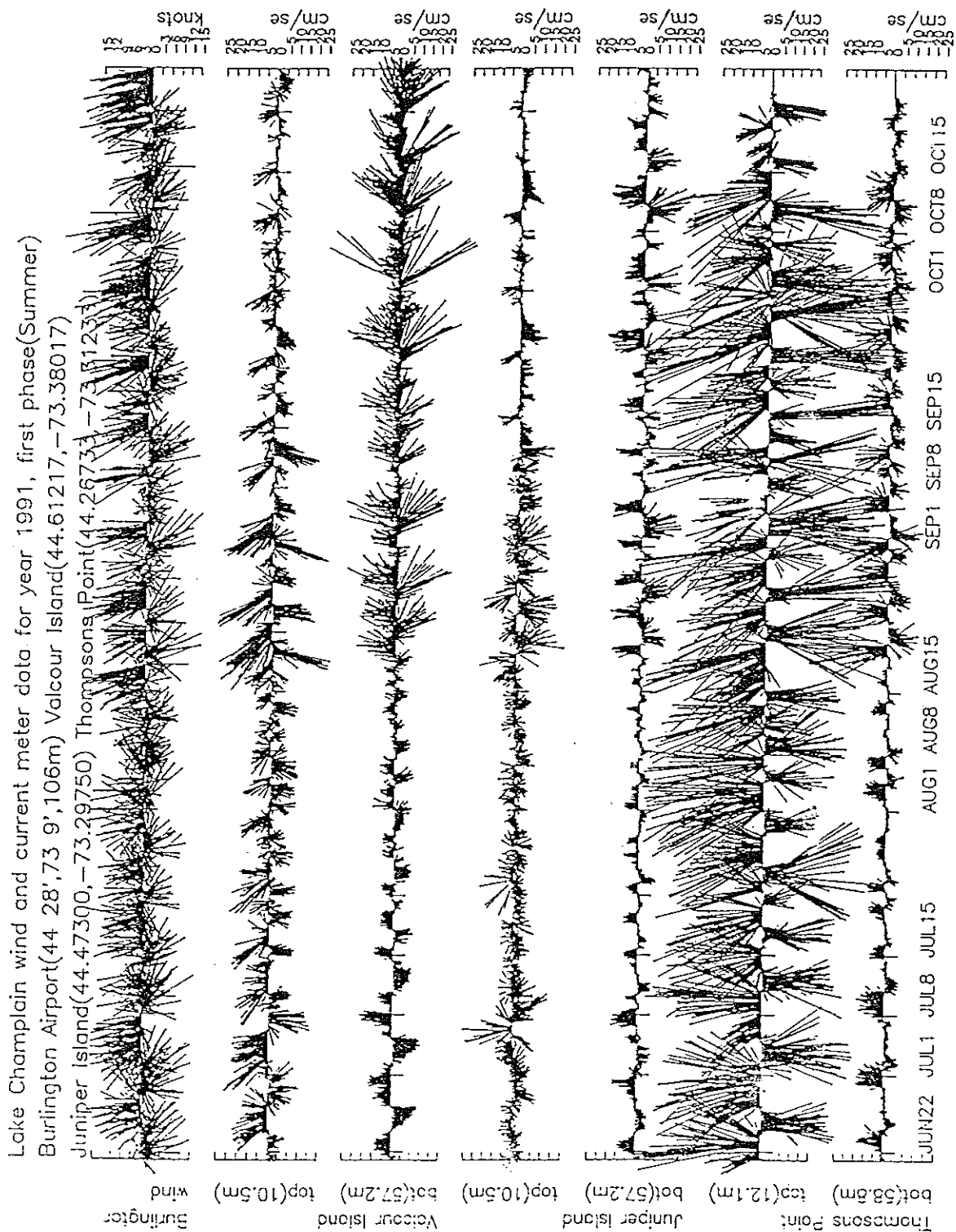


Figure 2.6 Field observed current during summer 1991.

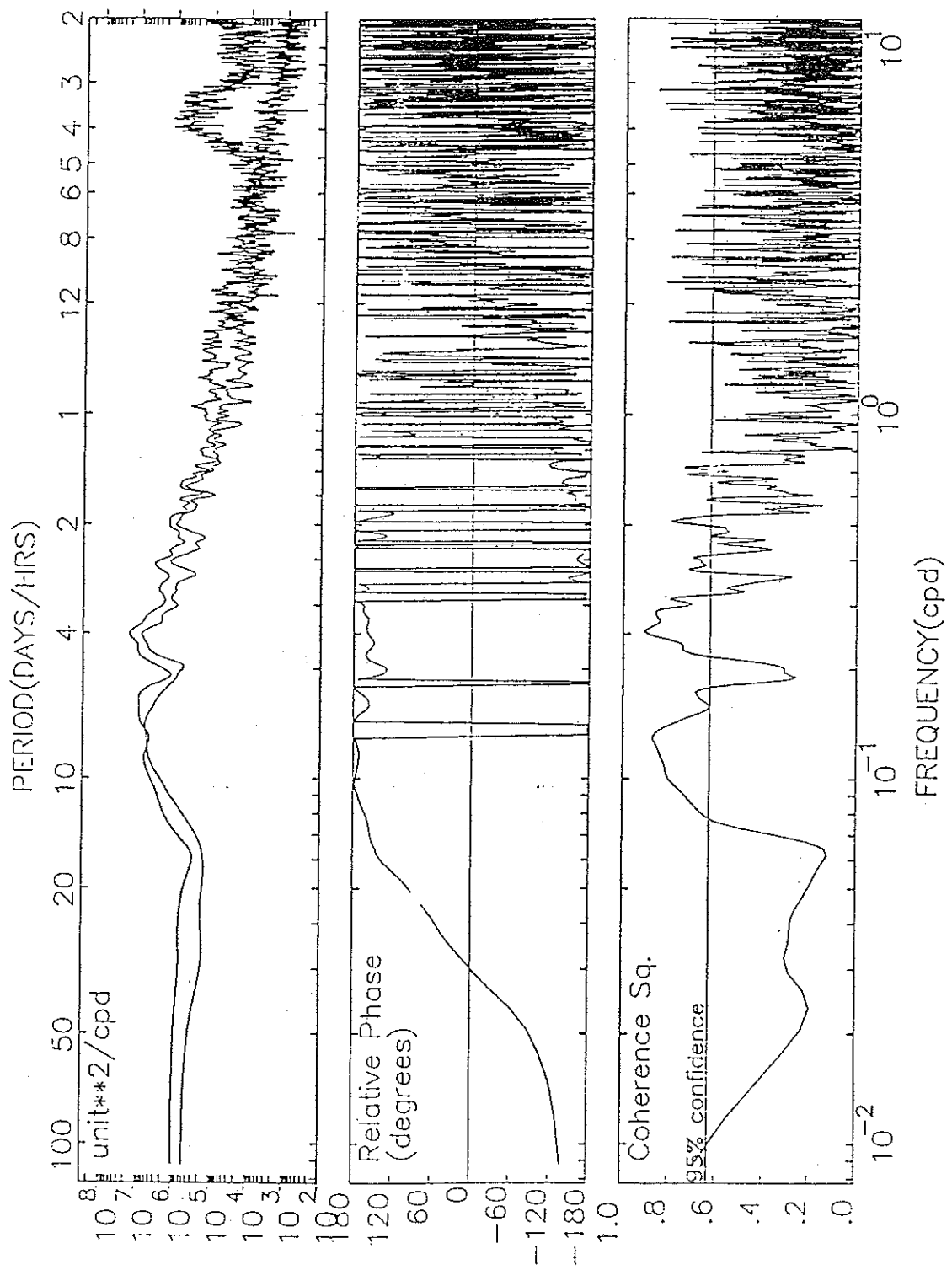


Figure 2.7a Power spectral densities and coherence square Valcour Island Mooring.

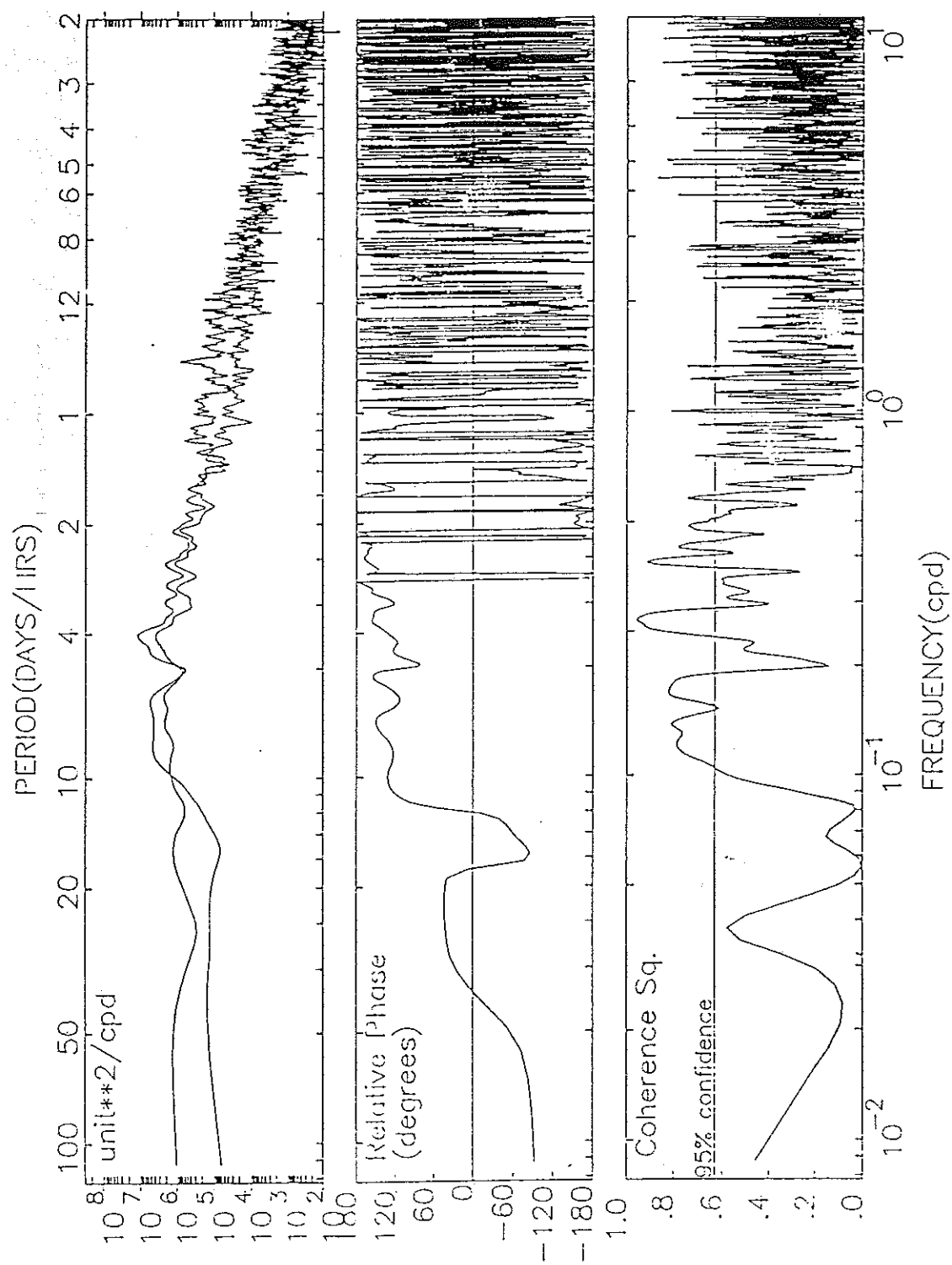


Figure 2.7b Power spectral densities and coherence square Juniper Island Mooring.

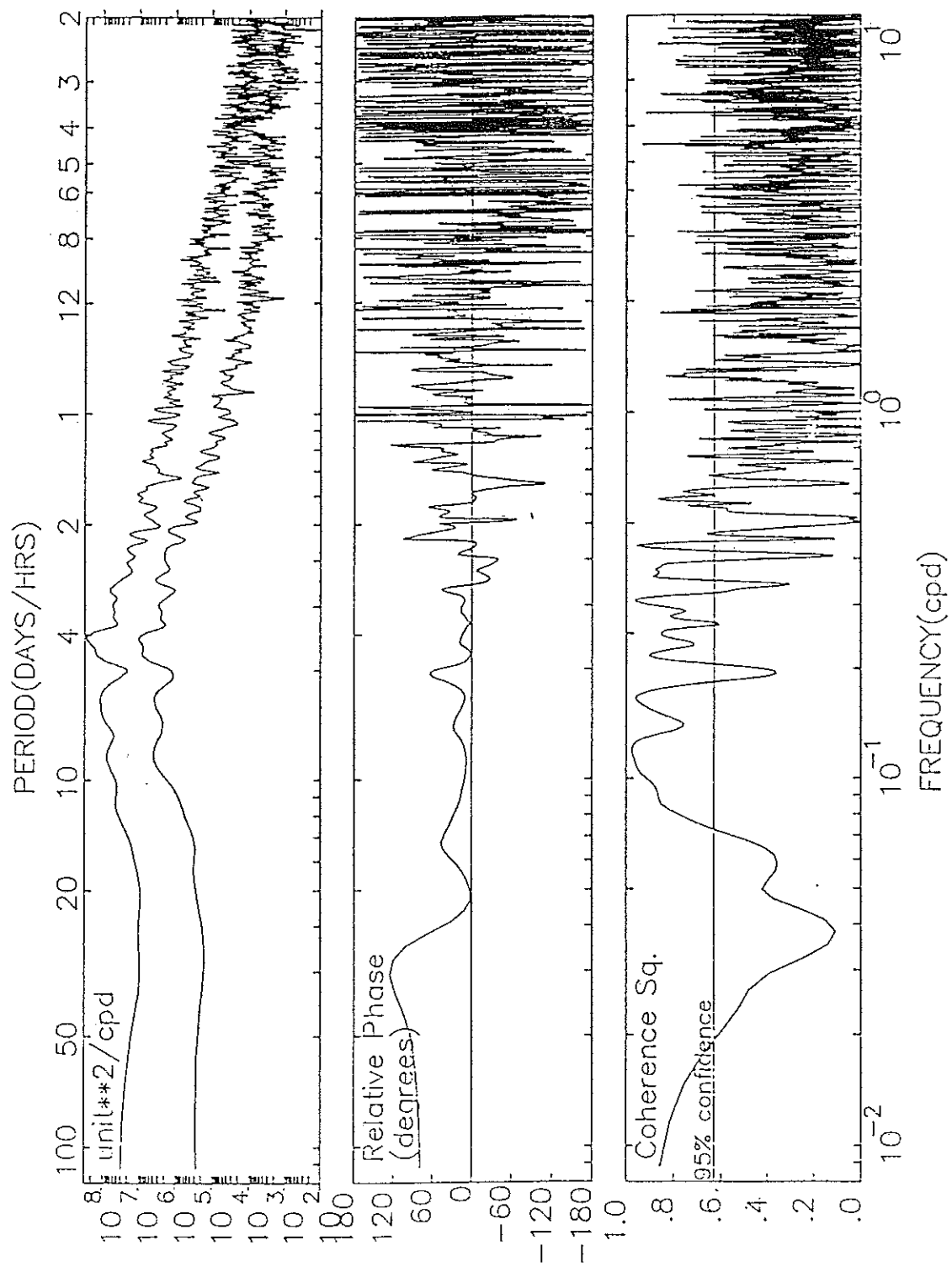


Figure 2.7c Power spectral densities and coherence square Thompsons Point Mooring.

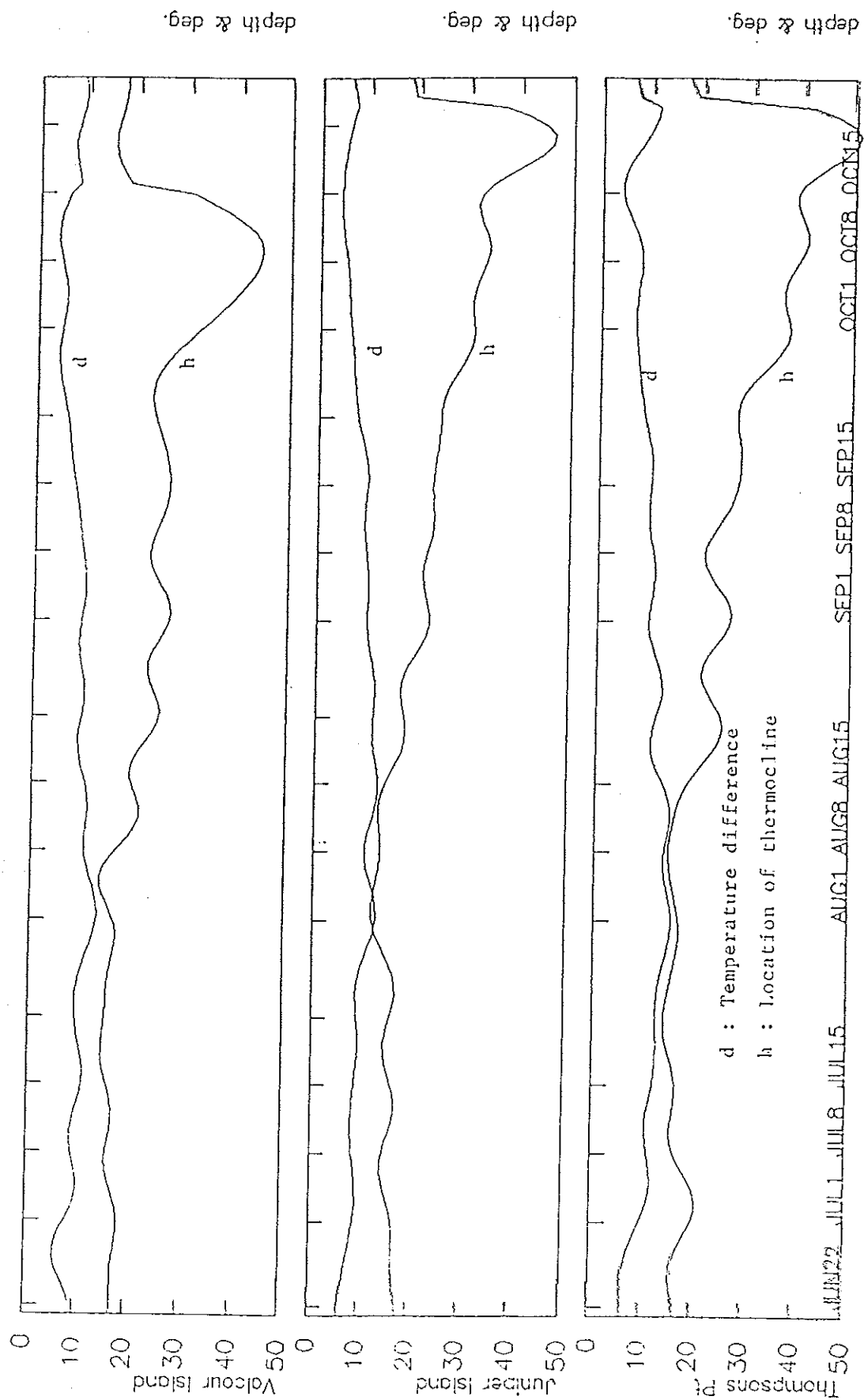


Figure 2.8 Field observed thermal structure during summer 1991.

Basic inputs to the model were wind data and stratification parameters. Hourly observations of wind data taken at Burlington Airport, Vermont were applied to the entire domain. The stratification parameters density difference and layer thickness were initialized for the entire domain. As the simulation proceeds the layer thickness is allowed to change but the gross water mass in each layer and the density difference remain the same.

Numerous runs were made with different values for the model parameters to assess the model response. The primary objective was to find the range of parameter values that would produce a reasonable simulation rather than to execute a complete sensitivity analysis. Several preliminary runs were made to find basic parameter values (such as minimum time step, interface friction, and horizontal diffusion) that produce a stable simulation. These are kept constant among the cases. Table 2.2 lists the base case parameters.

Table 2.2 Base case parameters for hydrodynamic simulations.

Horizontal Resolution	1000 meters
Number of Layers	2
Horizontal Diffusion	7.5 meters/sec ²
Time Step	25 seconds
Interface Friction	0.0001
Bottom Friction	0.001

Sensitivity parameters examined were the layer thickness (15 and 20 m) and the density difference (0.5, 1.0, 1.5 kg/m³). This combination yielded five case runs (no run for the 1.5 kg/m³, 20 m case). Several additional exploratory runs were made to examine the effect of added bottom friction, extended period simulation (2 months), and changes in grid resolution (not presented). Table 2.3 lists the values for each parameter and the associated case names and figure numbers of the simulation output and observations for comparison. Figures 2.9a-g display the results.

Table 2.3 Description of cases for summer simulation.

Number	Case Name	Figure Number	Period Layer	Density Thickness	Difference
1	1K_AUG10	2.9a	aug1-31	15 m	0.5 kg/m ³
2	1K_AUG11	2.9b	aug1-31	15 m	1.0
3	1K_AUG13	2.9c	aug1-31	15 m	1.5
4	1K_AUG12	2.9d	aug1-31	20 m	0.5
5	1K_AUG3	2.9e	aug1-31	20 m	1.0
6	*1K_AUG11	2.9f	aug1-31	15 m	1.0
7	1K_JUL1	2.9g	jul1-aug	15 m	1.0

* bottom friction $cd=0.003$

All figures plot simulated currents comparing three mooring sites and wind stress in stacked stick plot form. The differences between cases were relatively small. General observations were:

- 1) Relative amplitude of observed and calculated currents agree, with the exception of the surface observations at Thompsons Point.
- 2) During strong wind periods, the model-predicted and observed currents agree well in both amplitude and phase.
- 3) During weak wind periods, current amplitudes agree with observations but the phase is often shifted.
- 4) The effect of bottom friction is not significant.
- 5) The fine grid (0.5 km) simulations do not show any improvement over the coarse grid (1.0 km) simulations.
- 6) The case, 1K_AUG13 (15 m layer thickness and 1.5 kg/m³ density difference) shows the best agreement with observations.

It is apparent that wind is an important forcing function, as seen in all cases. The simulated currents responded strongly to strong wind events. It is questionable how well the lake surface wind can be represented by Burlington Airport wind, particularly for weak winds. It became apparent that a short term simulation (less than several internal seiche

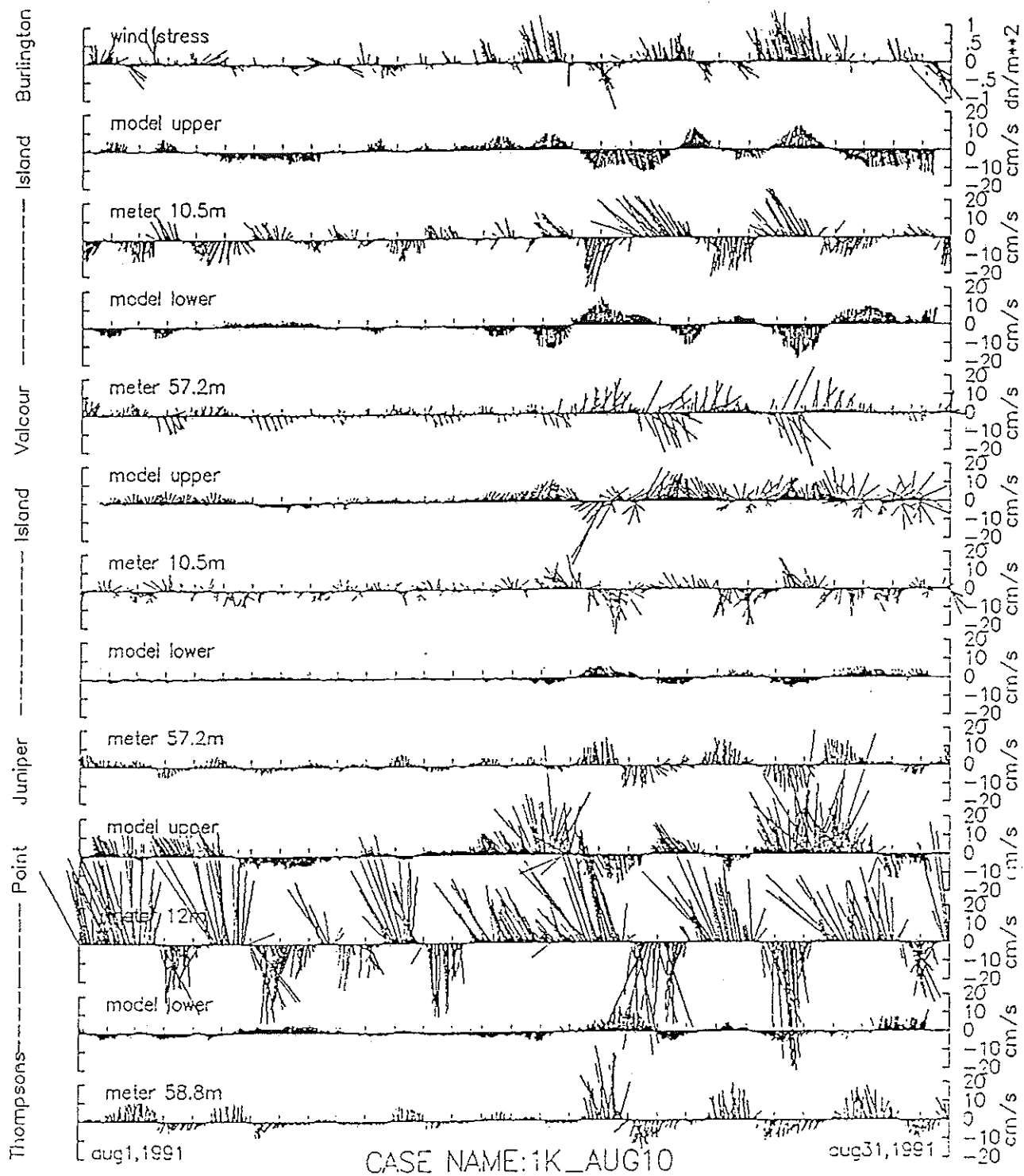


Figure 2.9a Hydrodynamic simulation for August 1991, with run parameters density difference = $0.5 \text{ (kg/m}^3\text{)}$, stratification at 15 m.

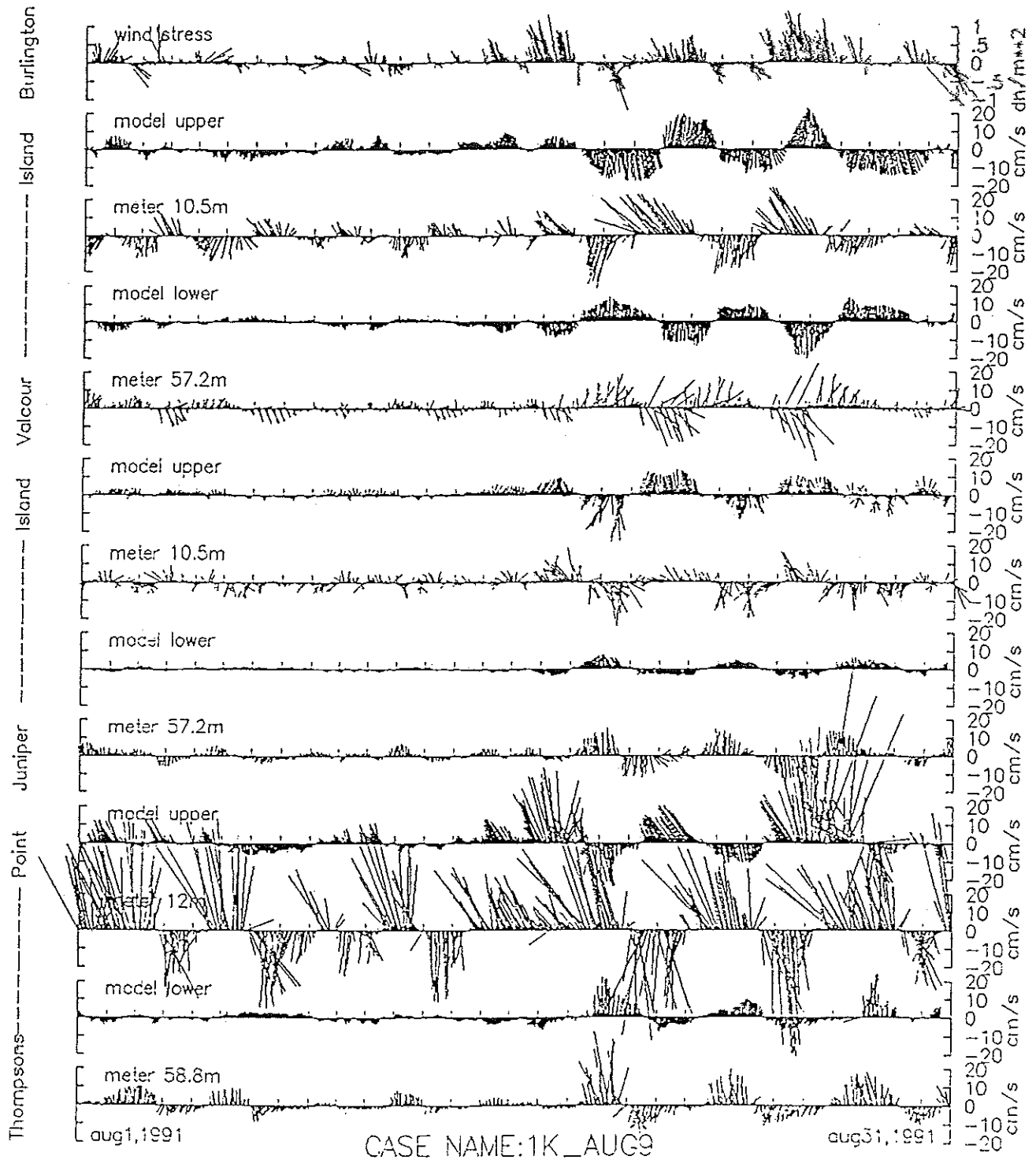


Figure 2.9b Hydrodynamic simulation for August 1991, with run parameters density difference = $1.0 \text{ (kg/m}^3\text{)}$, stratification at 15 m.

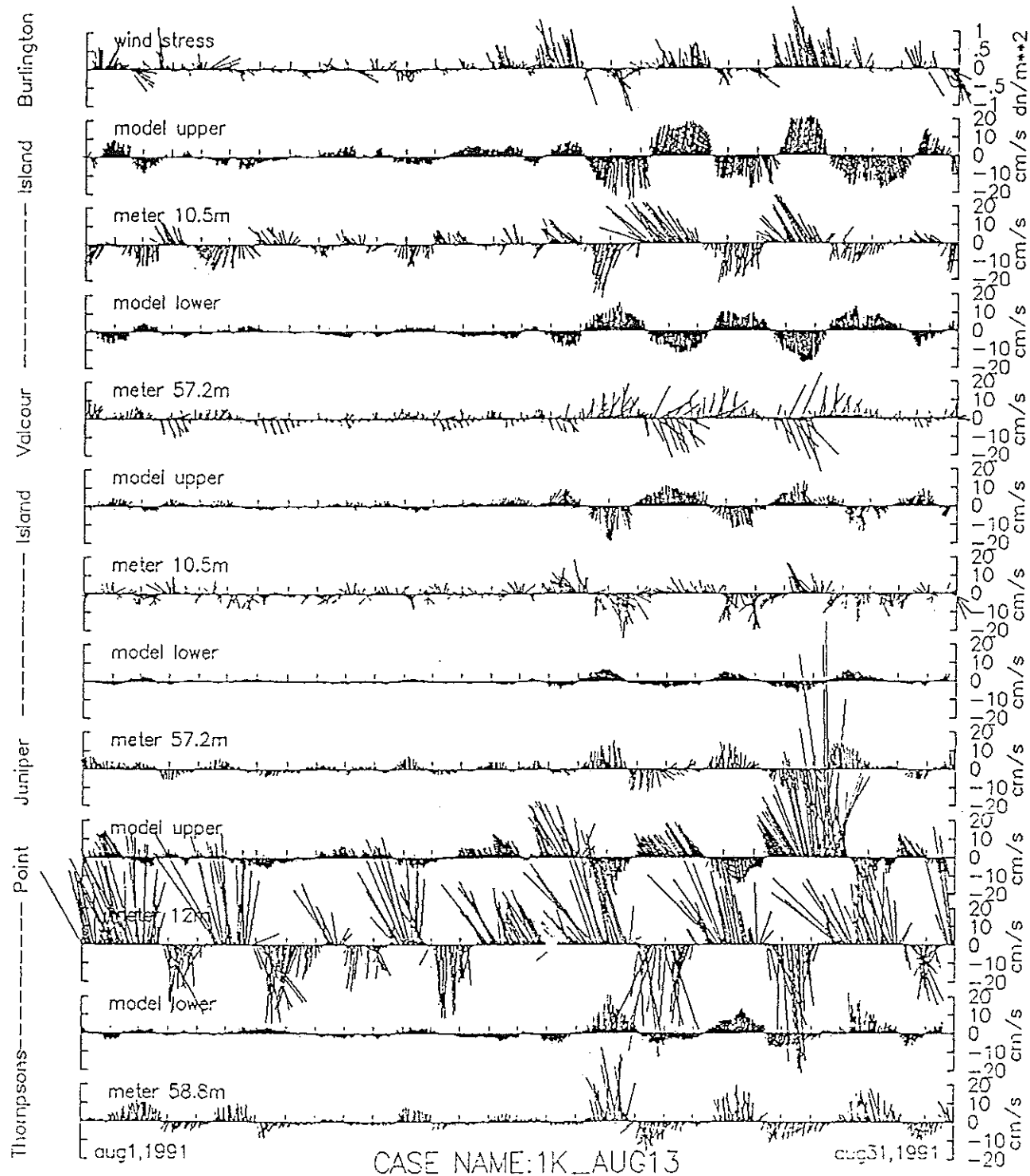


Figure 2.9c Hydrodynamic simulation for August 1991, with run parameters density difference = $1.5 \text{ (kg/m}^3\text{)}$, stratification at 15 m.

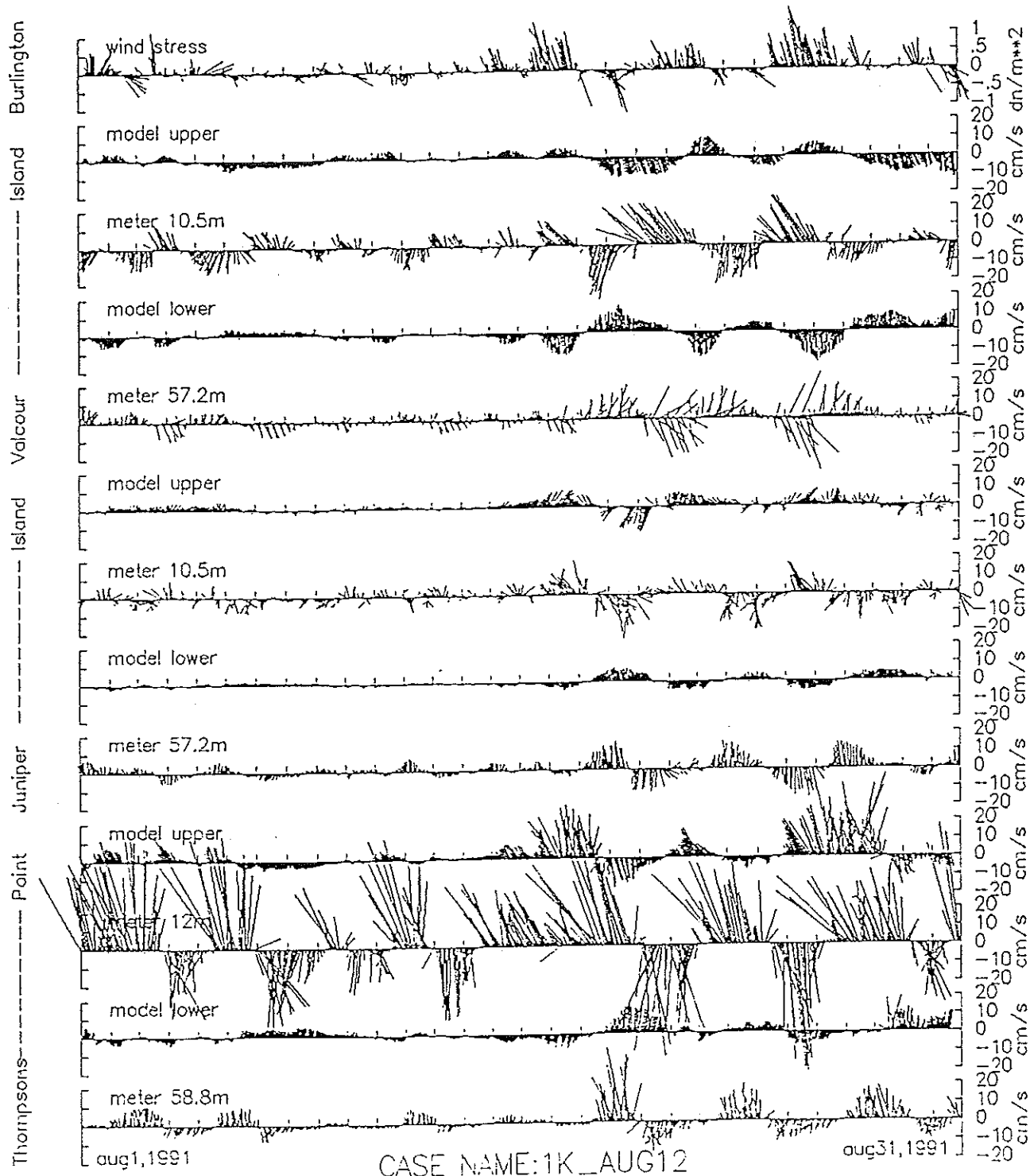


Figure 2.9d Hydrodynamic simulation for August 1991, with run parameters density difference = 0.5 (kg/m³), stratification at 20 m.

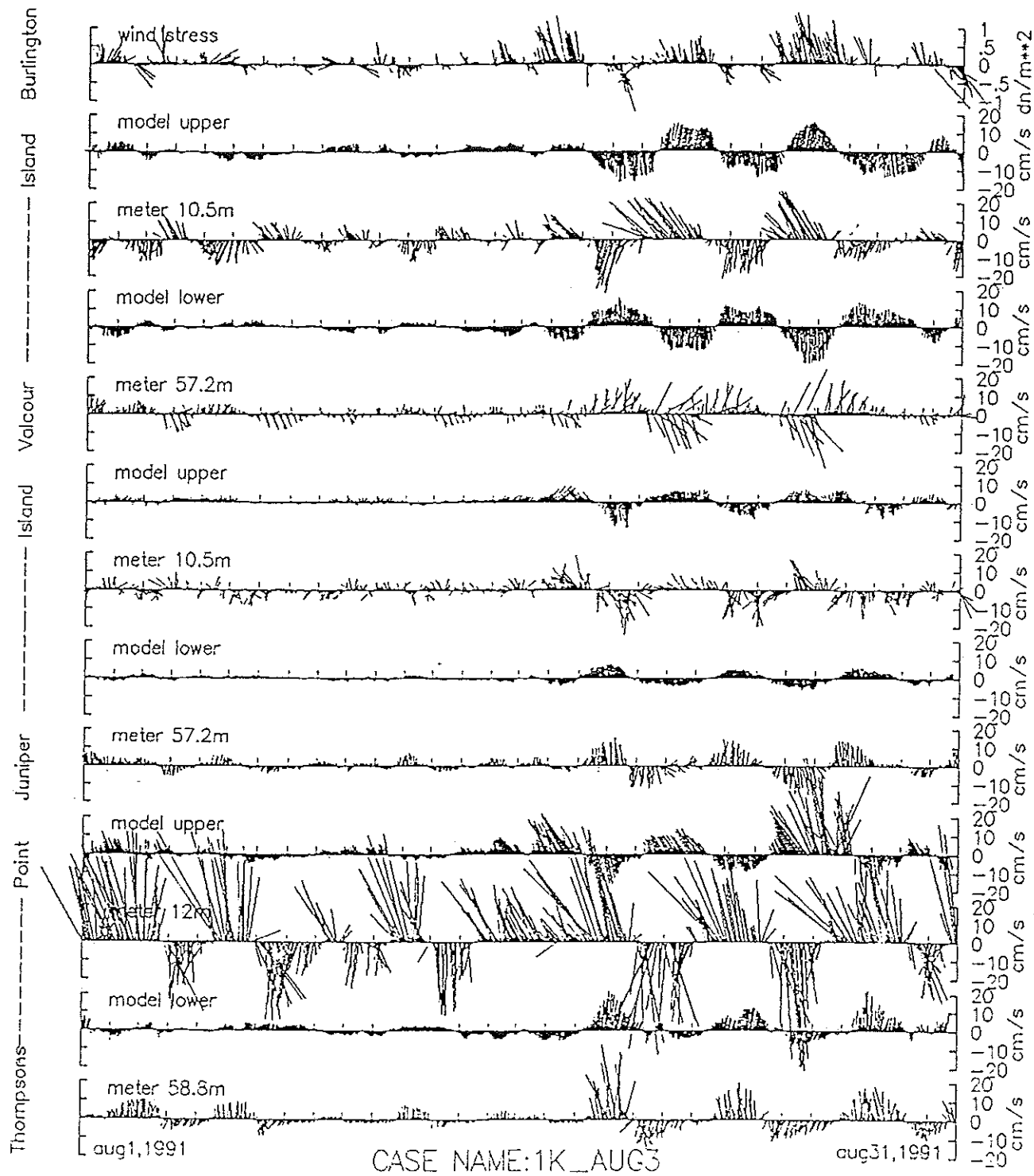


Figure 2.9e Hydrodynamic simulation for August 1991, with run parameters density difference = $1.0 \text{ (kg/m}^3\text{)}$, stratification at 20 m.

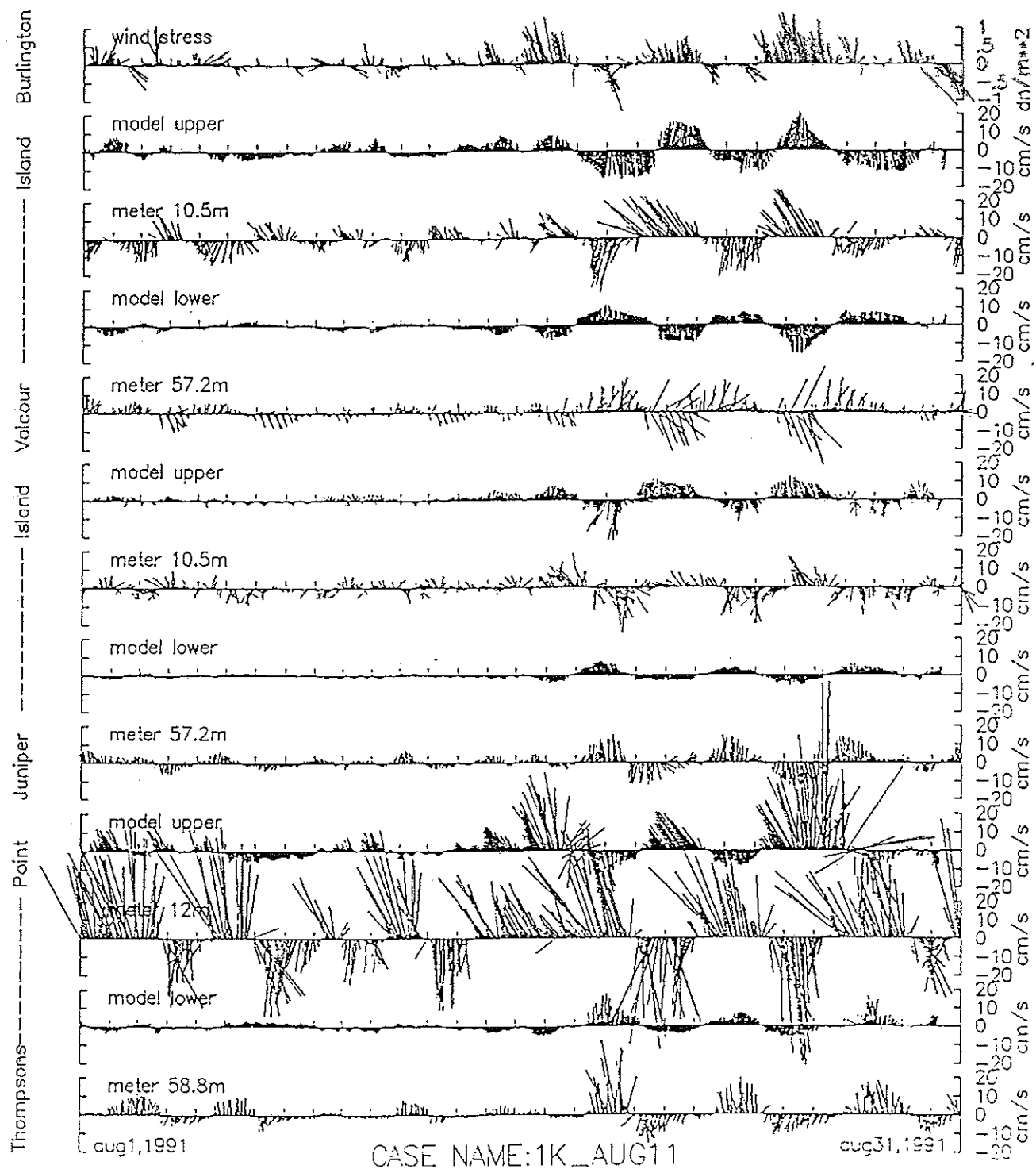


Figure 2.9f Hydrodynamic simulation for August 1991, as case 1K_AUG9, except bottom friction of 0.003.

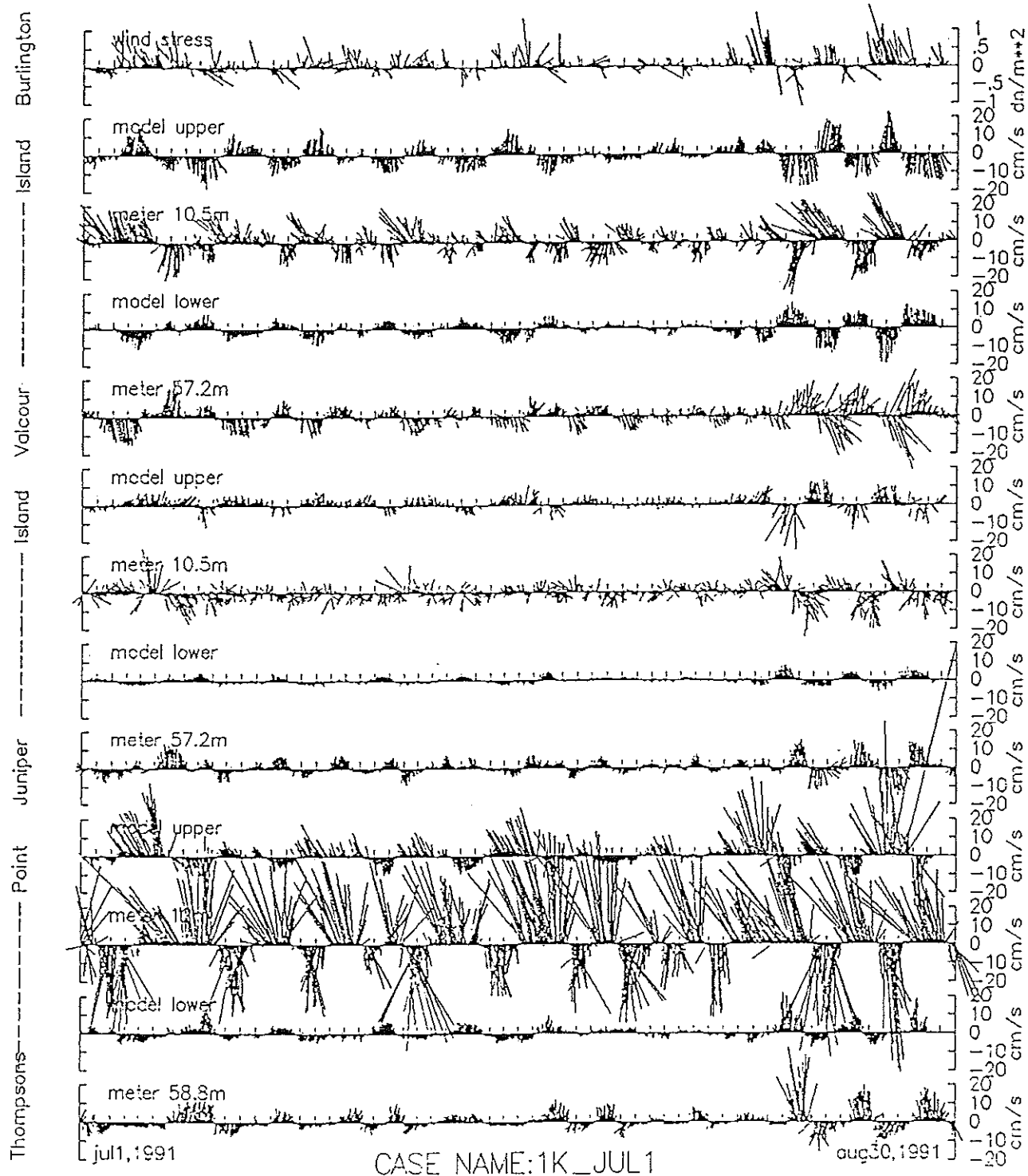


Figure 2.9g Hydrodynamic simulation for July-August 1991, with run parameters density difference = 1.0 (kg/m³), stratification at 15 m.

periods, 12 days) requires appropriate initial conditions to reproduce the observed currents. The case, 1K_JUL1 was run for two months, one month longer than the other cases to see if a longer simulation period would result in better agreement. The improvement was marginal. For weak wind events it may not be possible to synchronize the model predicted internal seiche with the naturally occurring oscillation observed in the lake without extensive and detailed initial conditions unless a strong wind event can restart and force the oscillation.

2.3.3 Model Simulation of Winter 1991

Winter observations were quite different than those of the summer. After fairly large oscillations for the later part of the summer and fall, the stratification collapsed and currents decreased dramatically (Figure 2.10) in spite of a relatively high wind speed for the entire winter period. As current meters were kept at nearly the same depth as in summer, it is not clear what current structure the measurements represent in the absence of stratification. The currents seemed to correspond as bulk water movement due to wind forcing at the surface and return flow at the bottom. For the winter simulation there is no particular period of interest. The month of November was selected for study (Figures 2.11a,b). Two simulations were made, with two layers and one layer respectively as shown in Table 2.4.

Table 2.4 Description of cases for winter simulations.

Number	Case Name	Figure	Period	Density	Difference
1	1K_Nov1	2.11a	nov9-dec9	25 m	0.kg/m ³
2	1K_Nov2	2.11b	nov9-dec9		

Since the water column is unstratified there is no potential force to return currents and cause oscillation. A prolonged wind therefore induces vertical advection of water mass. When multiple layers are used in this simulation, mass exchange through the interface must be allowed. It is not clear what to expect from these cases at this stage. The two cases produced similar current patterns to the observations although one to one comparisons reveal some currents were entirely out of phase (opposite direction). It is also unclear however how well the observed currents corresponded to the Burlington Airport winds.

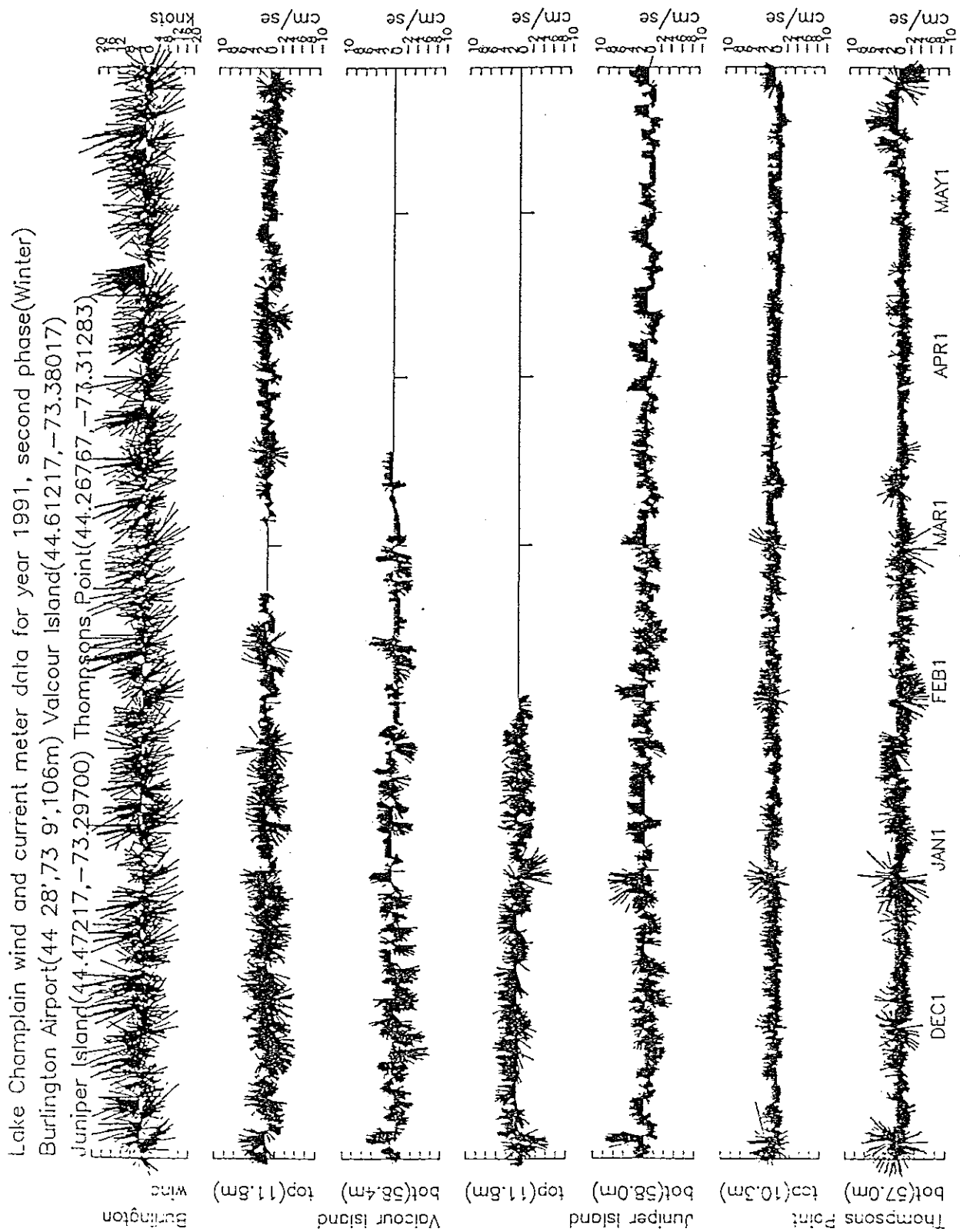


Figure 2.10 Field observed current during winter 1991-1992.

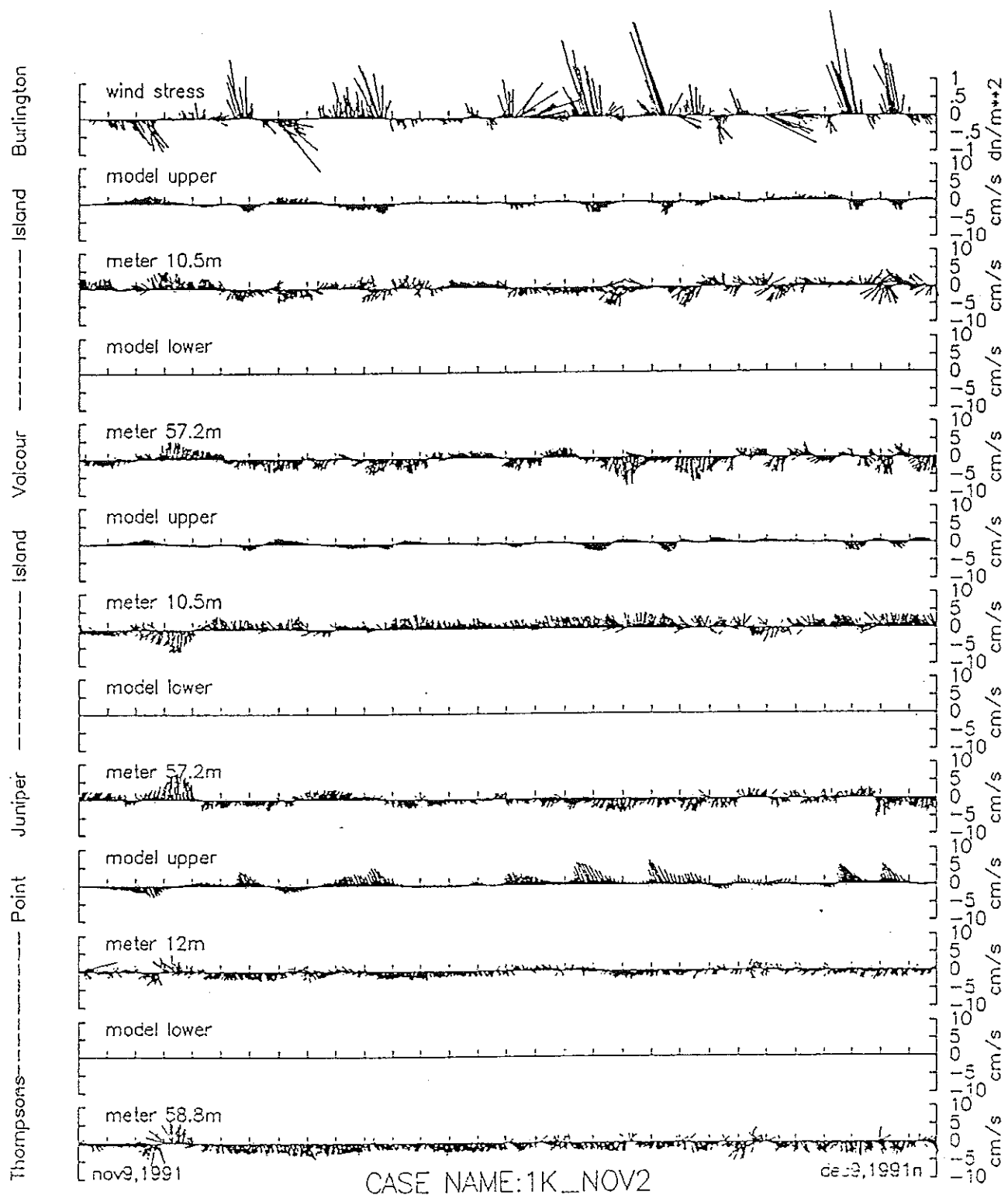


Figure 2.11b Hydrodynamic simulation for November 1991, with one layer, the labeled 'model upper' corresponds to one layer result (vertical mean) and the label 'model lower' is null.

2.4 Discussion and Recommendations

The field investigation that for the first time yielded extensive coverage in Lake Champlain is now in its second year. The additional observations will undoubtedly give us far more insight and understanding of the lake hydrodynamics. It is premature to make any judgement with respect to the field data that we have so far. The expected data report and analysis are essential for further studies.

From the modeling perspective the following items need to be addressed:

- 1) Verification of wind field. An adequate wind field is of prime importance. It is necessary to verify how well the lake surface wind can be represented by the Burlington Airport observations. Additional wind stations may be needed.
- 2) Variable layer depth and density. For long term simulations, it is not reasonable to keep constant density and layer thickness. Some form of exchange between layers should be applied without solving the full conservation of heat.
- 3) Additional current measurements. Currents and circulation patterns in Malletts Bay, the northeast arm and Missisquoi Bay need to be studied. Little more than qualitative information is now available in these areas.
- 4) Interbasin passage data. Detailed interbasin passage geometry in concert with long term passage current measurements and subsequent analyses are essential in the determination of interbasin fluxes. Simultaneous current measurements at each of the passages between the main lake, Malletts Bay, the northeast arm and Missisquoi Bay would make basin-wide flux calculations possible.

3. LAKE CHAMPLAIN PHOSPHORUS MODEL

3.1 Background

The issue of whether a simplified water quality model can accurately portray the processes of a system is dependent upon the physics and chemistry of the water body. There has been, however, a long and successful history of box model applications to estuarine (Officer, 1980; Thomann and Mueller, 1987 and Swanson and Jayko, 1988) and lake problems (Chapra and Reckhow, 1983; DiToro and Connolly, 1980; Thomann and Mueller, 1983). The approach taken here is a more sophisticated version of a simple concept and provides hydrodynamic information about advective and dispersive flows in three dimensions deduced from the distribution of a conservative tracer, chloride, given flow rates and loads to the system. Although the conservation of momentum equation is not involved directly in the approach taken, the effects of current movement and circulation are accounted for in an integrated sense. It should be noted that hydrodynamic exchange coefficients are sufficient to represent the hydrodynamics in many water quality models such as the EPA WASP model (Ambrose et al., 1993).

As an alternative to the tracer method the exchange coefficients can be generated by integrating the hydrodynamic model output currents in time and space. The hydrodynamic simulations necessary to create exchange coefficients that would be meaningful for calibration and use in the water quality model are difficult to develop with the present lack of interbasin flow data and circulation data in the Northeast Arm. Hydrodynamic model predicted exchange coefficients are calculated, however, for the main lake and connected basins and compared to data derived values from VTDEC and ASA.

This section describes the simplified approach to modeling lake circulation and water quality. The model is based on the box model methodology presented by Officer (1980) linked with the WASP5 (Ambrose et al., 1993) phosphorus kinetic rate equations. This methodology has a number of desirable features: both conservative and nonconservative constituents can be examined; with two layers both advective and nonadvective exchange estimates can be made; and the approach is sufficiently general to handle complex geometries.

The assumptions implicit in this type of model are the following:

1. The lake can be divided into a series of boxes which enclose volumes of constant properties such as chloride and phosphorus concentration.

2. The time independent conservation equations for water and the tracer (chloride) can adequately describe the flow. No momentum equations are used.
3. Exchanges occur only at box faces, which allows a finite difference representation of the equations.
4. Constituent mass transport can be described by a conservation equation including kinetics, sources, sinks, and exchanges.

The box model requires that the lake be represented by a number of boxes of known area, volume, river flow and tracer concentration. Three equations are then solved for each box: conservation of water, chloride and constituent, to give the exchanges between boxes and the constituent concentration within the box.

One unique feature of this model is that the exchange rates are determined directly from observed sets of chloride. This approach sought to eliminate the "trial and error" and tuning necessarily used by modelers in other approaches.

Box models have several inherent limitations. They present extreme simplifications of the actual hydrodynamic processes occurring, including information on currents in an integrated sense only. Predicted constituent concentrations are highly dependent on the input tracer data set. Pollutant concentrations which are weakly correlated with the tracer distribution are very difficult to predict accurately. However, box models have been shown to be valuable for first order approximations of exchange coefficients and constituent distributions in lakes and estuaries (Officer, 1980; Chapra and Reckhow, 1983; Thomann and Mueller, 1987).

One of the major water quality issues facing managers on Lake Champlain is the problem of excessive nutrient enrichment of the lake and the associated eutrophication problems. Phosphorus has been identified as the limiting nutrient and has been the focus of a number of studies (Henson and Gruendling, 1977; VTDEC and NYSDEC, 1992) and management and load allocation plans (Lake Champlain Basin Study, 1979; VTDEC and NYSDEC, 1993). The Lake Champlain Diagnostic Feasibility Study (VTDEC and NYSDEC, 1992) conducted a comprehensive, concurrent lake and tributary sampling program for a two year period focussing on phosphorus and chloride. Sufficient data were collected to form the basis of a whole lake phosphorus mass balance, concentration model and load allocation study as reported in Part I of the Feasibility Study. Final Report. The

VTDEC modeling effort, although focussing on total phosphorus, with appropriate calibration was able to make predictions of the steady state, in-lake concentration that agreed well with observations.

The present model development seeks to expand the capabilities for predictive phosphorus modeling, and ultimately eutrophication modeling, through better understanding of phosphorus dynamics and kinetics in the lake. The development effort focusses on mixing exchange coefficient calculations based on the concentrations of a conservative tracer as well as the phosphorus cycle constituent concentration calculations, (i.e., organic phosphorus, inorganic phosphorus and phytoplankton) through the incorporation of the WASP5 kinetic rate equations.

3.2 Model Development

In a box model the water body under consideration is segmented into a number of boxes within which the physical characteristics are approximately constant. Each box can have either one or two layers in the water column and one sediment layer. Mean time averaged values are used for all input parameters and therefore the exchange coefficients and concentrations calculated by the model are likewise time-invariant solutions. There is a provision, however, for the time variable solution of the phytoplankton population and phosphorus cycle as described below.

The model, as presented by Officer, has two-layered boxes, where each box has only one upstream and one downstream face for flow to enter and leave the box. The flow has no such restriction in the present model. The current application has extended the methodology to represent three dimensions by allowing each box to have an unlimited number of vertical faces through which flow may enter or leave, in addition to two water column layers and one sediment layer.

3.2.1 Exchange Coefficients

3.2.1.1 Exchange Coefficients Calculated from Data

The model equations are based on the principles of continuity of mass and conservation of a tracer, chloride in this case. Observed values of chloride and river flow are used to determine the hydrodynamic exchange coefficients. All exchanges occur at the

boundaries of the boxes. The vertical boundaries may be located fairly arbitrarily but should enclose regions of similar properties; the horizontal boundary between upper and lower layers is often determined by the thermocline.

Following the approach of Officer (1980) longitudinal exchange coefficients (E) rather than dispersion coefficients are used to describe the dispersive exchange. Nonadvective chloride transfer is therefore represented by a term $E_{ij}S_i$ instead of $(K_x A / \Delta x) S_i$ where:

$$E_{ij} S_i = \left(\frac{K_x A}{\Delta x} \right) S_i$$

- E_{ij} = longitudinal exchange coefficient from box i to box j
- S_i = salinity of box i
- K_x = longitudinal dispersion coefficient
- A = cross-sectional area
- x = longitudinal distance

This relationship assumes that the exchange coefficient E_{ij} from box i to box j is equal to the exchange coefficient E_{ji} from box j to box i .

In a one-layer simulation both mixing and diffusive exchanges (nonadvective) and net circulation (advective) effects are included in the longitudinal exchange coefficient. When two layers are used, these effects can be separated. It is apparent from the analysis of the hydrodynamic model results that both advective and oscillatory processes are occurring in the lake. These processes may have differing relative importance on material transport from lake basin to basin. As an example, the transport of material through the narrow and shallow passages between the main lake and the Northeast arm will be governed by advective processes whereas transport between segments within the main lake will be influenced both by advective and oscillatory processes. At this point it is desirable to introduce the parameter ϕ which will be used to relate the advective and the non-advective effects within the system and which will supply the necessary relationship for closure of the solution equations. The parameter ϕ can be determined empirically or calculated directly from the hydrodynamic model output as the ratio of the mean net transport to the mean exchange between two basins.

A conceptual diagram of the hydrodynamic exchanges occurring across the vertical and horizontal faces of a box is shown in Figure 3.1. Several naming conventions are followed. E and Q represent nonadvective and advective exchanges, respectively, while R is the net river flow. The ratio α is used to proportion the net river flow between the upper and lower layers: αR is the river flow in the upper layer, $(1-\alpha)R$ is the flow in the lower layer. (The use of α is a generalization of the work done by Officer (1980) which assumes one-half the river flow in each layer.) The chloride in each box is represented by S . A prime (') indicates that the parameter represents conditions in the lower layer of the box. Lettered subscripts indicate the face through which the exchange occurs; e.g., E_{ij} is the nonadvective exchange between box i and box j . A subscript v indicates a vertical exchange between the upper and lower layers. The box under consideration is box i ; adjacent boxes are numbered $i-1$ to $i+1$ depending on the number of connections, but may be thought of in a finite difference sense where upstream is $i-1$, downstream is $i+1$ for convenience. There are no restrictions on the number of adjacent boxes a box may have. This is true since there is no directionality in the model, only flow in and out which is proportioned a priori. Flow into a box is considered positive; flow out of the box is negative. To simplify equation formulation a parameter δ is introduced to specify flow direction. If flow is into a box then $\delta=1$; for flow out $\delta=-1$.

Since the net circulation Q is depth dependent, its direction of motion varies with depth. In the upper layer Q is assumed to be in the same direction as the river flow. In the lower layer Q is in the opposite direction. This may or may not be true in the case of the seiche induced net circulation but little data exists for confirmation one way or the other.

Referring to Figure 3.1, it can be seen that there are $4N+2$ unknowns to solve for Q and Q' on each face, E and E' on each face and Q_v and E_v . For each face of a box the continuity of mass and the tracer conservation equations can be written. These equations can also be written for the box as a whole. Since the model provides a steady state solution, the conservation and continuity equations are valid for both the face and the entire box.

This assumption forces the sum of the surface and bottom net flows to equal the river flow which is a reasonable solution for lake flow in the two horizontal dimensions.

The sum of the flows across the upstream face of the box (both lower and upper layers) can be written

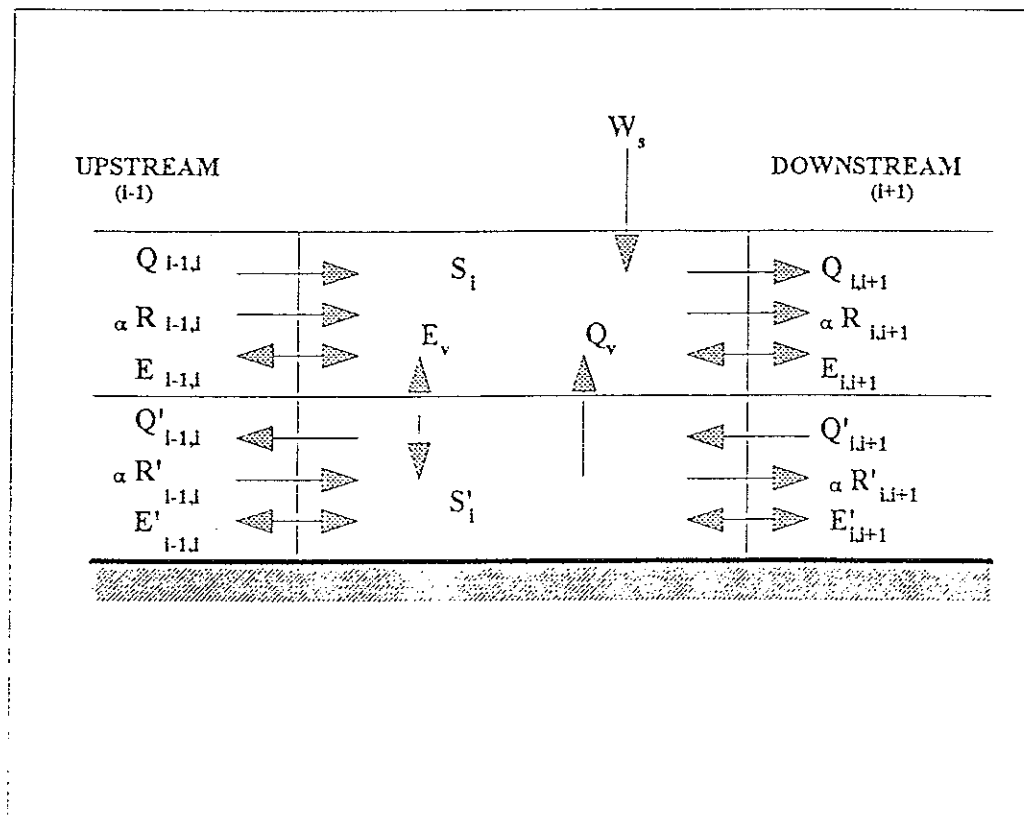
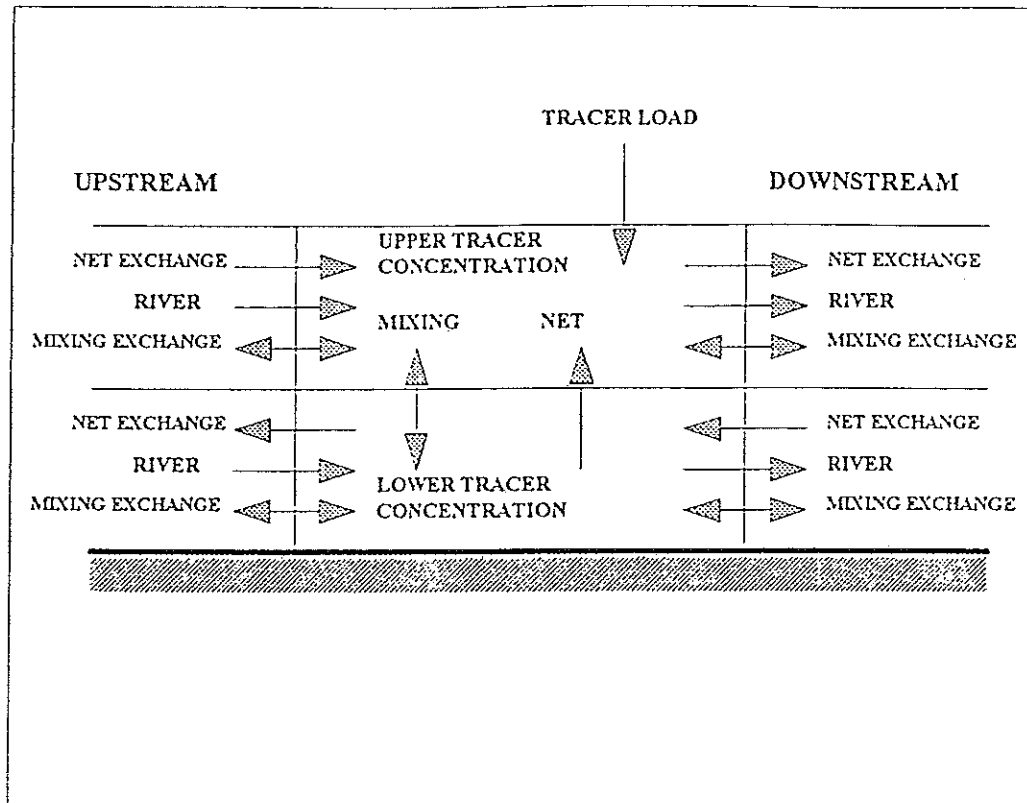


Figure 3.1 Conceptual diagram of hydrodynamic exchanges in the box model.

$$\alpha R_{i-1,j} + Q_{i-1,j} + (1-\alpha)R_{i-1,j} - Q'_{ij-1} = R_{i-1,j} \quad (3.1)$$

which reduces to

$$Q_{i-1,j} = Q'_{ij-1} \quad (3.2)$$

$E_{i,i-1}$ and $E'_{i,i-1}$ are not included in Equation 3.1 since $E_{i,i-1}$ equals $E_{i-1,j}$ and $E'_{i,i-1}$

equals $E'_{i-1,j}$ and they therefore cancel each other. Similar equations for flow across the downstream face of the box reduces to

$$Q_{i+1,j} = Q'_{ij+1} \quad (3.3)$$

These equations (3.2 - 3.3) remain valid regardless of the direction of river flow, e.g., $Q_{i+1,j} = Q'_{i,i+1}$ is the same as $Q_{i,i+1} = Q'_{i+1,j}$. Writing the tracer conservation equation for box i upper layer yields

$$\begin{aligned} V_i \frac{dS_i}{dt} = & W_s + (\alpha R_{i-1,j} + Q_{i-1,j}) S_{i-1} \\ & - (\alpha R_{ij-1} + Q_{ij-1}) S_i + E_{i-1,j}(S_{i-1} - S_i) \\ & + E_{ij-1}(S_{i-1} - S_i) + E_v(S'_i - S_i) + Q_v S'_i = 0 \end{aligned} \quad (3.4)$$

if the river flow is from box i-1 through box i to box i+1.

It should be noted that the introduction of additional tracer material into a box must be accounted for which is done here with the load W_s .

Following our one-dimensional example Equation 3.4 can be generalized for direction by the introduction of the flow direction parameter, δ , and by noting that flow continuity for

the upper layer of the box can be expressed as the sum of all the flows entering and leaving the upper layer:

$$\begin{aligned} & (\alpha R_{ij-1} + Q_{ij-1}) [\delta_{i-1} - (1-\delta_{i-1})] \\ & - (\alpha R_{ij+1} + Q_{ij+1}) [\delta_{i+1} - (1-\delta_{i+1})] + Q_v = 0 \end{aligned} \quad (3.5)$$

The nonadvective exchanges, E and E_v , are not included in Equation 3.5 since each exchange into the box is balanced by an equal exchange out of the box.

Similarly the tracer flux through the upper layer can be written

$$\begin{aligned} & W_s + (\alpha R_{ij-1} + Q_{ij-1}) [\delta_{i-1} S_{i-1} - (1-\delta_{i-1}) S_i] + E_{ij-1} (S_{i-1} - S_i) \\ & - (\alpha R_{ij+1} + Q_{ij+1}) [\delta_{i+1} S_i - (1-\delta_{i+1}) S_{i+1}] + E_{ij+1} (S_{i-1} - S_i) \\ & + Q_v S'_i + E_v (S'_i - S_i) = 0 \end{aligned} \quad (3.6)$$

An equation similar to Equation 3.6 can be formulated for the lower layer of the box as well. However, it is redundant and adds nothing to the solution for the $4N+2$ unknowns. To provide the remaining equations necessary for the solutions, the bulk parameter relating the advective and non-advective components, ϕ is introduced. The value of ϕ ranges from 0 when Q is large and E is 0 to 1 when E is large and Q is 0. At ϕ equal to zero the equations reduce to the set presented by Thomann and Mueller (1987). Following Officer (1980), assuming Q is 0 and solving the tracer conservation equation for exchange the downstream face of the upper layer of the box and introducing $\delta_i^m = (1-\delta_i)$, results in

$$E_{ij-1} = \frac{W_s + \phi [\alpha R_{ij-1} (\delta_{i-1} S_{i-1} - \delta_{i-1}^m S_i) - \alpha R_{ij+1} (\delta_{i+1} S_i - \delta_{i+1}^m S_{i+1})] + E_{ij-1} (S_{i-1} - S_i)}{(S_i - S_{i+1})} \quad (3.7)$$

This procedure can be repeated to solve for E and E' on each side of the box (remembering that $E_{i,i+1} = E_{i+1,i}$) to generate the additional equations needed to solve for the unknowns.

In general form for an N sided box, the exchange between box i and j can be written:

$$E_{ij} = \frac{W_i + \sum_{a=1, a \neq i}^N \{S_a[\delta_{ia}(\alpha R_{ia} + Q_{ia}) + E_{ia}] - S_i[\delta_{ia}^m(\alpha R_{ia} + Q_{ia}) + E_{ia}]\}}{(S_i - S_j)} + \frac{(\alpha R_{ij} + Q_{ij}) - (S_i \delta_{ij} - S_i \delta_{ij}^m)}{(S_i - S_j)} \quad (3.8)$$

The equation for E and E' are now in terms of S and R which are known inputs. Solutions for Q, Q', Q_v and E_v are then found which are also in terms of S and R.

3.2.1.2 Hydrodynamic Model Calculated Exchange Coefficients

One of the interesting considerations for the predicted circulation in the lake is the estimation of what effect the various forces that move water have on the mixing and net transport of constituents. The two largest of these forces are river flow and the wind induced flow, the latter can be broken down into the direct wind induced motion and the motion associated with the complicated internal seiche dynamics. The river induced flow may be thought of entirely as transport, (no mixing due to its predominantly steady state) for the present application and as such is straightforward to calculate. The mixing and transport associated with the inherently dynamic nature of the wind on, the other hand, is more complex. Once a hydrodynamic simulation has been run for a certain time period a postprocessor can be used to calculate the exchange rate coefficients and transport that are associated with that period. The calculations necessarily use the same grid as the hydrodynamic model and therefore a value for both exchange coefficient and net transport are determined for each grid cell and layer on which the hydrodynamics simulation calculated currents.

For the net transport calculation the current vector components of a cell, multiplied by the layer depth of that cell, are summed in the east and north directions in positive and negative bins to generate total per unit width positive and negative transport components in the east and in the north directions, respectively. The sums are averaged to determine a mean positive and a mean negative value. The mean net transport in the east-west direction is then the difference between the positive (east) and negative (west) mean vector components multiplied by the cell width in the north-south direction as given in equation (3.9).

$$T_{east} = \left[\frac{\sum_1^N HU_+ + \sum_1^N HU_-}{N} \right] \Delta y \quad (3.9)$$

where

- T_{east} = mean net east-west transport (m^3/s)
- H = layer depth (m)
- U_+ = east velocity vector component (m/s)
- U_- = west velocity vector component (m/s)
- N = number of points in the time series (-)

The same method is followed for the north-south component equation (2.11).

$$T_{north} = \left[\frac{\sum_1^N HV_+ + \sum_1^N HV_-}{N} \right] \Delta x \quad (3.10)$$

where

- T_{north} = mean net north-south transport (m^3/s)
- V_+ = north vector in the east-west direction (-)
- V_- = south velocity vector component (m/s)
- Δx = east-west cell width (m)

The two components then determine the vector quantity for each cell and layer (equation 3.11).

$$T_{net} = \langle T_{east} \hat{i}, T_{north} \hat{j} \rangle \quad (3.11)$$

where

- T_{net} = mean net transport vector (m^3/s)
- \hat{i} = unit vector in the east-west direction (-)
- \hat{j} = unit vector in the north-south direction (-)

The mean exchange coefficients are determined in a manner similar to the transport calculation. Once the mean positive and mean negative transport have been calculated the exchange coefficient is determined by definition as the magnitude of the transport that flows equally in both directions. Equations 3.12 and 3.13 shows the calculation method for the east-west and north-south components respectively.

$$E_{e-w} = \min \left\| \frac{\sum_1^N HU_+}{N}, \frac{\sum_1^N HU_-}{N} \right\| \Delta y \quad (3.12)$$

$$E_{n-s} = \min \left\| \frac{\sum_1^N HU_+}{N}, \frac{\sum_1^N HU_-}{N} \right\| \Delta x \quad (3.13)$$

where

E_{e-w} = mean hydrodynamic exchange in the east-west direction (m^3/s)
 E_{n-s} = mean hydrodynamic exchange in the north-south direction (m^3/s)

The mean hydrodynamic exchange components calculated in equations 3.12 and 3.13 can be used to calculate the exchange coefficients, for use in the water quality model, once the study domain has been segmented. The exchange coefficient between two segments is calculated by integrating the normal component of exchange along the segment boundary. For example, if the segment boundary runs along a north-south path then the east-west mean exchanges would be integrated along that line for the inter-segment exchange coefficient. For segment boundaries not aligned with either axis, the larger resultant value of the two components projected onto the normal would be used. Some examples of exchange coefficients calculated for Lake Champlain are presented in section 3.3.2.2.

3.2.2 Conservation of Constituent Mass

To solve for a constituent concentration, C , in each box, the conservation of constituent mass equation is written for each of the constituents in both the upper and lower layers. The EPA WASP model kinetic rate equations are then integrated into the box model formulation to simulate the phosphorus cycle term interaction. Additional terms are included to allow for flux in (loading), flux out and settling as shown in Figure 3.2. For the upper layer of box i , the conservation of constituent equation becomes

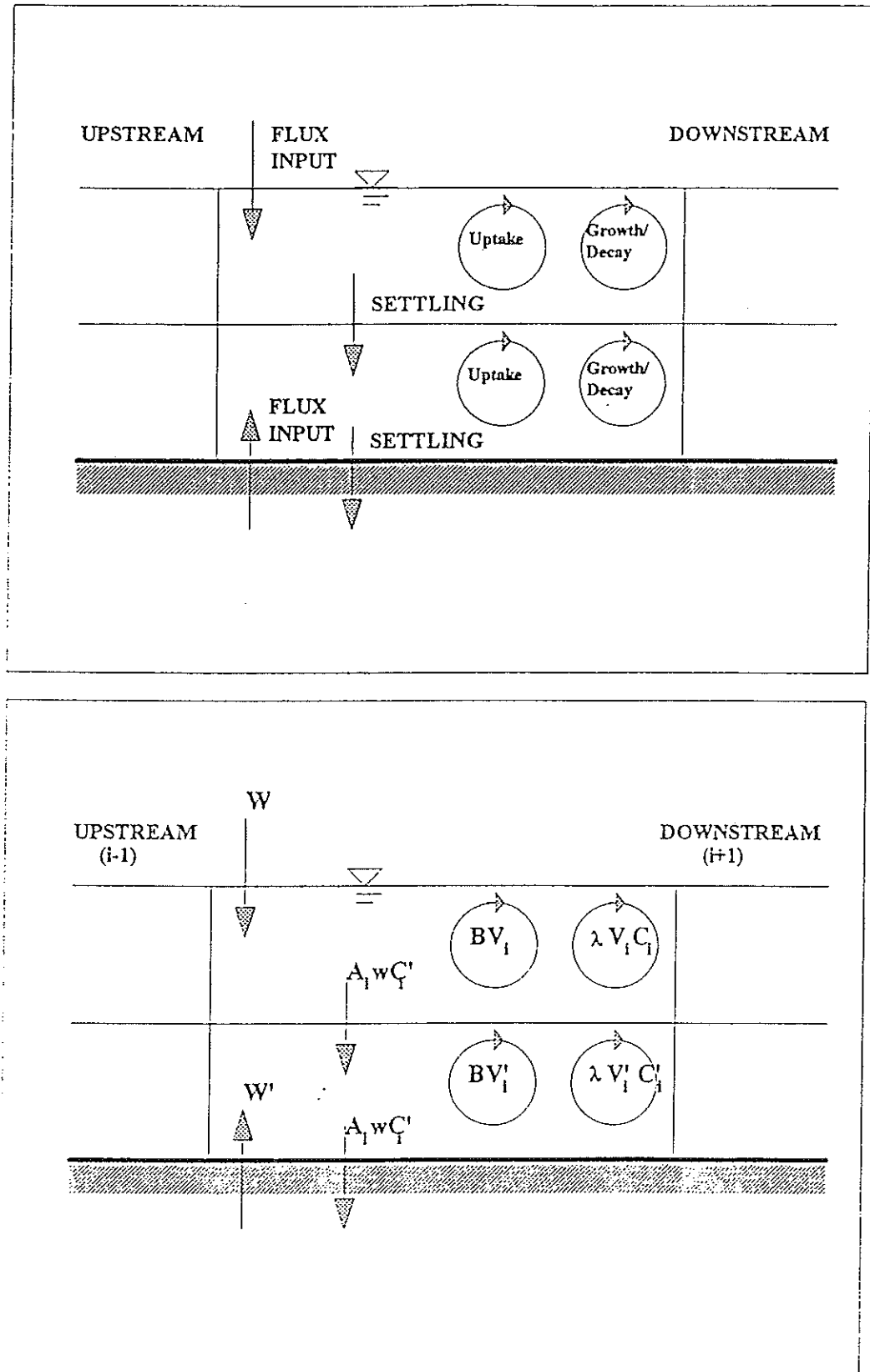


Figure 3.2 Conceptual diagram of non-exchange mechanisms affecting concentration.

[illegible]

$$\begin{aligned}
V_i \frac{dC_i}{dt} = & (\alpha R_{ij-1} + Q_{ij-1}) [\delta_{i-1} C_{i-1} - (1-\delta_{i-1}) C_i] + E_{ij-1} (C_{i-1} - C_i) \\
& - (\alpha R_{ij+1} + Q_{ij+1}) [\delta_{i+1} C_i - (1-\delta_{i+1}) C_{i+1}] + E_{ij+1} (C_{i+1} - C_i) \\
& + Q_v C_i + E_v (C'_i - C_i) + W_i - BV_i - \lambda C_i V_i - A_w C_i = 0
\end{aligned} \tag{3.14}$$

The additional terms are defined as

- W_i = flux input or output of constituent (mass/time)
- BV_i = uptake of constituent, where
- B = mass uptake rate (mass/volume/time)
- V_i = volume of the upper layer of the box
- $\lambda C_i V_i$ = exponential growth/decay of constituent, where
- λ = exponential growth/decay rate (1/time)
- V_i = volume of the upper layer of the box
- $A_{iw} C_i$ = settling of constituent, where
- A_i = cross-sectional area between upper and lower layers of the box
- w = settling velocity (distance/time)

For simplicity the area over which settling occurs on the bottom of the box is assumed equal to the horizontal area of the thermocline, through which the constituent can settle from the upper to the lower layer. The same is true for settling from the lower layer to the sediment layer.

Equation 3.14 can be recast into a form more amenable to solution by grouping the terms associated with the concentration in each adjacent box. Again for our one-dimensional example Equation 3.14 becomes

$$\begin{aligned}
& (\delta_{i-1} \alpha R_{ij-1} + \delta_{i-1} Q_{ij-1} + E_{ij-1}) C_{i-1} + [\delta_{i+1}^m \alpha R_{ij+1} + \delta_{i+1}^m Q_{ij+1} + E_{ij+1}] C_{i+1} \\
& + (Q_v + E_v) C'_i + W_i - BV_i - [\delta_{i-1}^m \alpha R_{ij-1} + \delta_{i-1}^m Q_{ij-1} + E_{ij-1} \\
& + \delta_{i+1} \alpha R_{ij+1} + \delta_{i+1} Q_{ij+1} + E_{ij+1} + E_v + \lambda V_i + A_{iw}] C_i = 0
\end{aligned} \tag{3.15}$$

Equation 3.10 is of the form

$$AC_{i-1} + BC_{i+1} + CC'_i + D = EC_i \tag{3.16}$$

where A through E are algebraic combinations of river flow, advective exchanges, and the addition flux terms described above. It can be seen that the concentration in a box is affected by the concentration in each adjacent box, in addition to flux inputs and losses of the constituent. Equation 3.16 is used to iteratively solve for constituent concentrations using a successive-over-relaxation technique for steady state simulations and an explicit time stepping method for transient cases (Roache, 1976).

The constituent kinetics are all contained in terms D and E of Equation 3.16. The box model has been set up to solve for four constituents; a tracer, total organic phosphorus, total inorganic phosphorus and phytoplankton. For the tracer constituent the simple kinetics described above are used. For the phosphorus and phytoplankton, term D is replaced by the WASP5 kinetic rate equations. The WASP kinetics are described more fully below.

3.2.3 Phosphorus Cycle Kinetics

Although total phosphorus inputs may be suitable for a first order estimation of lake eutrophication, the problem remains that a large portion of the input total is associated with the particulate matter that rapidly settles out after entering the lake (see Figure 3.3). It is clear that this fraction of the total would have little effect on mid lake productivity. To analyze this and other effects that influence phosphorus concentrations and lake trophic status such as phytoplankton-phosphorus interactions, a model needs to differentiate between the various forms of phosphorus.

The phosphorus cycle used here models three variables; organic phosphorus, inorganic (orthophosphate) phosphorus and phytoplankton phosphorus. The organic and inorganic phosphorus variables are partitioned into dissolved and particulate fractions based on the total and a designated fraction for each. Both organic and inorganic phosphorus are coupled to phytoplankton through basic biological functions (see Figure 3.4). Dissolved inorganic or "available" phosphorus is taken up by phytoplankton growth and returned from the phytoplankton biomass to both dissolved and particulate organic and dissolved inorganic phosphorus through endogenous respiration and mortality. A temperature dependent fraction of the organic phosphorus also undergoes a biologically driven mineralization into dissolved inorganic phosphorus. The set of coupled phosphorus cycle rate equations are presented below with a brief description of the variables. The interested reader is referred to the

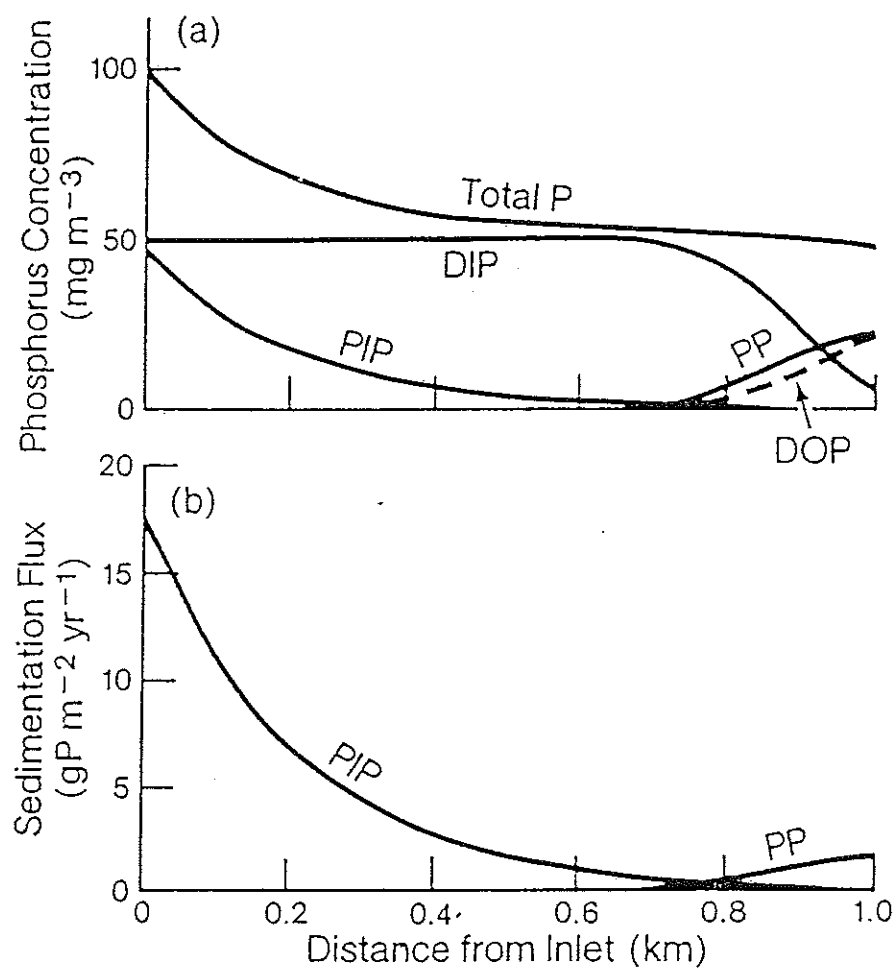


Figure 3.3 Phosphorus concentration and sedimentation flux versus distance from tributary (Chapra and Reckhow, 1983).

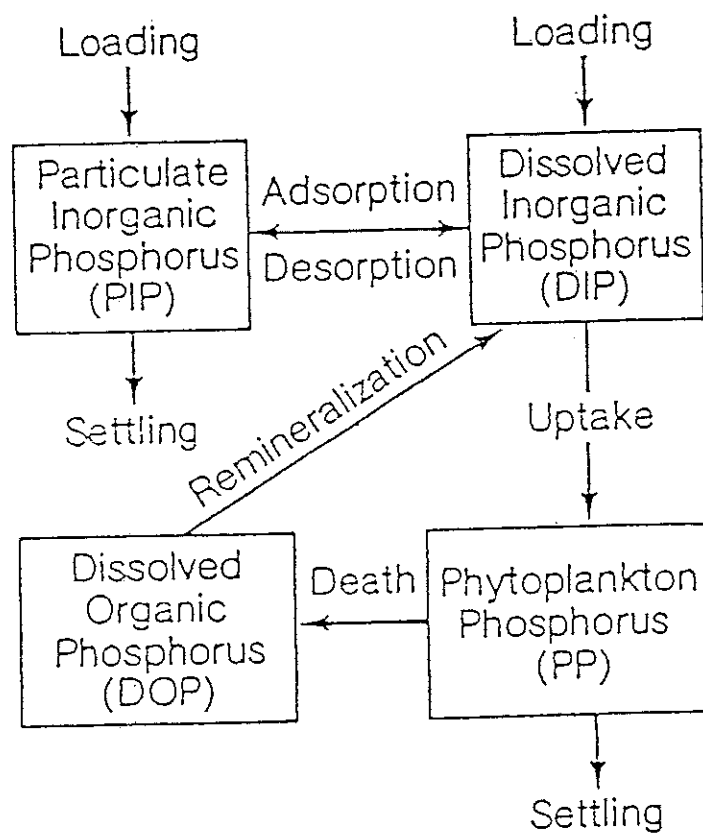


Figure 3.4 Schematic of a multispecies phosphorus model (Chapra and Reckhow, 1983).

Water Quality Analysis Simulation Program, WASP5: Model Documentation (Ambrose et al., 1993) for a more detailed description of the complex kinetics.

The phytoplankton phosphorus rate equation (i.e., the change in phosphorus as phytoplankton biomass with time) may be written as:

$$\frac{\partial(C_4 a_{PC})}{\partial t} = \underset{\text{growth}}{G_{PI} a_{PC} C_4} - \underset{\text{death}}{D_{PI} a_{PC} C_4} - \underset{\text{settling}}{\frac{v_{S4}}{D} a_{PC} C_4} \quad (3.17)$$

where

- C_4 = phytoplankton population, (mg Carbon/l)
- a_{PC} = phosphorus to carbon ratio, (mg P/mg C)
- t = time, (days)
- G_{PI} = specific phytoplankton growth rate, (1/day)
- D_{PI} = phytoplankton loss rate, (1/day)
- v_{S4} = settling velocity, (m/day)
- D = segment depth, (m)

The growth rate is a function of temperature, light limitation and nutrient limitation given by

$$G_{PI} = K_{IC} \theta_{IC}^{(T-20)} X_{RI} \left(\frac{DIP}{K_{mp} + DIP} \right) \quad (3.18)$$

where

- K_{IC} = maximum growth rate, (1/day)
- θ_{IC} = temperature coefficient
- T = temperature, (°C)
- X_{RI} = light limitation factor
- K_{mp} = half-saturation constant for phosphorus, (mg P/l)
- DIP = dissolved inorganic phosphorus, (mg P/l)

The light limitation factor X_{RI} takes into account the seasonal, depth and turbidity-induced light attenuation effects and supersaturation (photoinhibition) effects on phytoplankton population growth. The user has a choice of two similar light modeling formulations; from DiToro et al. (1971) and Smith (1980). Equation 3.19 presents the formulation developed by DiToro et al. which averages conditions over a given depth and over a fixed interval of time (one day in the present units)

$$X_{RI} = \frac{e}{K_e D} f \left[\exp \left\{ -\frac{I_a}{I_s} \exp(-K_e D) \right\} - \exp \left(-\frac{I_a}{I_s} \right) \right] \quad (3.19)$$

where

- e = natural base of logarithms = 2.71828...
- K_e = light extinction coefficient, (1/m)
- I_a = average daily surface solar radiation, (langley/day)
- I_s = saturation light intensity, (langley/day)
- f = fraction of the day that is daylight

A clearer representation of the variable described above may be found in the graphical comparison of actual variation in solar radiation over a day and the average value as shown in Figure 3.5 (from Thomann and Mueller 1987).

As an alternative the similar formulation developed by Smith (1980) as shown below in equation 3.20 may be used.

$$X_{RI} = \frac{e}{K_e D} \left[\exp \left\{ -\frac{I_o}{I_s} \exp(-K_e D) \right\} - \exp \left(-\frac{I_o}{I_s} \right) \right] \quad (3.20)$$

where

- I_o = time variable incident light intensity, (langley/day)

which is calculated within the model, from the total daily solar radiation and the fraction of sunlight per day, as a half sine curve.

The phytoplankton death plus respiration is modeled as a function of temperature and is given by:

$$D_{PI} = K_{IR} \theta_{IR}^{T-20} + K_{ID} + K_{IG} Z \quad (3.21)$$

where

- K_{IR} = endogenous respiration, (1/day)
- θ_{IR} = temperature coefficient, (-)
- K_{ID} = death rate, (1/mg C-day)
- K_{IG} = grazing rate, (1/mg C-day)
- Z = herbivorous zooplankton population grazing on phytoplankton, (mgC/l)

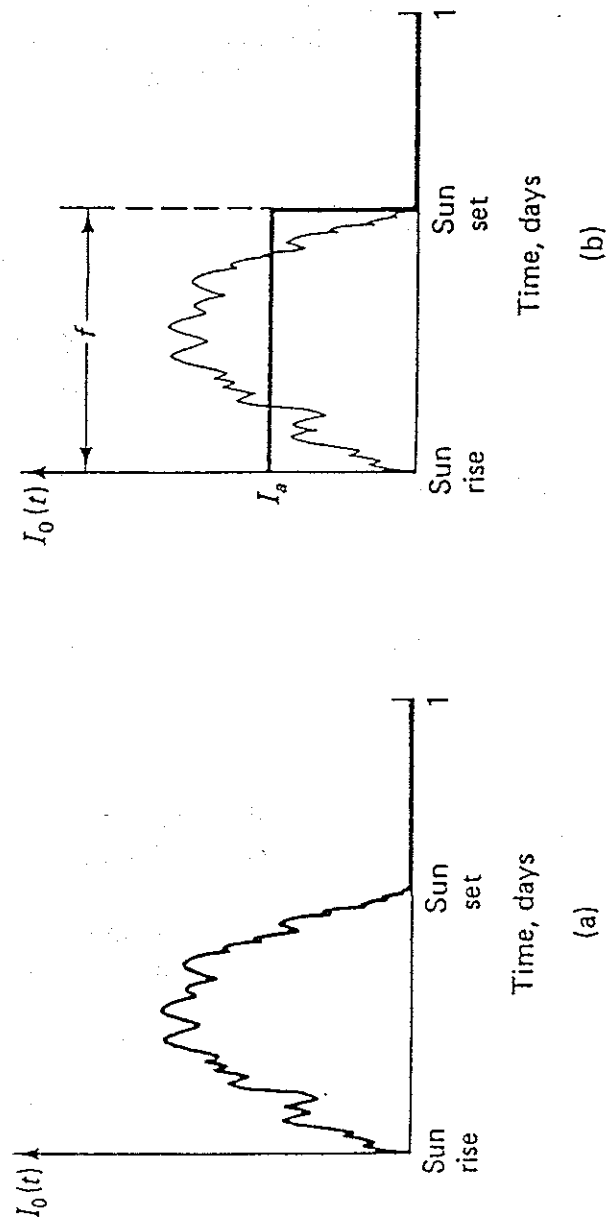


Figure 3.5 Actual and approximate solar radiation (Thomann and Mueller, 1983).

The kinetic rate of change of organic phosphorus in the system is given by:

$$\frac{\partial C_8}{\partial t} = \underbrace{D_{PI} a_{PC} f_{OP} C_4}_{\text{phytoplankton death}} - \underbrace{K_{83} \theta_{83}^{T-20} \left(\frac{C_4}{K_{mPC} + C_4} \right) C_8}_{\text{mineralization}} - \underbrace{\frac{v_{S8}}{D} (1-f_{D8}) C_8}_{\text{settling}} \quad (3.22)$$

where

- C_8 = organic phosphorus concentration, (mg/l)
- f_{OP} = fraction of dead and respired phytoplankton recycled to organic phosphorus
- K_{83} = dissolved organic phosphorus mineralization rate at 20°C, (1/day)
- θ_{83} = temperature coefficient
- K_{mPC} = half saturation constant for phytoplankton limitation of phosphorus recycle, (mg C/l)
- v_{S8} = organic matter settling velocity, (1/day)
- f_{D8} = fraction organic phosphorus in the water column that is dissolved

The remainder of the constants and variables are as previously designated.

Finally, the inorganic phosphorus kinetic rate of change equation is given by:

$$\frac{\partial C_3}{\partial t} = \underbrace{D_{PI} a_{PC} (1-f_{OP}) C_4}_{\text{death}} + \underbrace{K_{83} \theta_{83}^{T-20} \left(\frac{C_4}{K_{mPC} + C_4} \right) C_4}_{\text{mineralization}} - \underbrace{G_{PI} a_{PC} C_4}_{\text{growth}} - \underbrace{\frac{v_{S3}}{D} (1-f_{D3}) C_3}_{\text{settling}} \quad (3.23)$$

where

- C_3 = inorganic phosphorus concentration (mg/l)
- $(1-f_{OP})$ = fraction of dead and respired phytoplankton recycled to the inorganic phosphorus pool
- v_{S3} = inorganic sediment settling velocity, (m/day)
- f_{D3} = fraction inorganic phosphorus in the water column that is dissolved

A summary of all of the assignable rate equation constants and coefficients and the value for each reported in the WASP manual is given in Table 3.1. Nomenclature consistent with the WASP documentation has been retained here and in the model program code for easier reference and greater user accessibility.

Table 3.1 Phosphorus cycle kinetic rate equations terms (Ambrose et al., 1993).

Phytoplankton Net Growth Terms		Exogenous Variables	
Description	Notation	Values	Units
Extinction Coefficient	K_e	0.1-5	m^{-1}
Segment Depth	D	0.1-30	m
Water Temperature	T	0-35	$^{\circ}C$
Fraction of day that is daylight	f	0.3-0.7	---
Average Daily Surface Solar Radiation	I_s	200-750	langleys/day
Zooplankton Population	Z	0	mgC/L
Rate Constants			
Maximum Growth Rate	K_{lc}	2.0	day^{-1}
Temperature Coefficient	θ_{lc}	1.068	---
Maximum Photosynthetic Quantum Yield	Φ_{max}	720.0	mg C/mole photon
Phytoplankton Self-Light Attenuation	K_e	0.017	$m^2/mg \text{ Chl } a$
Carbon-Chlorophyll Ratio	θ_c	20-50	---
Saturating Light Intensity	I_s	200-500	langleys/day
Half Saturation Constant for Phosphorus	K_{mPg}	0.001	mgP/l
Endogenous Respiration	K_{IR}	0.125	day^{-1}
Temperature Coefficient	θ_{IR}	1.045	---
Settling Velocity	V_{s4}	0.1	m/day
Death Rate	K_{ID}	0.02	day^{-1}
Grazing Rate	K_{IG}	0	L/mgC-day
Phosphorus Reaction Terms			
Phosphorus to Carbon Ratio	a_{PC}	0.025	mg P/mg C
Dissolved Organic Phosphorus Mineralization at $20^{\circ}C$	K_{83}	0.22	day^{-1}
Temperature Coefficient	θ_{83}	1.08	---
Half Saturation Constant for Phytoplankton Limitation of Phosphorus Recycle	K_{mPC}	1.0	mg C/L
Fraction of Dead and Respired Phytoplankton Recycled to the Organic Phosphorus Pool	f_{OP}	0.5	---
Fraction of Dead and Respired Phytoplankton Recycled to the Phosphate Phosphorus Pool	$(1-f_{OP})$	0.5	---
Fraction Dissolved Inorganic Phosphorus in the Water Column	f_{D3}	0.85, 0.70	---
Organic Matter Settling Velocity	V_{s3}	---	m/day
Inorganic Sediment Settling Velocity	V_{s5}	---	m/day

3.3 Application to Lake Champlain

The control volume approach assumes that the region under consideration, the entire Lake Champlain water body in this case, can be segmented into a number of boxes in which the physical characteristics remain approximately uniform throughout. For a two layer system the thermocline is used to differentiate between the upper and lower layers. Since the calculated mixing exchange coefficients are assumed to be an integrated value over time, mean values of chloride concentration, load and freshwater flow must be specified for each box. The model then solves the equations of continuity and conservation of chloride to calculate the exchange coefficients on the faces of each box. Similarly, for use of the time dependent hydrodynamic model calculations, the output current fields must be integrated over time to determine the mean mixing exchange for the desired period. For the present study the exchange coefficients will be determined by the available chloride data for the lake. A follow up study will focus on the interdependent calibration of the hydrodynamic and water quality models through exchange coefficient determination for specific study periods.

Regardless of the source, these exchange coefficients define the hydrodynamic transport in the system. Since no momentum equations are used in the box model solution, the values calculated represent mean conditions for the period under consideration. The primary forcing mechanisms for mean circulation in the lake is river flow, and although some net circulation may be generated by the internal seiche this component has been ignored at present.

The objective of the water quality model application to Lake Champlain was to test the model's ability to:

- (1) predict meaningful hydrodynamic exchange coefficients from a given system wide conservative tracer, (chloride), mass balance data set;
- (2) reproduce the chloride concentration field in the lake;
- (3) use the calculated exchanges to calibrate the system response to loadings of a non-conservative constituent, phosphorus, over the same period;

The objective here was not to perform a detailed data analysis but rather to estimate and tune the model's skill at reproducing a given data set. This study relied heavily on the comprehensive water, chloride and phosphorus data set collected and analyzed by the combined efforts of the NYSDEC and the VTDEC and presented in Lake Champlain

Diagnostic-Feasibility Study Interim (1992) and Final Reports (1993). The reader is referred to the study report for a complete description of the data set.

The VTDEC/NYSDEC data set has been analyzed and averaged over two different periods. Initially the data was analyzed over the entire two year survey, but based on comparison with long term stream flow gauge data, it was determined that the calendar year 1991 better represented the long term annual mean flows. The 1991 calendar year was therefore selected as a hydrologic "base year" for determining long term average conditions and for subsequent use in the phosphorus modeling effort.

3.3.1 Lake Segmentation

In order to be able to compare results with and build on previous studies the lake segmentation developed by the VTDEC was used. This segmentation divides the lake into thirteen sections based on phosphorus concentration water quality criteria and present conditions. The geographic location and area/coverage of each segment is shown in Figure 3.6. A schematic of the lake segmentation indicating connections between segments, river inputs and net flow directions is shown in Figure 3.7. Table 3.2 presents the model segment morphometric data as developed by the VTDEC.

Table 3.2 Lake model segment morphometric data, and listing of lake sampling stations within each segment, (NYSDEC and VTDEC, 1992).

Segment	Area (km ²)	Volume (km ³)	Mean Depth (m)	Length (km)	Lake Sampling Stations
1. South Lake B	5.79	.0078	1.35	20.1	1, 2
2. South Lake A	43.27	.125	2.89	33.5	3, 5
3. Port Henry	75.55	1.463	19.36	20.1	6, 7
4. Otter Creek	28.49	.955	33.52	10.1	8, 9
5. Main Lake	414.14	16.787	40.53	47.0	10-15, 17-20, 22, 23, 26, 27, 28, 31
6. Shelburne Bay	9.62	.140	14.55	3.4	16
7. Burlington Bay	5.51	.063	11.43	2.0	21
8. Cumberland Bay	10.75	.063	5.86	3.4	33
9. Malletts Bay	55.06	.722	13.11	6.7	24, 25
10. Northeast Arm	248.25	3.380	13.62	33.5	29, 30, 34, 35, 37, 38, 39, 43, 45
11. St. Albans Bay	7.21	.023	3.19	3.4	40, 41

Segment	Area (km ²)	Volume (km ³)	Mean Depth (m)	Length (km)	Lake Sampling Stations
12. Missiquoi Bay	89.94	.205	2.28	16.8	47, 48, 50, 51, 52
13. Isle LaMotte	185.59	1.892	10.19	40.3	32, 36, 42, 44, 46, 49
Total	1179.17	25.826	21.90		

Water, chloride and phosphorus sources to Lake Champlain consist of rivers, municipal and industrial waste water treatment facilities (WWTF), ungaged drainage areas, groundwater inflow and direct precipitation. Outflow from the lake consists of the Richelieu River outlet, direct water withdrawals, evaporation and groundwater outflow. The water, chloride and phosphorus mass balance results for the NYSDEC/VTDEC two year study data set are presented in Table 3.3.

Table 3.3 Water, chloride and total phosphorus budgets for Lake Champlain for the period of March 1990 to February 1992. "ND"="no data", (NYSDEC and VTDEC, 1992).

Source	Water (hm/yr)	Chloride (mt/yr)	Phosphorus (mt/yr)
Inputs			
Gaged Tributaries	11,387	106,980	780
Ungaged Tributaries	552	4,838	29
Direct Wastewater Discharges	52	12,423	57
Direct Precipitation	1085	312	18
Groundwater Inflow	ND	ND	ND
Total Inputs	13, 076	124,553	884
Outputs			
Outlet Flow	12,809	131,933	181
Water Withdrawals	46	549	1
Evaporation	735	0	0
Groundwater Outflow	ND	ND	ND
Total Outputs	13,590	132,482	182
Change in Storage	-701	-7,220	-10
Error/Retention	187	-709	712
(% of Total Inputs)	(1%)	(1%)	(81%)

Mean flow rates and chloride and phosphorus concentration data were determined and tabulated for the entire 2 year survey and for the hydrologic "base year". These flow rates and concentrations were then grouped geographically according to which segment would receive their input. For clarity these data are presented here as Table 3.4 and 3.5. For the

Table 3.4 Model input data for gaged tributaries, ungaged areas, and direct wastewater treatment facility (WWTF) discharges, for the period of March 1990 to February 1992, (NYSDEC and VTDEC, 1993).

Segment/Source	Flow (hm ³ /yr) Mean	Chloride (mg/l) Mean	Tot. P (µg/l) Mean	Diss P. (µg/l) Mean
South Lake B				
Mt. Hope	19	0.8	8	4
Mettawee/Barge Canal	621	11.6	79	28
Poultney	371	10.5	87	22
Ungaged E	16	11.1	80	24
Ungaged W	62	0.8	8	4
Whitehall WWTF	.74	55.0	960	960
South Lake A				
Mill (Putname Sta.)	14	7.3	53	23
East	35	9.2	52	30
LaChute	365	8.4	4	2
Putnam	95	5.5	24	6
Ungaged E	33	9.1	55	34
Ungaged W	48	5.6	23	8
Ticonderoga WWTF	1.3	96.0	1120	1120
International Paper Co. WWTF	24	415.0	340	340
Port Henry				
Mill (Port Henry)	37	9.7	35	7
Hoisington	13	9.5	67	20
Ungaged E	10	9.1	55	34
Ungaged W	66	9.6	43	9
Port Henry WWTF	.81	56.0	1920	1920
Westport WWTF	.12	78.0	1810	1810
Otter Creek				
Otter	1427	9.7	99	61
Little Otter	80	11.0	122	75
Lewis	116	7.4	89	26
Ungaged E	12	9.5	98	58
Ungaged W	2.3	9.5	62	18
Vergennes WWTF	.65	70.0	700	700
Main Lake				
Bouquet	361	9.3	60	11
Highlands Forge	12	7.7	12	5
Winooski	2003	12.3	77	12
Ausable	804	5.8	30	7
Little Ausable	84	9.5	55	24
Salmon	62	5.8	32	12
Ungaged E	18	12.3	74	12
Ungaged W	55	6.9	34	9
Burlington North WWTF	1.8	71.0	1910	1910

Table 3.4 continued.

Segment/Source	Flow (hm ³ /yr) Mean	Chloride (mg/l) Mean	Tot. P (µg/l) Mean	Diss. P. (µg/l) Mean
Shelburne Bay				
LaPlatte	58	27.0	253	190
Ungaged E	16	27.0	254	190
Shelburne F.D. #2 WWTF	.38	119.0	700	700
Shelburne F.D. #1 WWTF	.42	101.0	670	670
So. Burlington Bar. Bay	1.0	118.0	580	580
WWTF				
Burlington Bay				
Ungaged E	1.3	27.0	254	190
Burlington Main WWTF	5.4	104.0	2120	2120
Cumberland Bay				
Saranac	877	5.4	22	8
Ungaged W	58	5.2	21	8
Plattsburgh City WWTF	11.5	76.0	1740	1740
Plattsburgh/Champlain Park	.18	150.0	1620	1640
WWTF				
Mallets Bay				
Indian	15	43.2	81	17
Malletts	40	14.9	63	23
Lamoille	1423	8.8	33	11
Ungaged E	34	9.3	35	11
Northeast Arm				
Stone Bridge	13	17.6	86	34
Ungaged E	40	17.5	83	34
St. Albans Bay				
Mill	39	25.9	135	62
Stevens	16	61.4	238	101
Ungaged E	2.8	35.2	155	71
St. Albans City WWTF	2.9	78.0	270	270
Northwest Correctional WWTF	.02	56.0	170	170
Missiquoi Bay				
Missiquoi	1534	6.5	72	18
Rock	85	9.8	353	100
Pike	347	11.9	173	68
Ungaged	43	7.6	105	31
Swanton WWTF	1.0	112.0	2380	2380
Isle Lamotte				
Little Chazy	56	14.3	74	54
Great Chazy	366	10.1	52	19
Ungaged W	34	10.5	50	24
Wyeth-Ayerst, Chazy WWTF	0.054	466.0	83800	83800

Table 3.5 Model input data for gaged tributaries, ungaged areas, and direct wastewater treatment facility (WWTF) discharges, for the hydrologic base year, January 1991 - December 1991, (NYSDEC and VTDEC, 1993).

Segment/Source	Flow (hm ³ /yr) Mean	Chloride (mg/l) Mean	Tot. P (µg/l) Mean	Diss P. (µg/l) Mean
South Lake B				
Mt. Hope	13	.8	7	4
Mettawee/Barge Canal	487	12.1	76	24
Poultney	273	11.3	62	19
Ungaged E	12	11.7	92	22
Ungaged W	44	.8	8	4
Whitehall WWTF	.74	55	960	960
South Lake A				
Mill (Putname Sta.)	9.0	7.7	47	24
East	24	9.3	53	30
LaChute	273	8.4	4	2
Putnam	67	6.3	19	6
Ungaged E	23	9.3	50	33
Ungaged W	33	6.5	20	1120
Ticonderoga WWTF	1.3	96.0	1120	340
International Paper Co. WWTF	24	415.0	340	
Port Henry				
Mill (Port Henry)	25	10.9	25	7
Hoisington	9.6	10.2	50	19
Ungaged E	7.1	9.3	54	33
Ungaged W	46	10.7	32	12
Port Henry WWTF	.81	56.0	1920	1920
Westport WWTF	.12	78.0	1810	1810
Otter Creek				
Otter	1119	10.1	98	62
Little Otter	55	11.4	99	64
Lewis	90	7.5	58	20
Ungaged E	9.3	10.0	95	59
Ungaged W	1.7	10.2	52	21
Vergennes WWTF	.65	70.0	700	700
Main Lake				
Bouquet	281	9.9	48	10
Highlands Forge	8.8	7.8	12	4
Winooski	1543	13.2	54	12
Ausable	639	6.3	26	8
Little Ausable	89	9.2	58	23
Salmon	55	5.8	32	12
Ungaged E	14	13.2	54	12
Ungaged W	45	7.5	35	10
Burlington North WWTF	1.8	71.0	1910	1910

Table 3.5 continued

Segment/Source	Flow (hm ³ /yr) Mean	Chloride (mg/l) Mean	Tot. P (μg/l) Mean	Diss. P. (μg/l) Mean
Shelburne Bay				
LaPlatte	44	30.4	270	209
Ungaged E	13	30.4	270	209
Shelburne F.D. #2 WWTF	.38	119.0	700	700
Shelburne F.D. #1 WWTF	.42	101.0	670	670
So. Burlington Bar. Bay	1.0	118.0	580	580
WWTF				
Burlington Bay				
Ungaged E	1.0	30.4	270	209
Burlington Main WWTF	5.4	104.10	2120	2120
Cumberland Bay				
Saranac	776	5.5	21	8
Ungaged W	51	5.5	21	8
Plattsburgh City WWTF	11.5	76.0	1740	1740
Plattsburgh/Champlain Park	.18	150.0	1620	1620
WWTF				
Mallets Bay				
Indian	13	44.5	68	17
Malletts	31	15.5	54	22
Lamoille	1100	9.4	27	10
Ungaged E	26	10.0	28	10
Northeast Arm				
Stone Bridge	10	19.0	76	33
Ungaged E	31	19.0	77	29
St. Albans Bay				
Mill	26	26.4	131	60
Stevens	14	61.5	257	102
Ungaged E	2.1	38.9	176	714
St. Albans City WWTF	2.9	78.0	270	270
Northwest Correctional WWTF	.02	56.0	170	170
Missiquoi Bay				
Missiquoi	1307	6.6	63	18
Rock	69	9.5	401	100
Pike	296	12.0	169	69
Ungaged	36	7.7	96	30
Swanton WWTF	1.0	112.0	2380	2380
Isle Lamotte				
Little Chazy	44	14.4	72	54
Great Chazy	320	10.0	54	20
Ungaged W	29	10.5	56	24
Wyeth-Ayerst, Chazy WWTF	.054	466.0	83800	83800

present study all of the flow rates for a particular segment were summed to create a single input flow rate per segment. The loads were determined by first multiplying the particular source mean flow rate by the mean concentration to create a mean load by source. These individual loads were then summed according to their segment grouping to create a single mean load for each segment. The results for both the 2 year survey and the base year are presented in Tables 3.6 and 3.7, respectively. The loads generated for chloride and total

Table 3.6 Two Year Survey, March - February 1992.

Segment	Box #	Flow (m ³ /s)	Chloride Load (g/s)	TIP Load (g/s)	TOP Load (g/s)	TP Load (g/s)
South Lake B	1	34.56	360.93	0.629	2.034	2.663
South Lake A	2	19.51	465.07	0.323	0.319	0.642
Port Henry	3	4.02	40.01	0.076	0.165	0.241
Otter Creek	4	51.94	499.80	2.281	2.894	5.175
Main Lake	5	107.84	1098.30	0.952	5.831	6.783
Shelburne Bay	6	2.40	69.88	0.356	0.278	0.634
Burlington Bay	7	0.21	18.92	0.159	0.213	0.372
Cumberland Bay	8	30.44	188.31	0.651	0.738	1.389
Malletts Bay	9	47.95	446.56	0.403	1.242	1.645
Northeast Arm	10	1.68	29.45	0.042	0.098	0.141
St. Albans Bay	11	1.93	73.52	0.118	0.212	0.330
Missisquoi Bay	12	63.74	487.76	1.487	5.100	6.587
Ilse LaMotte	13	14.46	154.73	0.359	0.594	0.954
Total		380.68	3933.23	7.837	19.718	27.556

Table 3.7 Hydrologic Base Year, January 1991 - December 1991.

Segment	Box #	Flow (m ³ /s)	Chloride Load (g/s)	TIP Load (g/s)	TOP Load (g/s)	TP Load (g/s)
South Lake B	1	26.31	291.87	0.421	1.361	1.782
South Lake A	2	14.41	428.75	0.294	0.242	0.536
Port Henry	3	2.81	31.18	0.068	0.090	0.158
Otter Creek	4	40.45	404.61	1.776	2.087	3.863
Main Lake	5	84.87	920.59	0.779	3.239	4.019
Shelburne Bay	6	1.86	61.47	0.300	0.203	0.503
Burlington Bay	7	0.20	18.66	0.273	0.098	0.372
Cumberland Bay	8	26.59	169.86	0.631	0.658	1.290
Malletts Bay	9	37.10	347.07	0.285	0.761	1.046
Northeast Arm	10	1.30	22.78	0.029	0.071	0.100
St. Albans Bay	11	1.43	58.16	0.124	0.139	0.262
Missisquoi Bay	12	54.19	415.07	1.274	3.997	5.271
Ilse LaMotte	13	12.46	132.89	0.328	0.536	0.865
Total		304.00	3302.97	6.582	13.483	20.066

phosphorus (TP) are straightforward, as described above. Those generated for total organic phosphorus (TOP) and total inorganic phosphorus (TIP) require some explanation.

The first point that needs explanation is the partitioning of phosphorus load into TOP and TIP. Simply, TOP and TIP are two of the three independent variables in the phosphorus model, phytoplankton being the third. Loading values need, therefore, to be specified with that partitioning. In order to estimate the partitioning of TP into TOP and TIP the vertical profile data set from the 2 year survey was used. Of the five vertical profile stations orthophosphate phosphorus (DIP) was measured at three, along with dissolved and total phosphorus (see Table 3.8 for a complete list of phosphorus partitioning abbreviations used here). The arithmetic mean of the total dissolved to orthophosphate ratio (TDP/DIP) was determined for each station. The mean of the three stations was then taken resulting in a TDP/DIP ration of 1.69. This value was then used as a best estimate for phosphorus load partitioning.

Table 3.8 Phosphorus partitioning abbreviations.

TP	Total Phosphorus
TDP	Total Dissolved Phosphorus
DIP	Dissolved Inorganic Phosphorus (Orthophosphate)
DOP	Dissolved Organic Phosphorus
TIP	Total Inorganic Phosphorus
PIP	Particulate Inorganic Phosphorus
TPP	Total Particulate Phosphorus
POP	Particulate Organic Phosphorus
TOP	Total Organic Phosphorus
DOR	Total Dissolved to Orthophosphate Ratio
FD3	Fraction Dissolved Inorganic Phosphorus
Partitioning Equations	
DOR = TDP/DIP	
DIP = TDP/DOR	
DOP = TDP - DIP	
TIP = DIP/FD3	
PIP = TIP - DIP	
TPP = TP - TDP	
POP = TPP - PIP	
TOP = DOP + POP	

For both the 2 year survey and the hydrologic base year, (Tables 3.4 and 3.5) the dissolved phosphorus values were divided by the TDP/DIP ration to obtain DIP. Finally TIP is equal to DIP divided by the fraction dissolved which was taken as the recommended value of 0.8 from the WASP5 users guide. The total organic phosphorus load for each source was determined in a similar manner as summarized in Table 3.8. The total loads of TIP and TOP for each segment were determined by following the same procedure used in the chloride load determination.

The 52 station *in-situ* data set was also processed by the VTDEC to produce time weighted mean concentrations of chloride and total phosphorus by segment for the 2 year survey. The method used compensated for the greater number of samples taken in the summer months so that these values would not skew the data. The results are repeated here in Table 3.9. The chloride concentrations are used to calibrate the exchange coefficient calculations as are the total phosphorus used to calibrate the phosphorus cycle kinetics.

Table 3.9 Mean chloride and total phosphorus concentrations in each lake segment, 1990-1991. C.V. = coefficient of variation of the mean (NYSDEC and VTDEC, 1992).

Segment	Chloride (mg/l)		Total Phosphorus (μ g/l)	
	Mean	C.V.	Mean	C.V.
South Lake B	11.62	.042	57.55	.067
South Lake A	13.47	.045	33.88	.062
Port Henry	11.18	.007	14.97	.048
Otter Creek	10.72	.005	14.58	.050
Main Lake	10.61	.004	11.79	.025
Shelburne Bay	10.89	.008	15.09	.058
Burlington Bay	10.78	.006	13.34	.068
Cumberland Bay	10.18	.012	13.57	.067
Malletts Bay	9.43	.012	9.35	.059
Northeast Arm	9.29	.004	14.23	.024
St. Albans Bay	10.20	.010	23.71	.052
Missisquoit Bay	7.78	.019	35.24	.056
Isle LaMotte	10.33	.006	12.10	.027

3.3.2 Exchange Rate Coefficients

3.3.2.1 Exchange Coefficients from Data

The mean flows and chloride loads developed in the last section (Tables 3.6 and 3.7) were then used, along with the mean *in-situ* chloride concentrations (Table 3.9), to calculate the mixing exchange coefficients at the segment interfaces. A comparison of the results for the 2 year survey load means to the VTDEC exchange calculations is shown in Table 3.10a and to the values for the hydrologic base year in Table 3.10b. The segment designation indicates that the exchange value is given for the downstream (river flow out) face of that segment. Segment 9, Malletts Bay has two outlets, one to the west adjoining the main basin and one to the north adjoining the Northeast Arm (see Figure 3.6 and 3.7). The river flow was partitioned between the two outlets in Malletts Bay following the results of data given in Myer and Gruendling (1979) and the VTDEC analysis which reports that approximately 16% of the flow goes north to the Northeast Arm and the remainder flows to the Main Lake.

Table 3.10a Two year survey data exchange coefficient.

Segment	Box #	VTDEC Exchange (m ³ /s)	ASA Exchange (m ³ /s)
South Lake B	1	23	22
South Lake A	2	40	43
Port Henry	3	444	471
Otter Creek	4	1567	1693
Main Lake	5	281	100
Shelburne Bay	6	153	156
Burlington Bay	7	95	98
Cumberland Bay	8	275	283
Malletts Bay	9	9	5
Malletts Bay	9	2	1
Northeast Arm	10	62	33
St. Albans Bay	11	60	59
Missisquoi Bay	12	9	5
Ilse LaMotte	13	---	---

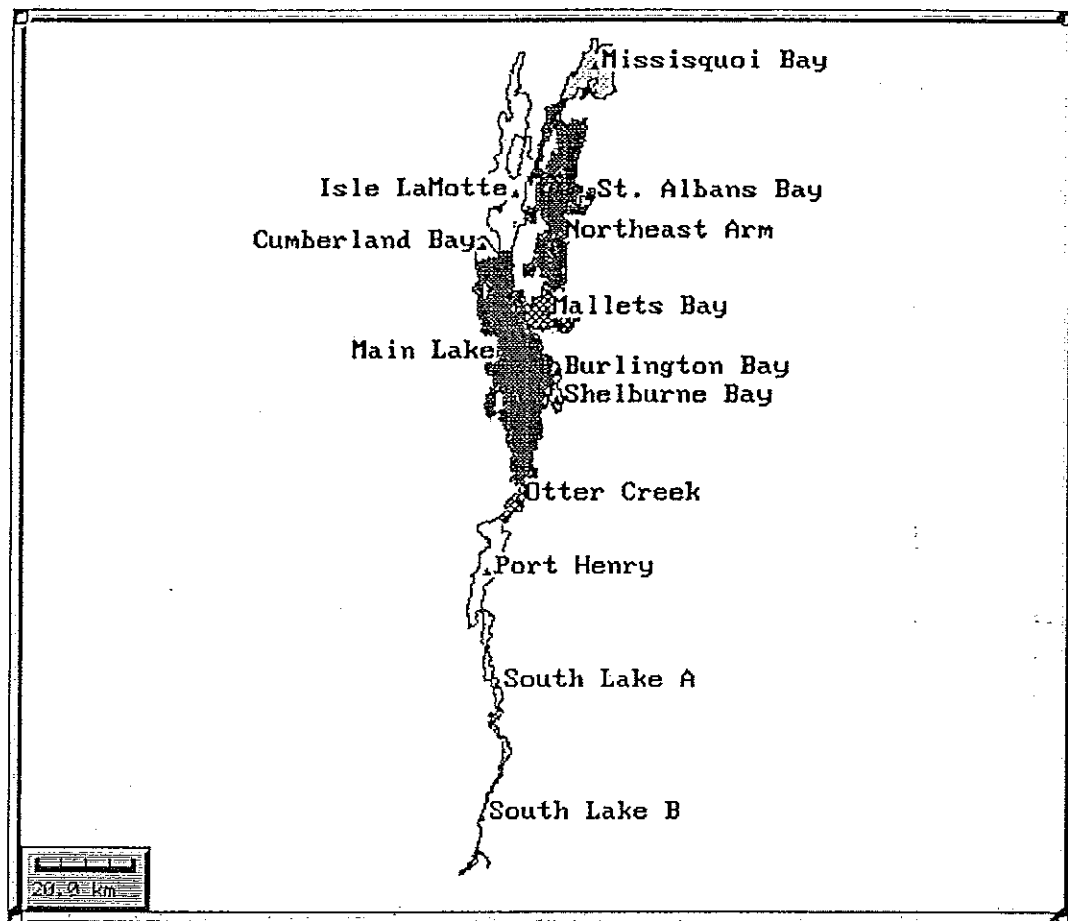


Figure 3.6 Phosphorous model segmentation geography.

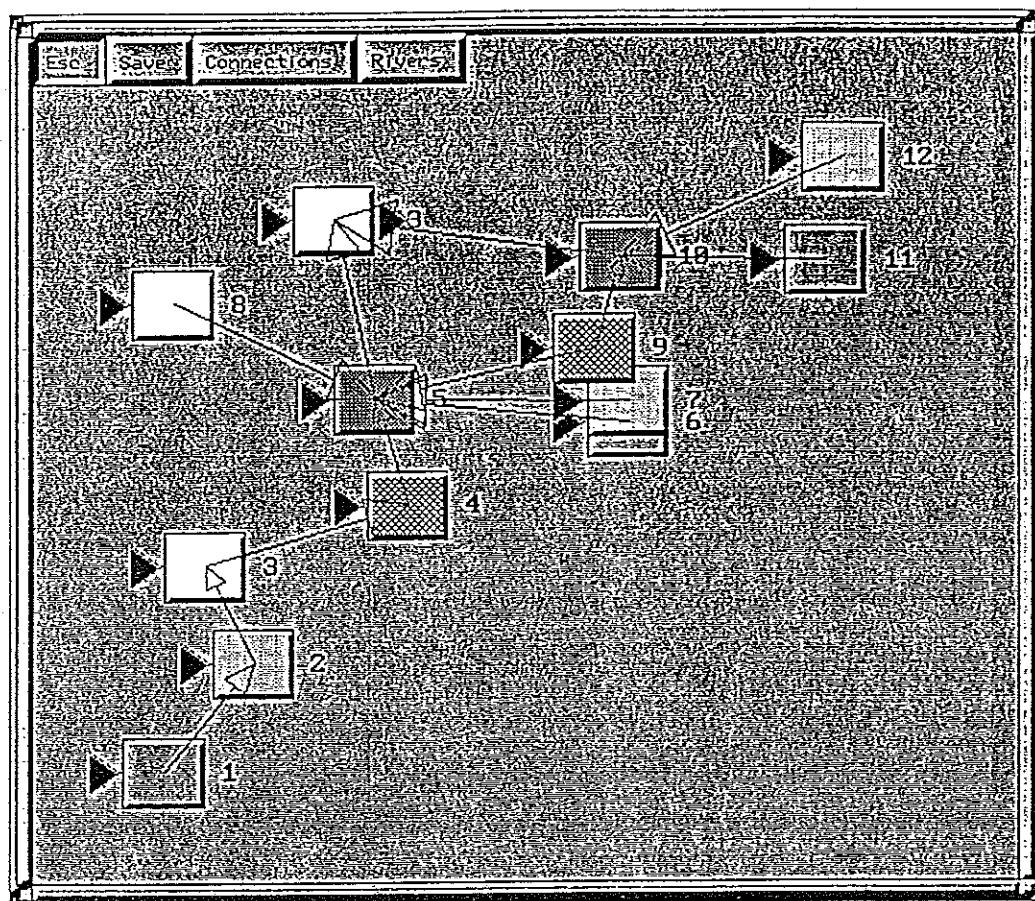


Figure 3.7 Schematic of the model segmentation, connections and net flow path.

Table 3.10b Hydrologic base year vs. two year survey.

Segment	Box #	2 Year Exchange (m ³ /s)	Base Year Exchange (m ³ /s)
South Lake B	1	22	8
South Lake A	2	43	75
Port Henry	3	417	576
Otter Creek	4	1693	2329
Main Lake	5	100	685
Shelburne Bay	6	156	147
Burlington Bay	7	98	97
Cumberland Bay	8	283	235
Malletts Bay	9	5	2
Malletts Bay	9	1	1
Northeast Arm	10	33	31
St. Albans Bay	11	59	48
Missisquoi Bay	12	5	4
Ilse LaMotte	13	---	---

The data from Tables 3.10a and b are plotted in Figures 3.8a and b, respectively. It is clear immediately that the values calculated for the exchange coefficients by the ASA model are very similar to those of the VTDEC model which is reassuring in that similar methods for the exchange calculation are used. This is a good baseline validation for the development and coding of ASA's water quality model.

The largest difference between the ASA and VTDEC calculations lies at the interface between segments 5 and 13, the main lake and Isle LaMotte segment to the north. A relatively small exchange would be expected here, compared to that between segments 4 and 5 for example, in that although the concentration gradient is not particularly large the net river flow rate between segments is, as can be seen in Figure 3.9a. Reviewing equation 3.8 it can be seen that as the river flow out, multiplied by the segment concentration, increases, the difference between that "load" out and the direct and river loads in decreases thereby decreasing the calculated exchange. The effect of the concentration gradient is much more straight-forward. Again referring to equation 3.8 it can be seen that as the difference between the concentration of segment 5 and that of 13 increases, ($S_i - S_{i+1}$, increases), the calculated exchange will decrease. Overall the comparison is quite favorable between the

ASA and VTDEC results. It is clear that the exchange coefficient calculation method used here, based entirely upon the data, is an effective method for use in lakes.

A comparison of calculated exchange coefficients of the hydrologic base year to the 2 year values was also made (Figure 3.9b). The increase in calculated exchanges in the main lake, segments 2 through 5 is attributable to the decreased flow input of the base year data set, as can be seen in Figure 3.9b. The remainder of the differences are not so easily explained. An important point to be made though is that for this analysis the data set is not completely consistent as with the 2 year survey calculations. The flow and load input data set was created from the hydrologic base year means whereas the *in-situ* concentrations of the 2 year survey means were retained. By inspection of the input flow and load data, Table 3.8, and the *in-situ* concentration data, Table 3.9, it can be seen that the total load in of 3303 g/s is greater than the total flow multiplied by the concentration in segment 13, (3140 g/s), by a difference of 163 g/s. Bound by the conservation of tracer mass, the model must also find this difference. The discrepancy can be handled in one of two ways. Left on its own the model will calculate the requisite storage or flushing in order to account for the imbalance (e.g., it could be assumed that the lake is losing an additional 163 g/s, or 15.75 m³/s to volume change, in this case), balancing the mass flux and given concentrations. Ideally, of course, the source of the discrepancy should be found and a balanced input data set created.

3.3.2.2 Hydrodynamic Model Calculated Exchange Coefficients

The method described by equations (2.10-13) was used to estimate the exchange coefficients and net transport in the lake for the better of the summer simulations. The case study 1K_AUG13, described in section 2.3.2, was chosen for its closer agreement with the observations. The current vector components, surface elevation and layer thickness were stored for each cell and layer at 1 day intervals.

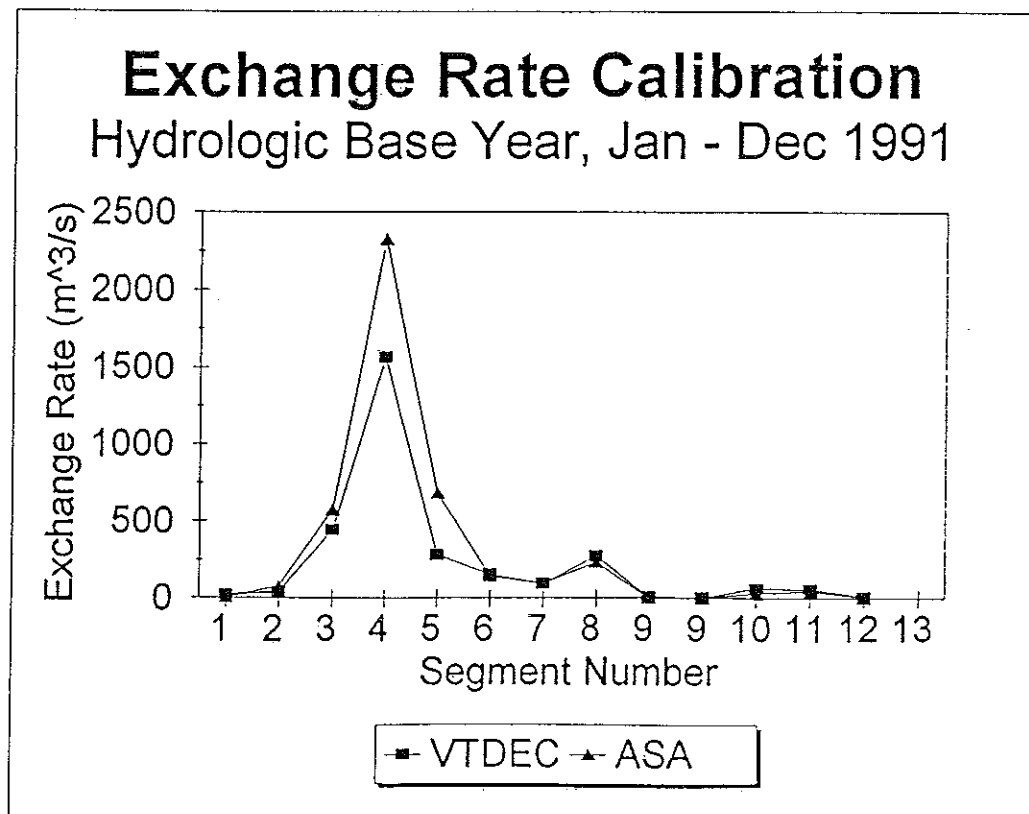
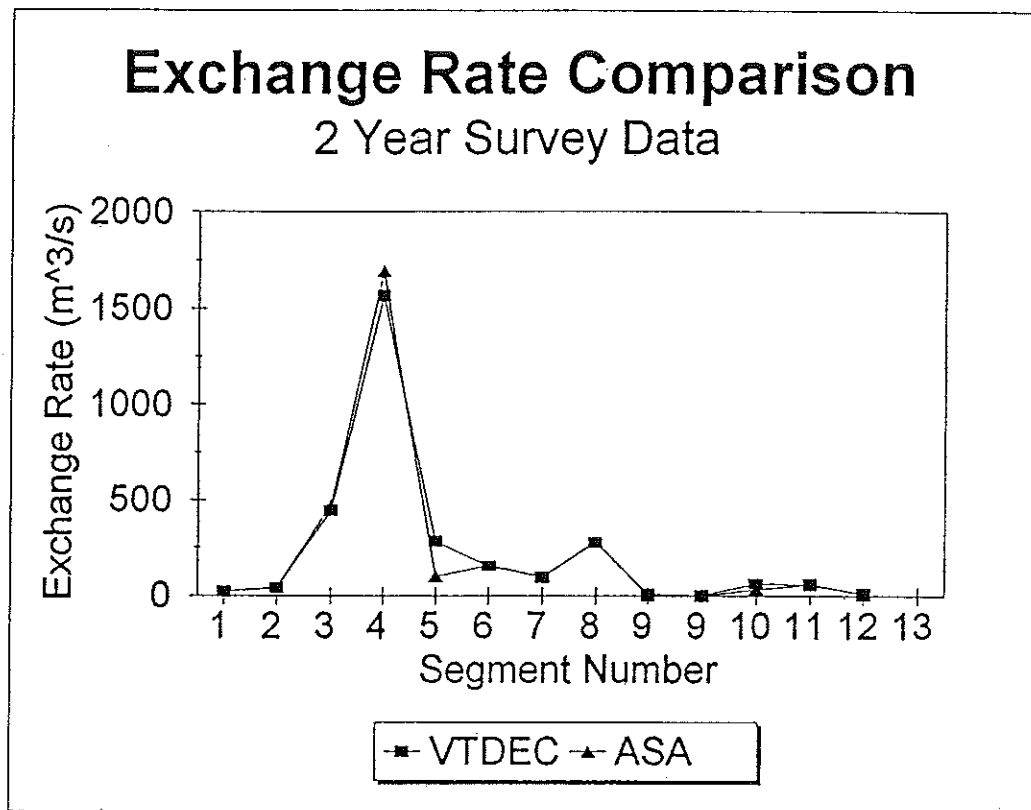


Figure 3.8 Comparison of mixing exchange coefficient calculations (a) VTDEC calculations versus ASA calculations (b) hydrologic base year versus 2 year data.

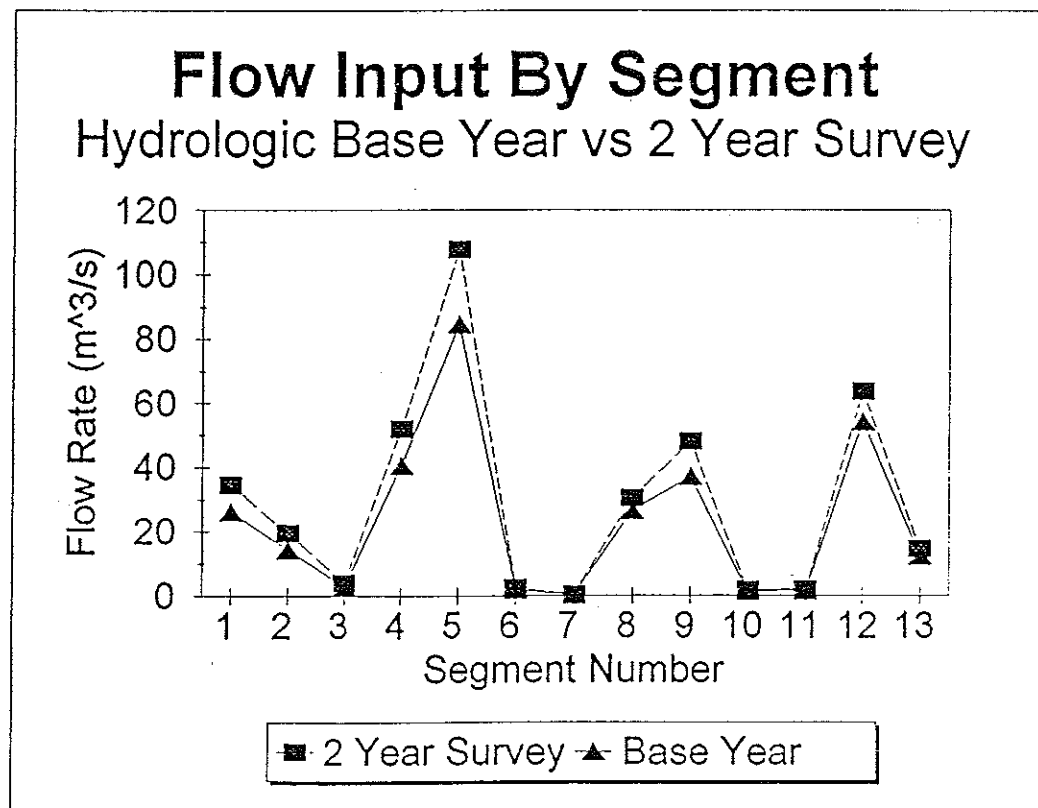
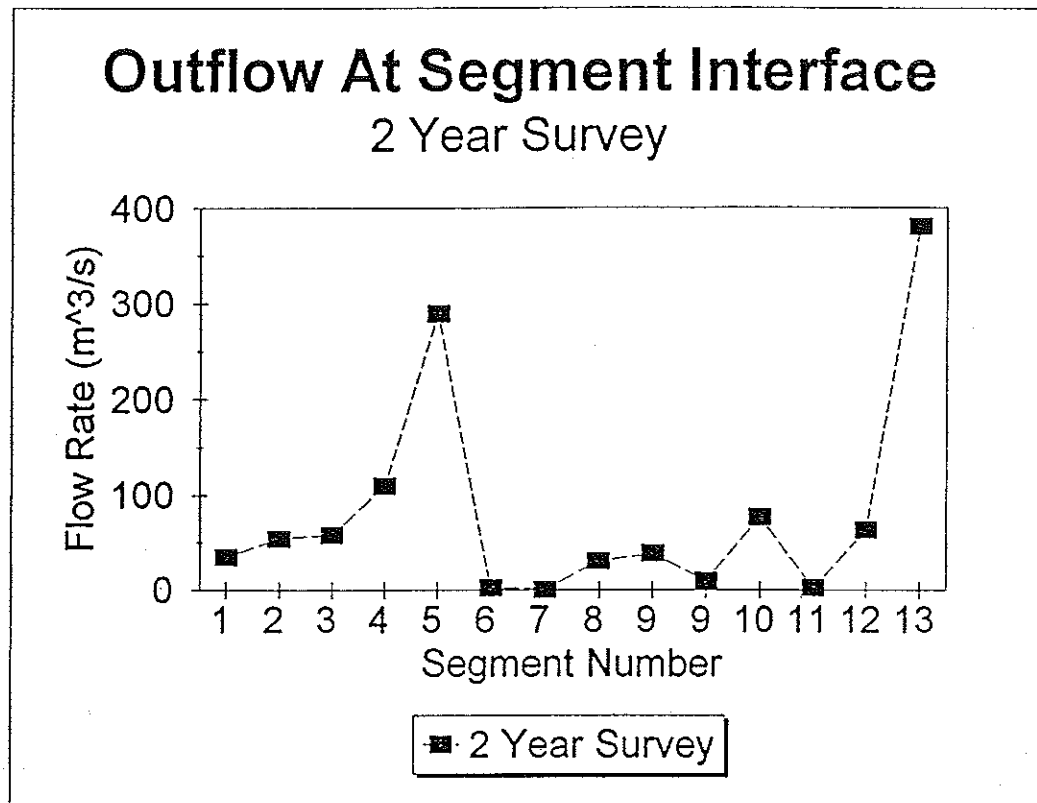


Figure 3.9 Flow rate by segment (a) outflow at the downstream face of each segment (b) flow input by segment for the hydrologic base year versus 2 year data.

Figure 3.10 shows the predicted mean net transport in the upper layer for the simulation. An interesting feature appears in Figure 3.10 which is generally consistent with earlier predictions made by Myer and Gruendling (1977), of the system of oscillating two layer, near baroclinic, geostrophic currents resulting here in a counter clockwise net transport rate gyre in the main basin of the lake. The gyre extends from Shelburne Point north to Colchester Point in the east then west to Trembleau Point and Schuyler Island and on south past Willsboro Point in New York. This is caused by the simultaneous north-south and east-west rocking motion of the interface at the thermocline due to the internal seiche. A clockwise mean transport rate gyre is also generated in the area north of Trembleau Point and south of Valcour Island. No evidence as yet exists for this phenomenon of two opposing mean net transport rate circulation patterns caused by the internal seiche and it may in turn be an artifact of the limited duration of the simulation, again highlighting the need for an analysis of the data now becoming available.

The net transport rate for the lower layer is shown in Figure 3.11. There the picture is quite different. Only a small net circulation is seen in comparison with the upper layer. This is attributable to the fact that the wind stress is applied to the surface layer adding energy to the system. A portion of the energy is transferred to the lower layer through the mechanisms of potential energy and interfacial stress. All of the energy in the lower layer must first pass through the upper layer where some of the energy is dissipated. The lower layer is therefore less dynamic.

The results of the hydrodynamic exchange rate calculation for the IK_AUG13 simulation for the upper and lower layers are shown in Figure 3.12 and 3.13, respectively. The darker the grid cell the larger the exchange as can be seen in the key to the left of the lake map in the figures. The upper layer of the main lake shows an evenly distributed exchange rate with values increasing at the north near the constricted area of Cumberland head and in the southern portion between The Four Brothers Islands and Thompsons Point. These are precisely the areas where increased exchange, due to the seiche, would be expected. The magnitudes of the exchange rate, on the order of 100-200 m^3/s throughout the main basin and increasing to 400-800 m^3/s at the northern and southern extremes, have yet to be verified as little or no data exists.

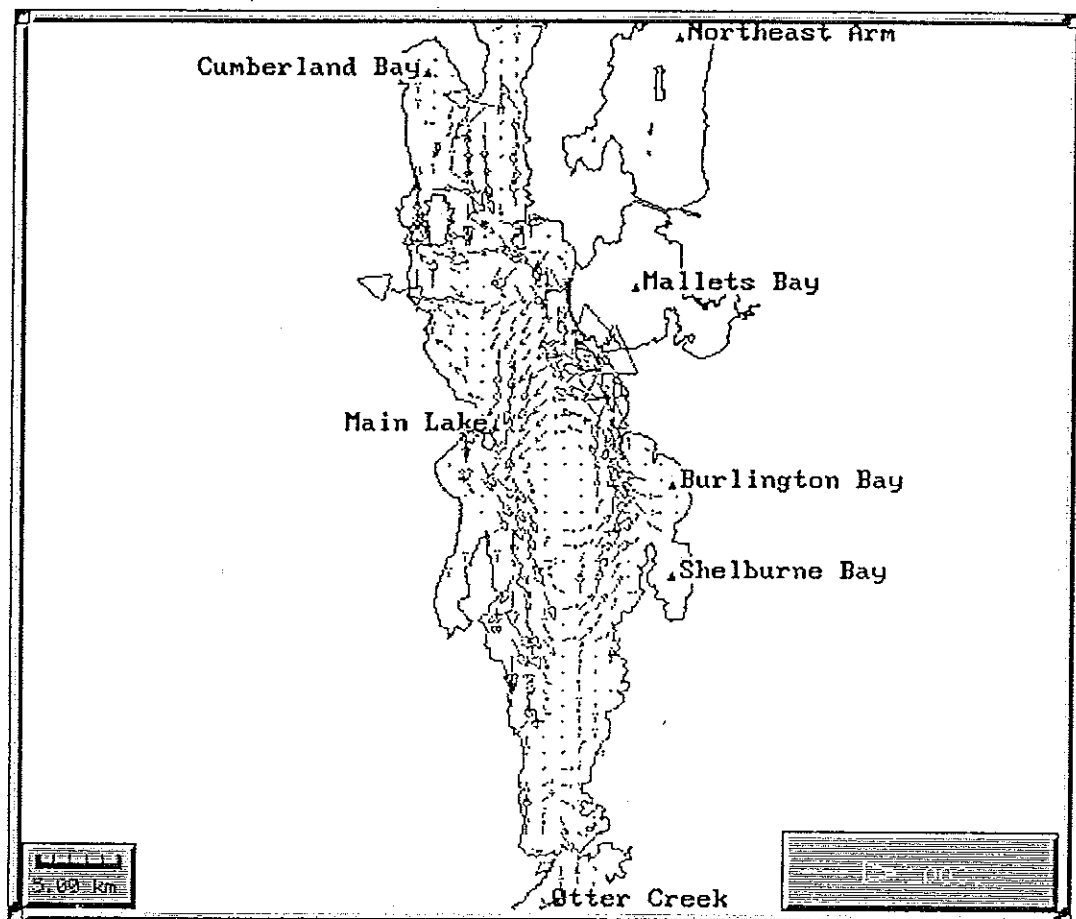


Figure 3.10 Predicted mean net transport rate in the upper layer for the 1K_AUG13 hydrodynamic simulation.

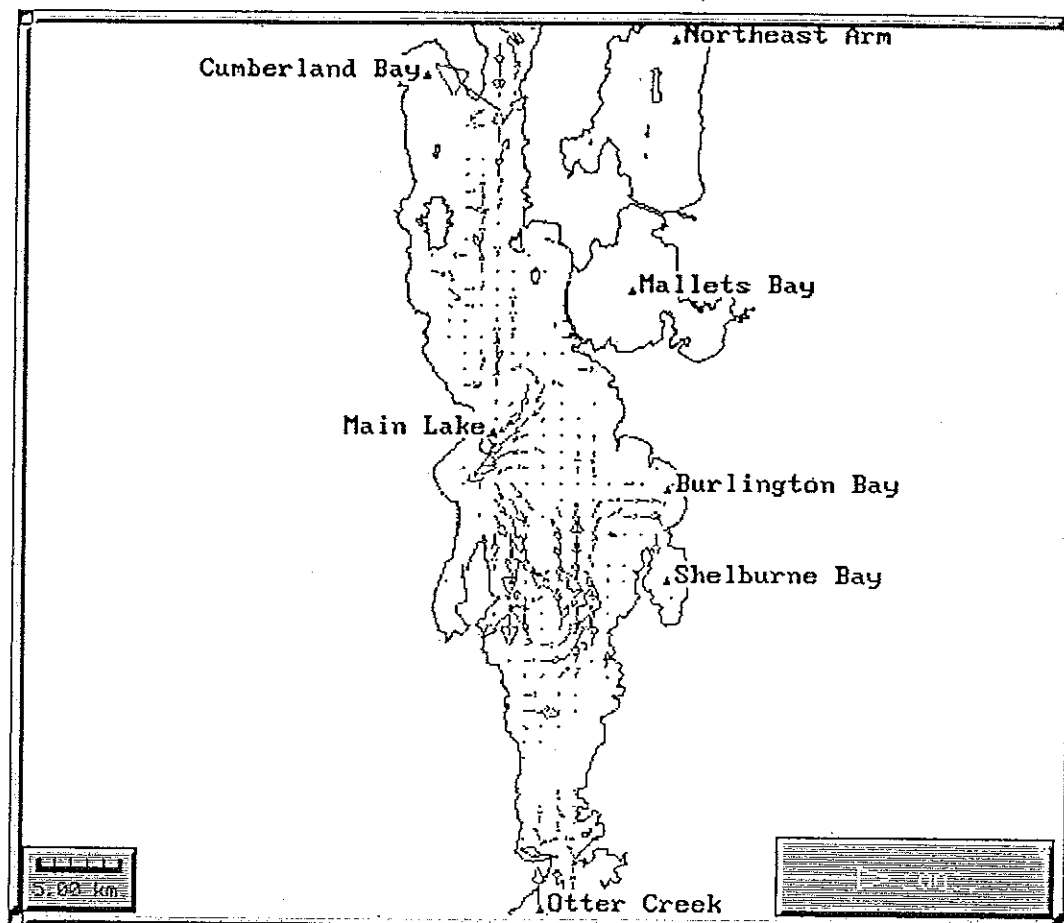


Figure 3.11 Predicted mean net transport rate in the lower layer for the 1K_AUG13 hydrodynamic simulation.

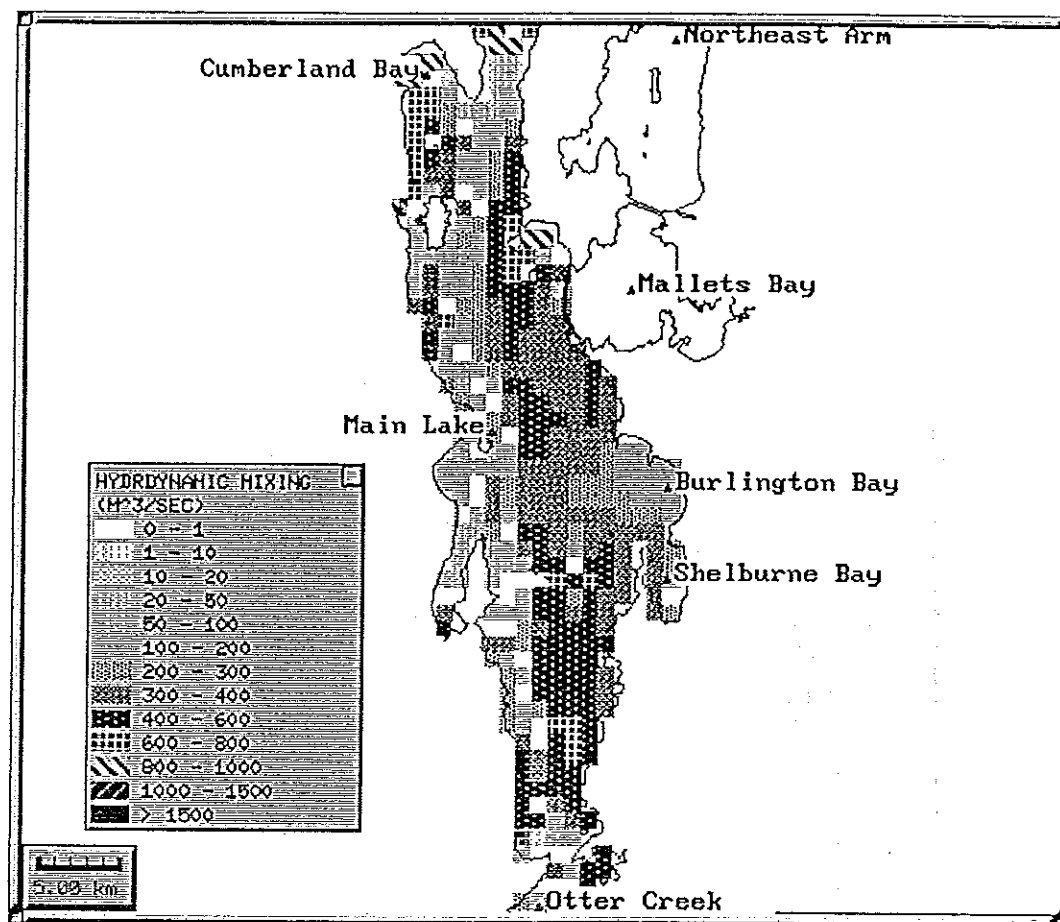


Figure 3.12 Predicted mean exchange rate in the upper layer for the 1K_AUG13 hydrodynamic simulation.

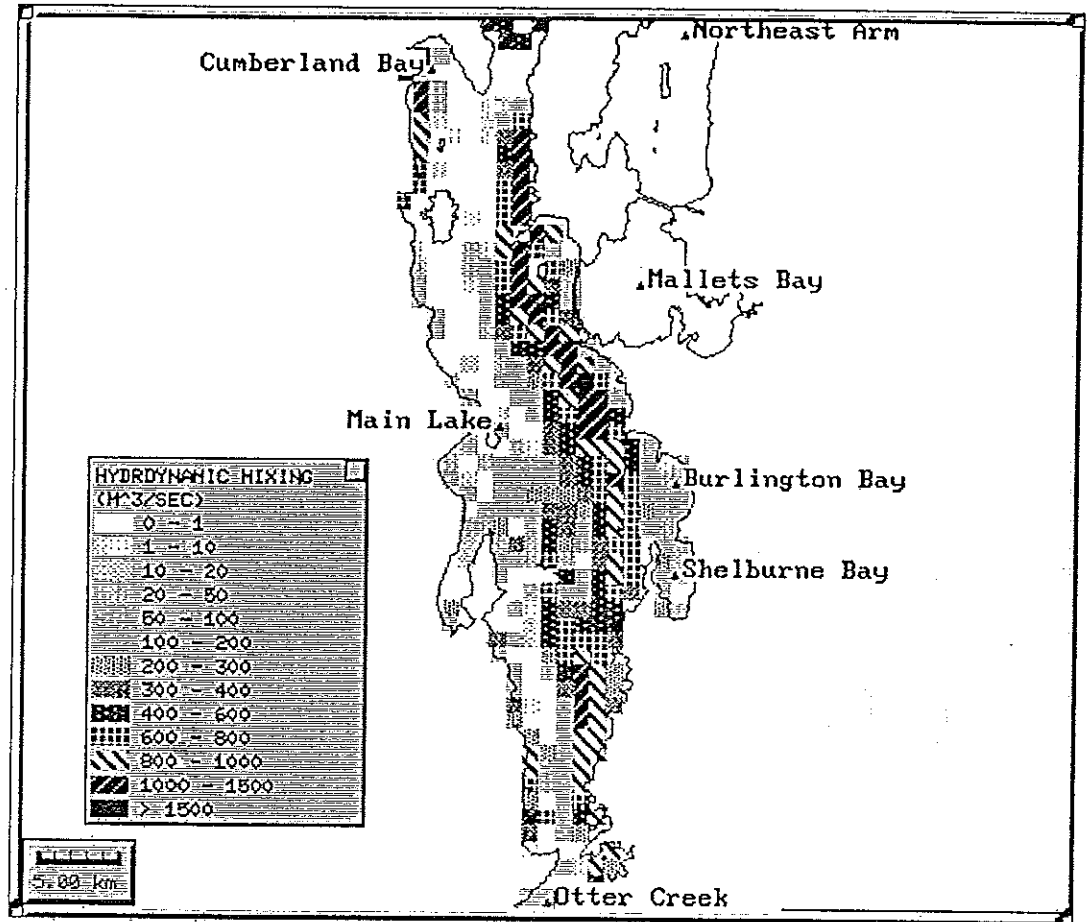


Figure 3.13 Predicted mean exchange rate in the lower layer for the 1K_AUG13 hydrodynamic simulation.

The lower layer exchange rate distribution is quite different, as seen in Figure 3.13. The larger exchange rates occur along the eastern side of the main basin for the entire length from Thompsons Point in the south to Cumberland Head in the north. This region of high exchange appears to follow a line drawn by the break in bathymetry between the extremely deep central lake and the shallow shelf area on the eastern side (see Figure 3.14). This indicates that a great deal of the motion in the lower layer, attributed to the seiche, is much like a simple sloshing back and forth, bounded by the steep bathymetric contours of the long, narrow and deep central lake.

One point of interest to note is that, although the central area of the main lake is extremely dynamic, the exchange rate between the main basin and the sub-basins, indicated in the figures, is relatively small. For example, at the entrance to Shelburne Bay in the upper layer exchange rates in the range of 50-100 m³/s are calculated. In the lower layer the range is also between 50-100 m³/s. It should be noted that where the line is drawn, demarking an embayment, could change the results but should not vary substantially at the entrance of a closed basin such as Shelbourne Bay. The results in this case are in the range of 100-200 m³/s summing upper and lower layers across the opening. It is interesting to compare this with the 150 m³/s obtained, by both VTDEC and ASA, directly from chloride tracer data analysis techniques as described in Section 3.3.2.1.

Values of the exchange rate may be calculated for the other basin interfaces in a similar manner. Table 3.10c shows values calculated for some of the other inter-segment boundaries in the main lake basin for which hydrodynamic data was generated. The magnitude and trend of the calculated exchange coefficients is similar to the values determined from the tracer data, with one notable exception. The exchange coefficient between the main basin and the Isle LaMotte segment is substantially higher in the hydrodynamic model calculated exchange. This may be partially accounted for by noting that the hydrodynamic model calculated exchange coefficients were determined for a one month period in the energetic summer stratified season whereas the tracer data calculated values derive from one year and two year average data sets respectively. This explanation of course, begs the questions of why the other exchange coefficients more closely represent their data derived counterparts. It is possible that a better resolution of the circulation would somewhat alter the calculated exchange coefficients although the hydrodynamic model

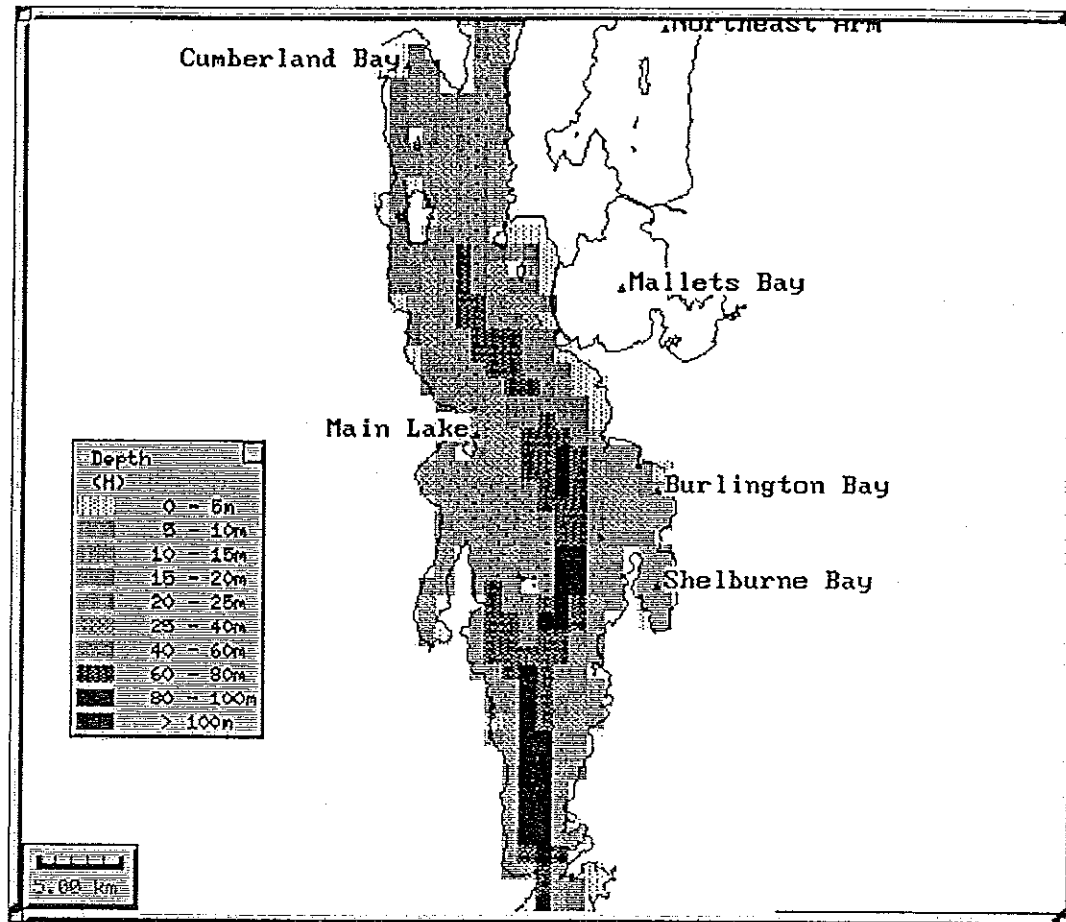


Figure 3.14 Lake Champlain gridded depths.

application described in Section 2 indicates that increased resolution did not substantially improve the simulation of the seiche. It is not yet known how a layer hydrodynamic simulation, of one year duration, for example, including the four seasonal variations in the lake, would affect the calculated exchange coefficients. It is expected, though, that both the magnitude and the distribution would change dramatically during the unstratified winter months. In that case, any expectation of developing exchange coefficients comparable to the annually averaged data derived values must include the seasonal variation in circulation patterns.

Table 3.10c Hydrodynamic model calculated exchange coefficients.

Segment	Box #	Base Year Exchange (m ³ /s)
Port Henry	3	1006
Otter Creek	4	1689
Main Lake	5	2587
Shelburne Bay	6	124
Burlington Bay	7	236
Cumberland Bay	8	164

3.3.3 Phosphorus Cycle Kinetics Calibration

The constituent concentration model described in Section 3.2 as adapted for modeling the phosphorus cycle predicts the response of three dependent variables, organic phosphorus, inorganic phosphorus and phytoplankton to a given loading. Two data sets for input loading have been developed from the VTDEC 2 year survey data, one set of means for the full two year survey and one for the hydrologic base year, as presented in Tables 3.6 and 3.7, respectively. The results for both input sets are compared to the two year mean *in-situ* total phosphorus concentration data presented in Table 3.9 as no statistically significant lakewide difference in total phosphorus concentrations exist between the two averaging periods (VTDEC, 1993).

The hydrologic base year inflow data set was used to calibrate the various coefficients and parameters described in Section 3.2.3 for phosphorus cycle kinetics as it better represents the long term mean inflow and loading conditions found in the lake, which was

the original justification of the base year. The skill of the calibrated model is then assessed on the predictions made for input based on the means of the 2 year data set as a whole. It should be kept in mind that the model as developed is capable of simulating more variables than we have data to support. A number of processes have therefore been lumped together under common values which under real conditions would be more fully expressed. An example of this is the herbivorous zooplankton grazing rate, for which no population or even type data was available to the authors.

After a series of preliminary runs were made using the base year data a sense of the model's sensitivity for certain parameters was determined. At the same time a set of "base case" parameters was arrived at, which represented no calibration. The base case parameters are listed in Table 3.11. A list of the parameters and the range over which they were varied is presented in Table 3.12. The parameters chosen for variation were selected with the intention of attempting to explain or at least investigate some of the anomalous behavior observed in the preliminary runs.

One measure of the success of a particular parameter selection is in the comparison of model prediction to the observed mean total phosphorus concentrations by segment. With the present model's ability to simulate the mean phytoplankton population another measure for comparison is to the chlorophyll *a* concentration means. In order to do that comparison a set of means was determined for the hydrologic base year which is shown in Table 3.13 by segment. The data set in Table 3.13 will necessarily have a bias towards the warm weather concentrations in that no time weighing was used to average the values and the data set was taken between the months of April and November.

One of the important variables affecting phytoplankton populations, aside from nutrient availability, is the amount of sunlight available for growth. Factors affecting the amount of light are latitude and time of year and extinction of light in the water column. The value for total daily solar radiation was determined for Burlington, Vermont by averaging the monthly average daily radiation over a one year period, (from NOAA meteorological station data; Duffie and Beckman, 1980). A measure of extinction can be made by use of the secchi depth data, again, averaged for the base year, by station then by segment. An extinction coefficient, k_e (m) was developed empirically by Sverdrup et al. (1942) and Beeton (1958) as given by

Table 3.11 Phosphorus cycle kinetic rate equations terms for the "Base" case.

Phytoplankton Net Growth Terms		Exogenous Variables	
Description	Notation	Values	Units
Extinction Coefficient	K_e	Table 3.13	m^{-1}
Segment Depth	D	Table 3.2	m
Water Temperature	T	14.5	$^{\circ}C$
Fraction of day that is daylight	f	0.5	---
Total Daily Surface Solar Radiation	I_o	422	langley/day
Zooplankton Population	Z	0	mgC/L
		Rate Constants	
Maximum Growth Rate	K_{lc}	2.0	day^{-1}
Temperature Coefficient	θ_{lc}	1.068	---
Phytoplankton Self-Light Attenuation	K_e	0.017	$m^2/mg \text{ Chl } a$
Carbon-Chlorophyll Ratio	θ_c	35	---
Saturating Light Intensity	I_s	300	langley/day
Half Saturation Constant for Phosphorus	K_{mP}	0.001	mgP/l
Endogenous Respiration	K_{IR}	0.125	day^{-1}
Temperature Coefficient	θ_{IR}	1.045	---
Settling Velocity	V_{s4}	0.25	m/day
Death Rate	K_{ID}	0.02	day^{-1}
Grazing Rate	K_{IG}	0	L/mgC-day
Phosphorus Reaction Terms			
Phosphorus to Carbon Ratio	a_{PC}	0.025	mg P/mg C
Dissolved Organic Phosphorus Mineralization at 20 $^{\circ}C$	K_{83}	0.22	day^{-1}
Temperature Coefficient	θ_{83}	1.08	---
Half Saturation Constant for Phytoplankton Limitation of Phosphorus Recycle	K_{mPC}	0.001	mg C/L
Fraction of Dead and Respired Phytoplankton Recycled to the Organic Phosphorus Pool	f_{OP}	0.5	---
Fraction Dissolved Inorganic Phosphorus in the Water Column	f_{D3}	0.8	---
Organic Matter Settling Velocity	V_{s3}	0.25	m/day
Inorganic Sediment Settling Velocity	V_{ss}	0.25	m/day

Table 3.12 Phosphorus kinetics sensitivity study parameters.

Term	Notation	Range	Units
Phytoplankton Settling	V_{s4}	0.05 - 0.5	m/day
Organic Matter Settling	V_{s3}	0.05 - 0.5	m/day
Inorganic Matter Settling	V_{s5}	0.05 - 0.5	m/day
Fraction Organic Phosphorus	f_{OP}	0.25 - 0.75	---
Endogenous Respiration	K_{IR}	0.05 - 0.125	1/day
Saturating Light Intensity	I_s	300 - 500	langley/day
Carbon to Chlorophyll Ratio	Θ_C	25 - 35	---
Chlorophyll River Concentration	---	Segment specific (Table 3.14)	$\mu\text{g/l}$
Phosphorus Mineralization Rate @ 20°C	K_{s8}	0.22 - 0.44	1/day
Exchange Coefficient Data Set	---	2 year, base year	m^3/s
Phytoplankton Death Rate	K_{ID}	0.02 - 0.6	1/day
Total Daily Insolation	I_0	312-422	langley/day

Table 3.13 Hydrologic base year data averaged by segment.

Segment	Chlorophyll a ($\mu\text{g/l}$)	Secchi Depth (m)	Extinction Coefficient	KESHD	Corrected Extinction Coefficient
1	9.97	0.39	4.33	0.34	3.99
2	6.65	1.12	1.52	0.25	1.27
3	4.14	3.63	0.47	0.18	0.29
4	3.00	4.50	0.38	0.14	0.24
5	2.21	5.38	0.32	0.11	0.20
6	3.33	4.74	0.36	0.15	0.21
7	3.06	5.16	0.33	0.14	0.19
8	2.06	4.43	0.38	0.11	0.28
9	2.14	5.31	0.32	0.11	0.21
10	3.67	4.85	0.35	0.16	0.19
11	7.12	2.54	0.67	0.26	0.41
12	9.53	1.64	1.04	0.33	0.71
13	2.59	4.80	0.35	0.12	0.23

$$K_e = \frac{1.7}{\text{secchi depth}(m)} \quad (3.19)$$

Both the Smith and the DiToro light models that appear in the WASP kinetics also take phytoplankton self shading into account following the method of Riley (1956) relating the extinction coefficient to the chlorophyll concentration (P) as follows:

$$K_{e,shd} = 0.0088P + 0.054P^{2/3} \quad (3.20)$$

Since the extinction associated with the chlorophyll *a* is inherently contained in the secchi depth, a correction to the segment-specific extinction coefficient used as input to the model must be made. These values have been tabulated for the base year data and are presented along with the chlorophyll data in Table 3.13.

Results of the model run using the base case parameters are shown in Figures 3.15a,b which compare model predictions with mean values for year one. Total P (TP) and chlorophyll *a* are the only variables consistently reported in the lake data. Thus these are the only variables available to which the model can be calibrated. The extent to which this limits the reliability of the calibration for any particular model parameter should be noted. For a first approximation, the base case provides reasonable simulation of mean conditions in the lake for TP and chlorophyll *a*. Fit of the TP data is especially good. Simulation of segments 3 to 9 are somewhat high and segment 1, 2, 10 and 11 simulations are somewhat low, while segments 12 and 13 are very close. Chlorophyll simulations were not as close, with a few segments (1, 10 and 11) showing appreciable departures from the mean data values.

To explore the model conditions responsible for the variations seen in the output, a series of runs were made varying average total daily insolation, saturation light intensity, carbon to chlorophyll ratio in the phytoplankton, endogenous respiration rate of phytoplankton, death rate of phytoplankton, fraction of phosphorus recycled to the organic pool, phytoplankton settling rate, phosphorus settling rate (organic and inorganic together), river chlorophyll load and water exchange rates between segments within the lake. In the

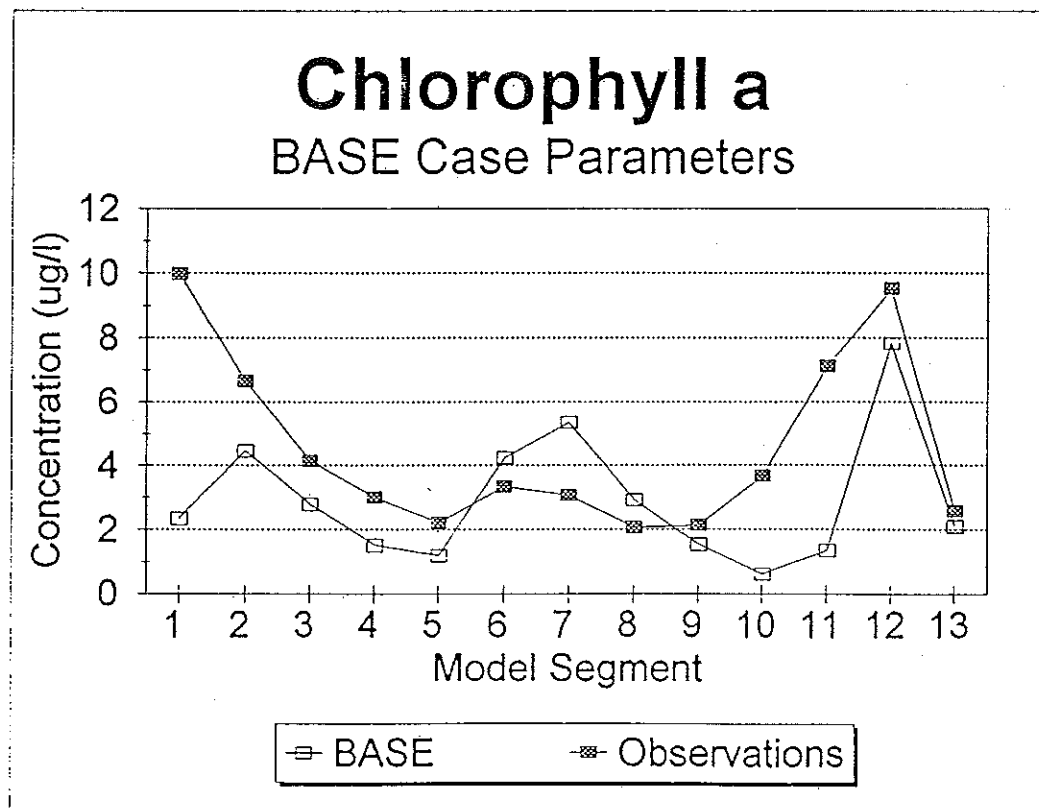
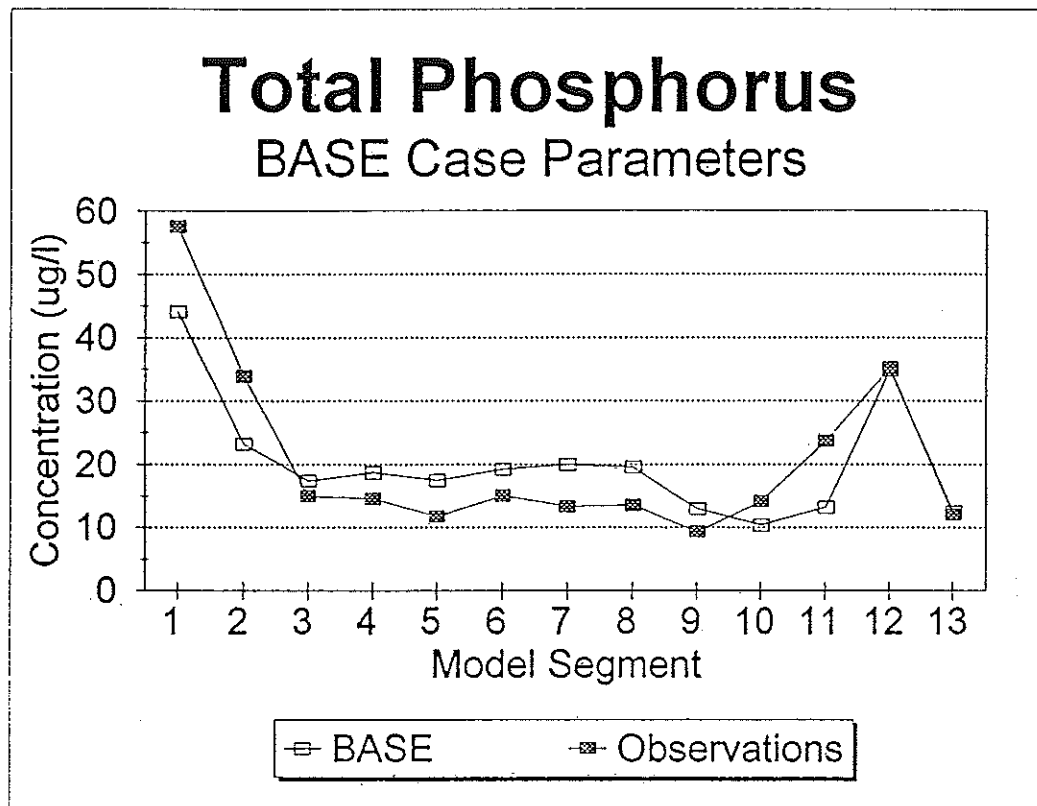


Figure 3.15 Mean observed concentration by segment and model-predicted concentrations using the base case parameters for (a) total phosphorus and (b) chlorophyll *a*.

following figures, the results of each simulation are shown along with the mean first year observations and the results of the base case run for comparison.

Average total daily insolation used for the base case was 312 langley's per day. This is the annual mean value for Burlington, Vermont. To evaluate the effect of using the mean for the sampling period (April to October) of 422 langley's per day instead, a comparison run was performed. The results are shown in Figures 3.16a,b. The differences are greater for chlorophyll than for TP, but in either case they are quite small. This may be in large part due to the use of a value of saturating light intensity (I_s) of 300 ly/day.

Saturating light intensity was varied between the base case of 300 ly/day and a value of 500 ly/day. The results are shown in Figures 3.17a,b. This primarily drives changes in chlorophyll levels which results in smaller changes in TP levels. It is not immediately apparent why differences show up uniformly for segments 1 to 8 and not for 9 to 13. The counterintuitive reduction in chlorophyll with an increase in I_s results from the fact that the maximum growth rate, set by a separate variable in the phytoplankton growth model used in these simulations, and was not altered. For such a condition, increased I_s requires a reduced quantum efficiency.

Decreasing the carbon to chlorophyll ratio in the phytoplankton from the base case of 35 to a value of 25 (Figures 3.18a,b) produced a fairly uniform increase in chlorophyll concentrations across all segments with only tiny changes in TP concentrations.

Endogenous phytoplankton respiration was set at 0.125 per day for the base case. A comparative run used 0.05 per day and is shown in Figures 3.19a,b. Large changes in chlorophyll concentrations are apparent with similar changes appearing in most segments. Changes in TP are also significant, with smaller changes occurring in the segments having higher concentrations. Death rate of phytoplankton is functionally identical to respiration in the phytoplankton kinetics so it is not surprising that similar results are seen when death (which should be considered to include grazing losses in this model) is reset from the base case of 0.02 per day to a value of 0.06 per day (Figures 3.20a,b). The direction of change is different because here we are increasing rather than decreasing losses. Also, the effect of a change in respiration will be altered somewhat by a temperature coefficient not used in the death rate calculation.

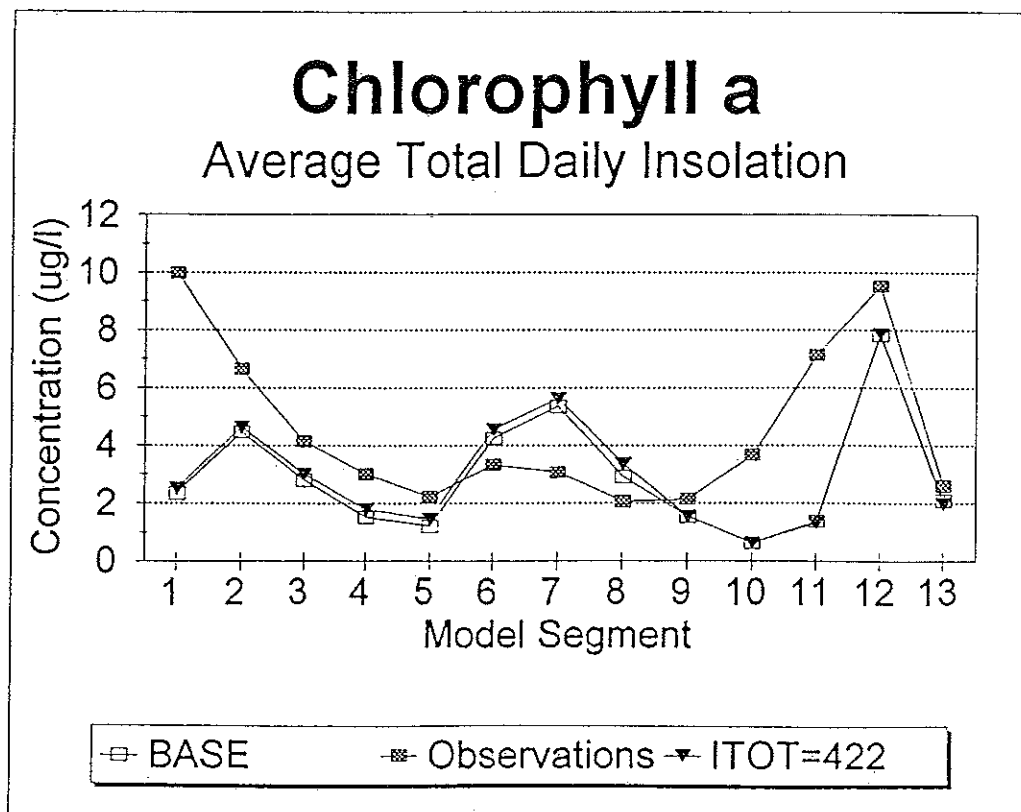
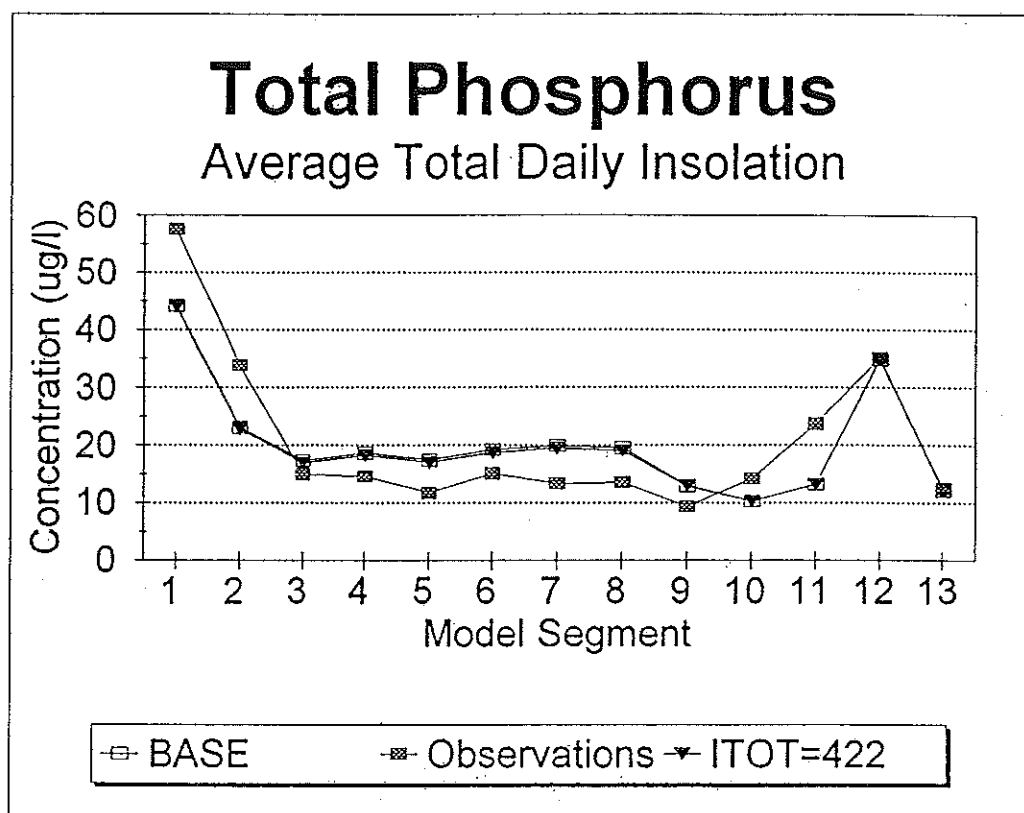


Figure 3.16 Effect on model-predicted concentrations of increasing total daily insolation from 312 to 422 langleys per day for (a) total phosphorus and (b) chlorophyll *a*. Mean annual observed concentrations and base case predictions are shown for comparison.

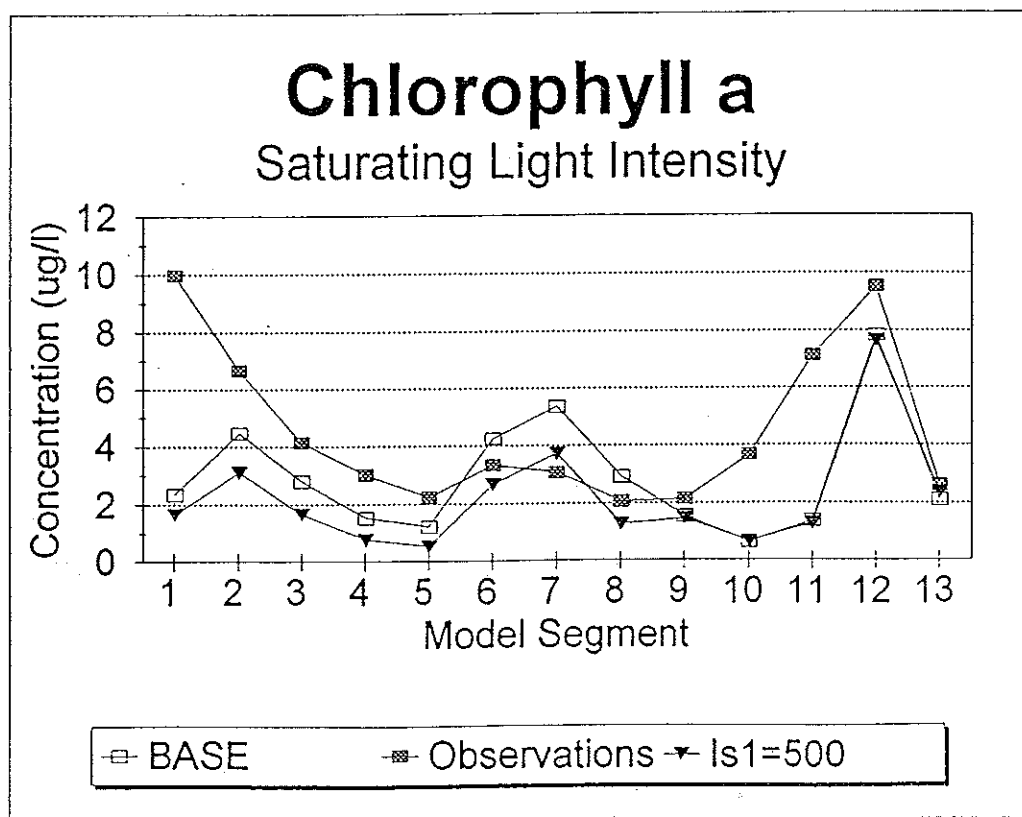
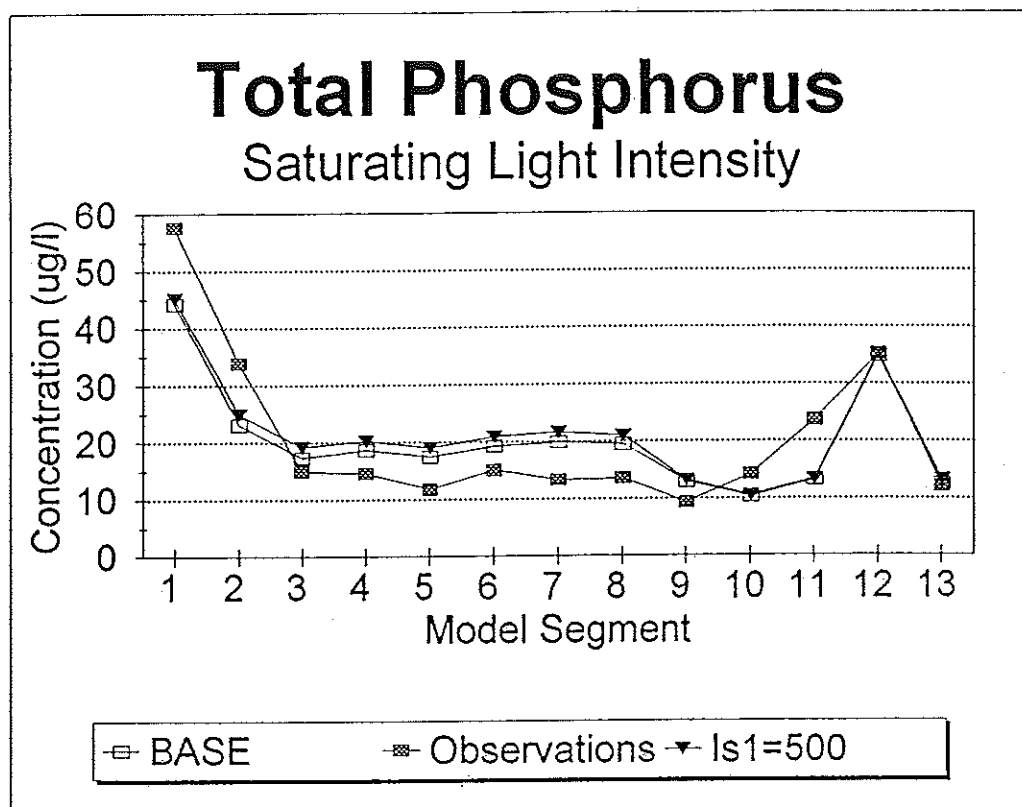


Figure 3.17 Effect on model-predicted concentrations of increasing saturating light intensity from 300 to 500 langleys per day for (a) total phosphorus and (b) chlorophyll *a*. Mean annual observed concentrations and base case predictions are shown for comparison.

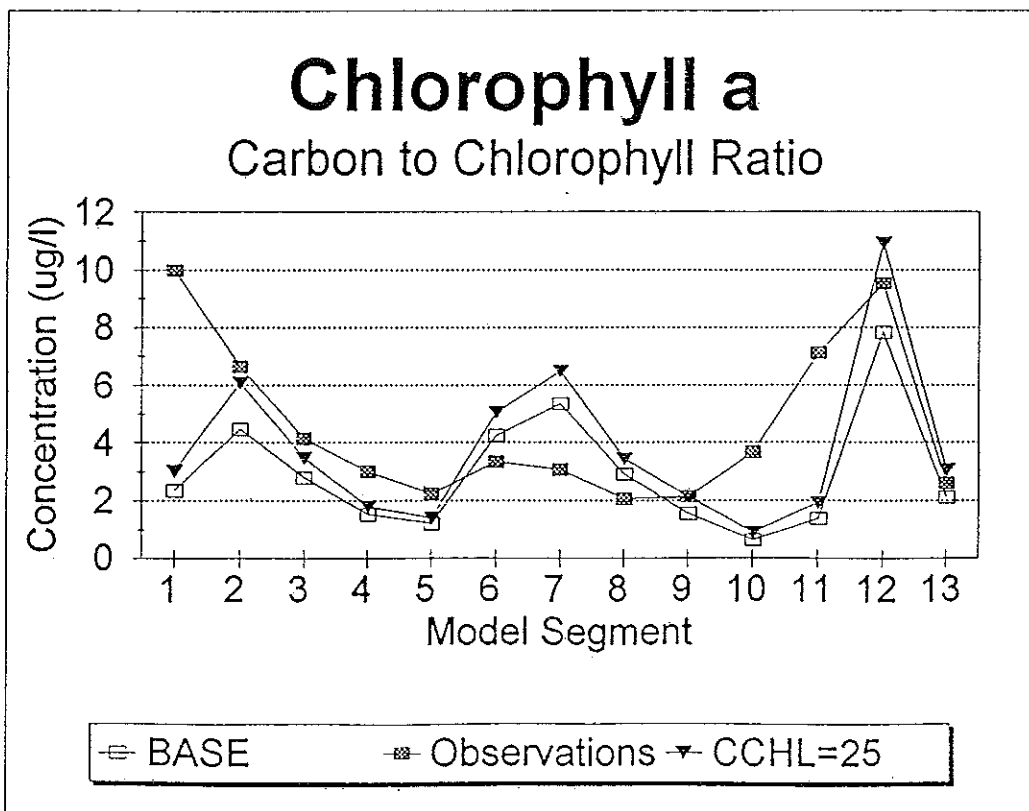
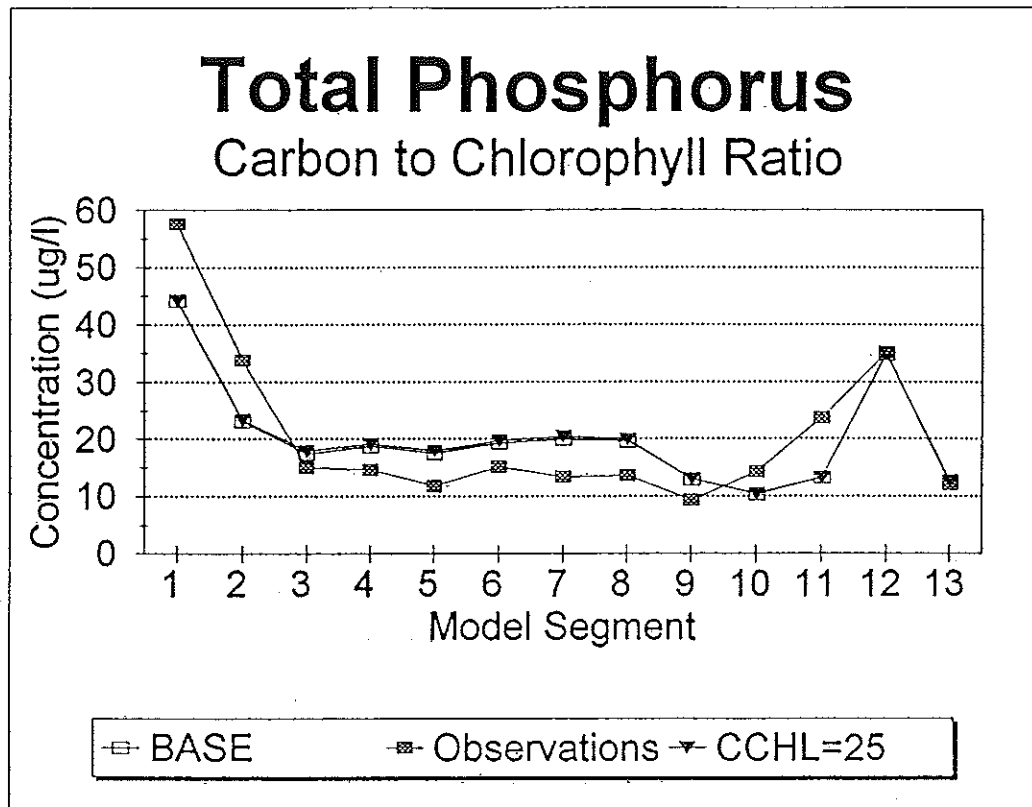


Figure 3.18 Effect on model-predicted concentrations of decreasing the phytoplankton carbon to chlorophyll ratio from 35 to 25 for (a) total phosphorus and (b) chlorophyll *a*. Mean annual observed concentrations and base case predictions are shown for comparison.

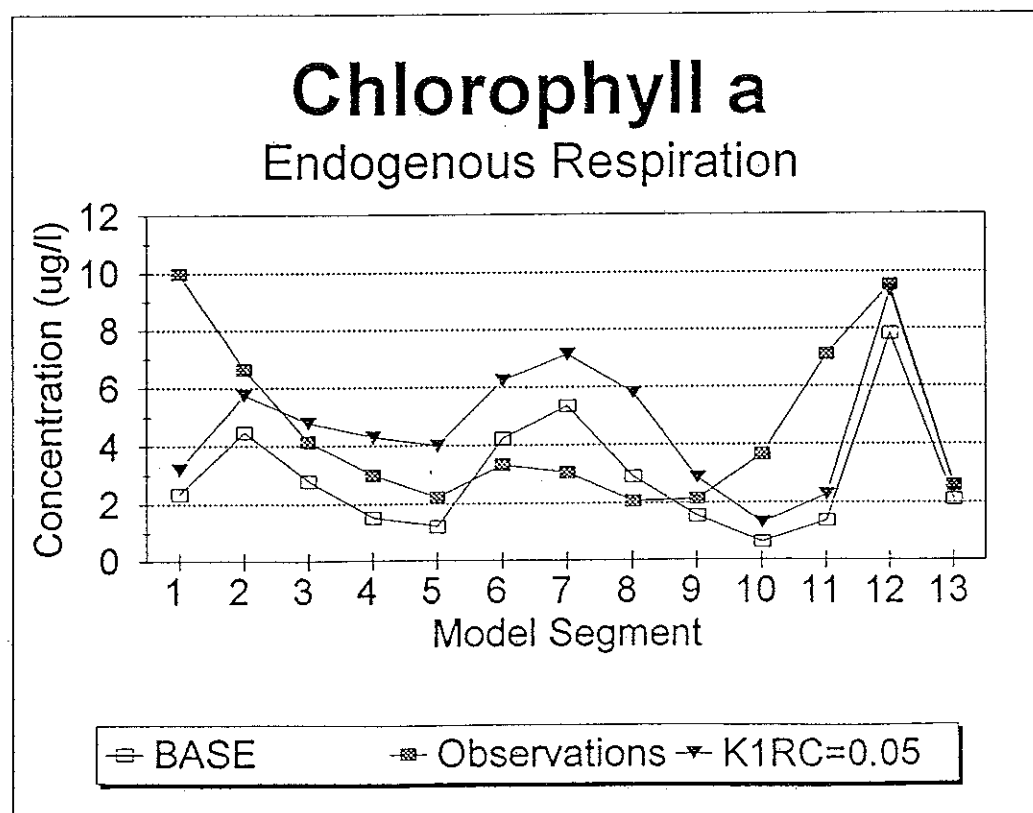
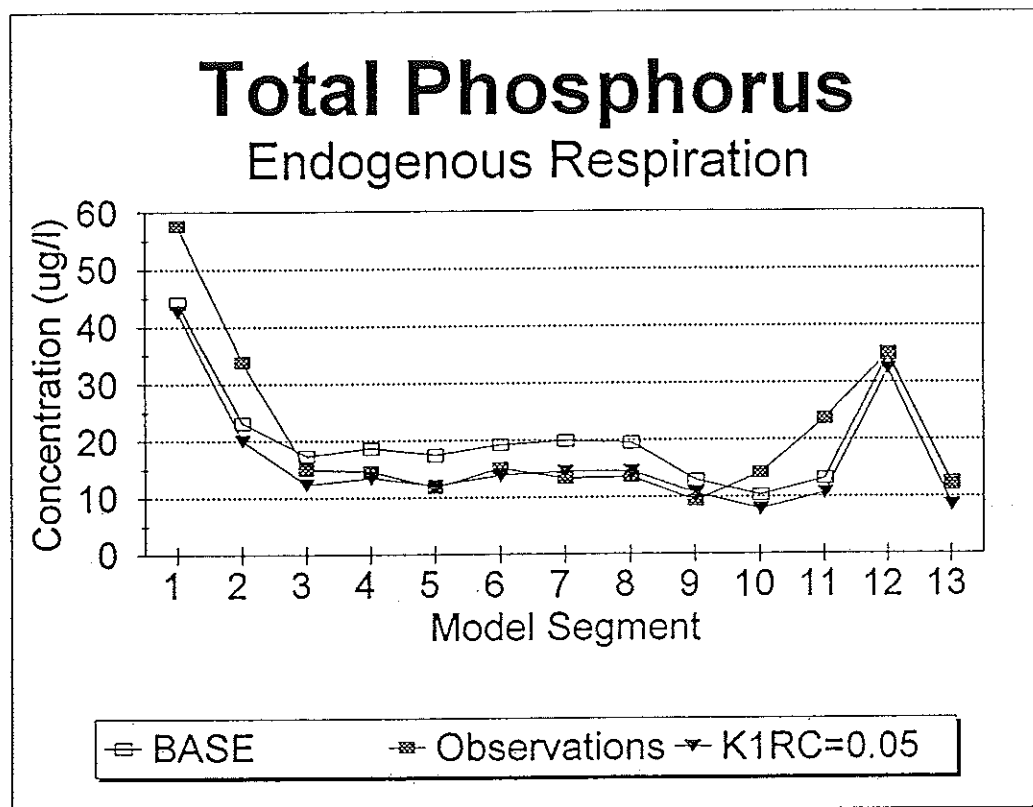


Figure 3.19 Effect on model-predicted concentrations of decreasing the phytoplankton respiration rate from 0.125 to 0.05 per day for (a) total phosphorus and (b) chlorophyll *a*. Mean annual observed concentrations and base case predictions are shown for comparison.

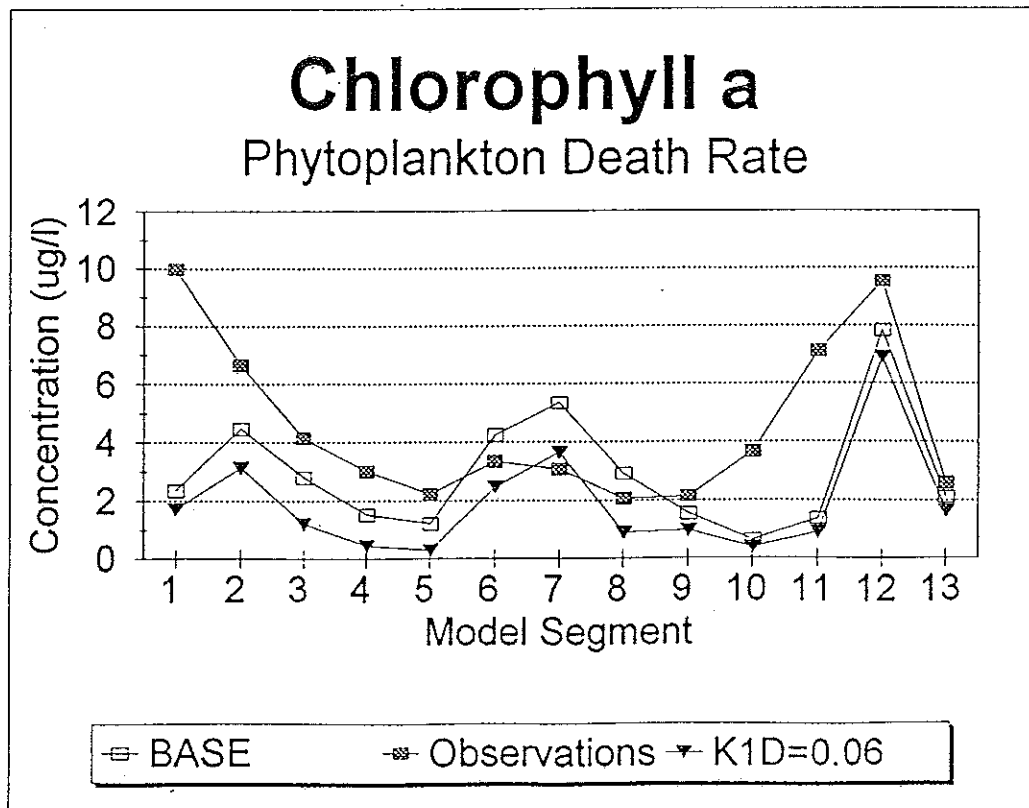
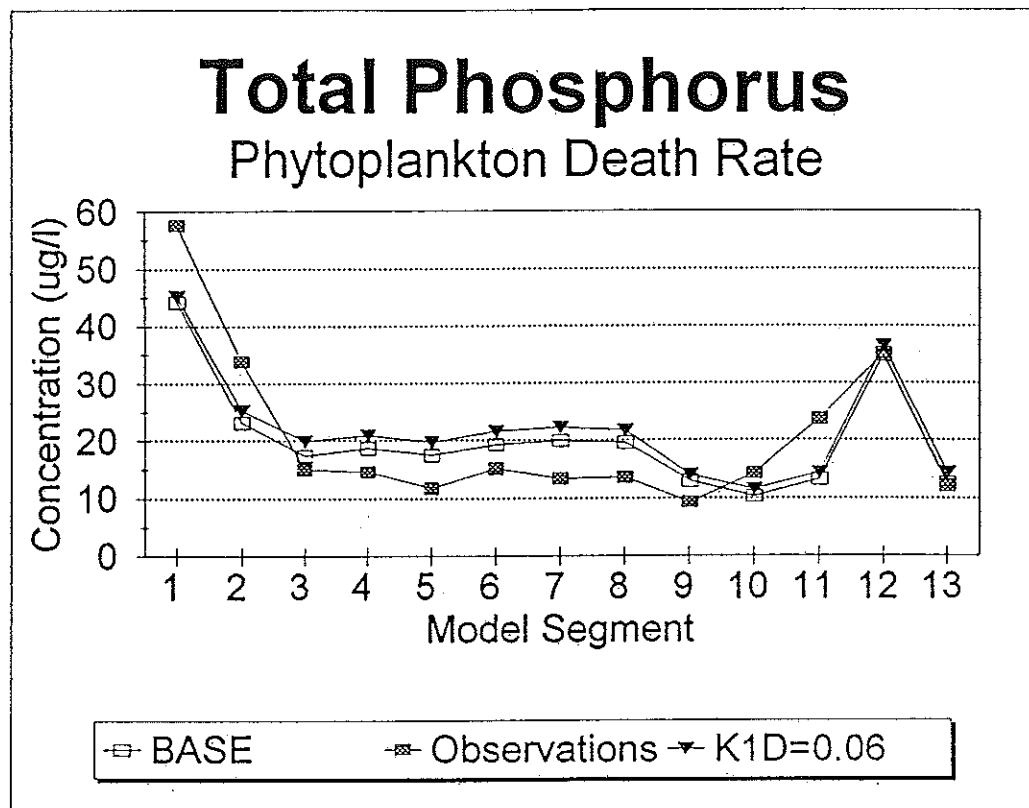


Figure 3.20 Effect on model-predicted concentrations of decreasing the phytoplankton death rate from 0.02 to 0.06 per day for (a) total phosphorus and (b) chlorophyll *a*. Mean annual observed concentrations and base case predictions are shown for comparison.

The fraction of phosphorus recycled to the organic pool (F_{OP} ; $1-F_{OP}$ is the fraction recycled to the inorganic pool) is set at 0.5 in the base case and was tested for values of 0.25 and 0.75, shown in Figures 3.21a,b. There is a uniform change in TP and chlorophyll *a* concentrations above or below the base case with changes in F_{OP} . Increasing F_{OP} reduces the fraction of recycled phosphorus immediately available to phytoplankton and reduces chlorophyll *a* concentrations, thus increasing TP concentrations. Decreasing F_{OP} has the reverse effect.

The base case phytoplankton settling rate is 0.25 m/day. Test cases were run using 0.05, 0.1, 0.4 and 0.5 m/day (Figures 3.22a,b). While results are not altogether uniform from segment to segment, there is a fairly predictable change in both chlorophyll *a* and TP of decreasing concentrations with increasing settling rates. The same series of rates were tested for phosphorus settling, modifying both organic and inorganic forms together (Figures 3.23a,b). Changes in both TP and chlorophyll *a* are more uniform from segment to segment than they are when phytoplankton settling rates are varied, and changes in TP are relatively larger than changes in chlorophyll *a* compared to results with phytoplankton settling.

One of the loads missing from the data set is chlorophyll *a* concentrations in the rivers. To simulate these loads, the mean value for the ratio of chlorophyll *a* to TP was determined for all the lake stations and this parameter was used to add chlorophyll to river inputs based on their reported TP concentrations. The results are shown in Figures 3.24a,b. There are small increases in TP predicted in every segment and moderate to very large increases in chlorophyll *a* in every segment. Clearly the chlorophyll *a*/TP ratio approach is a poor estimate of effective chlorophyll *a* load from the rivers.

Base case model runs were performed using both the two-year exchange rate calibration (the actual base case) and the exchange rates calculated for the hydrologic base year. Comparisons of the results are shown in Figures 3.25a,b. Only small differences show up for predicted TP and chlorophyll *a* for most segments, with the largest difference showing up in segment 1.

Based on the results of these sensitivity runs, a set of parameter value adjustments was selected to attempt calibration of the model for TP and chlorophyll *a*. Phytoplankton settling was reset to 0.15 m/day while organic and inorganic phosphorus settling was reset to 0.4 m/day. Though river chlorophyll *a* loads overall appeared to contribute poorly to model

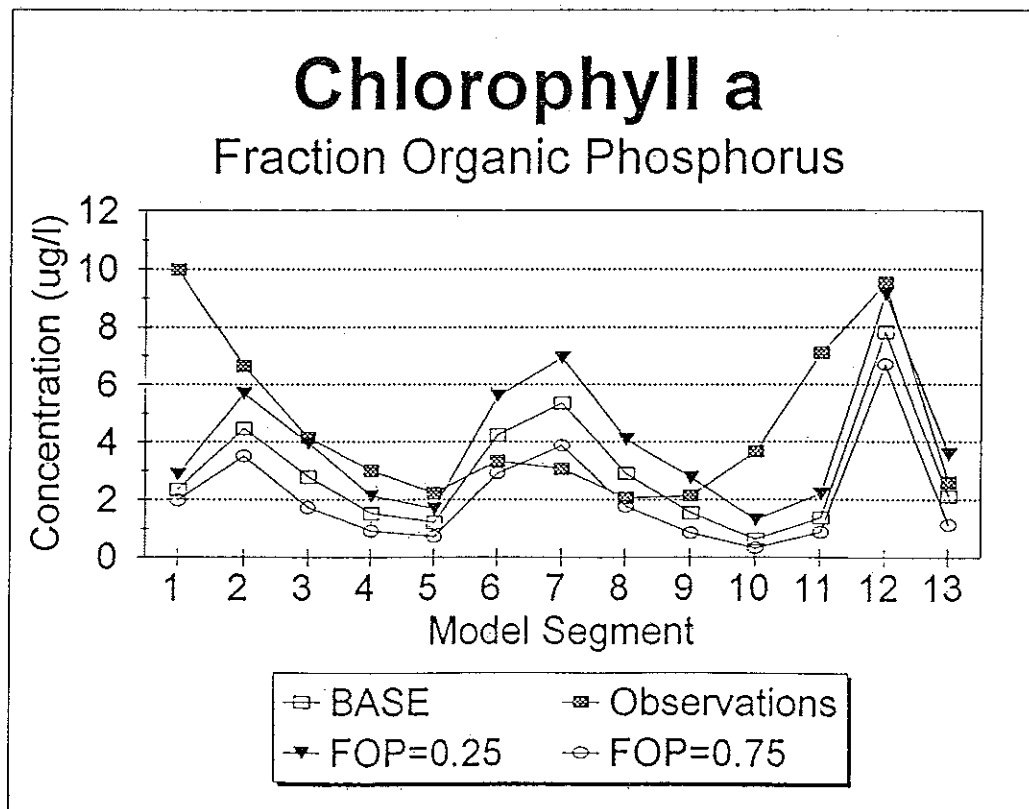
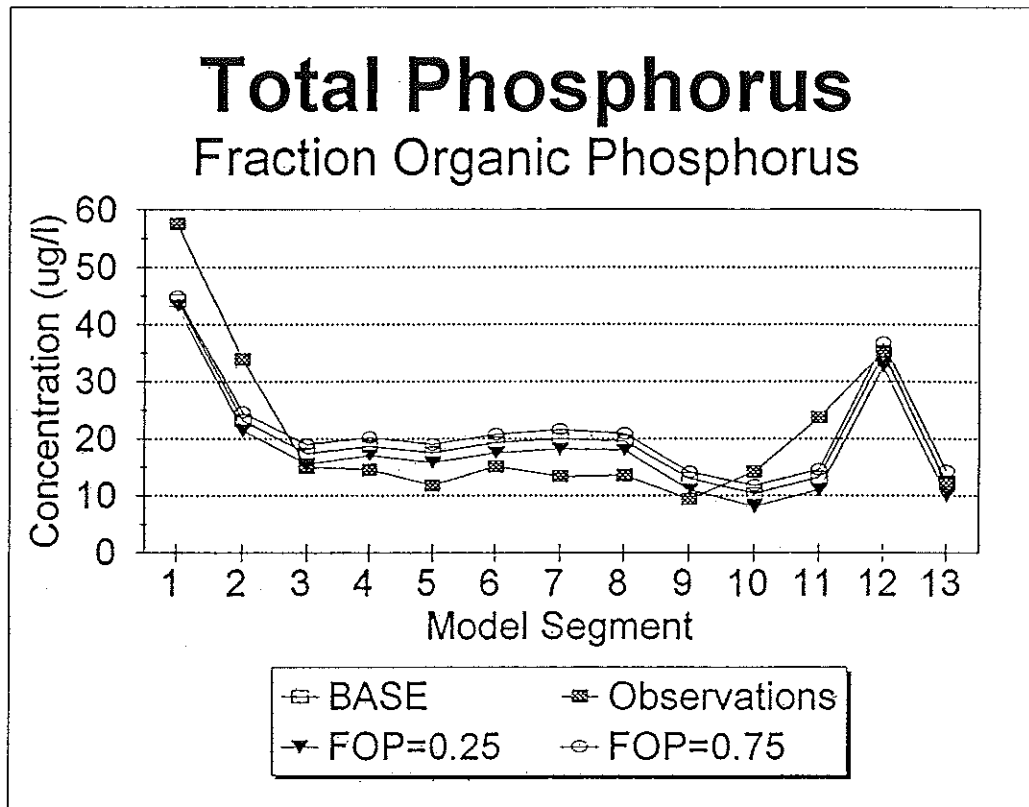


Figure 3.21 Effect on model-predicted concentrations of varying the fraction of phosphorus recycled to the organic pool, F_{op} , from a base case of 0.5 to values of 0.25 or 0.75 for (a) total phosphorus and (b) chlorophyll *a*. Mean annual observed concentrations and base case predictions are shown for comparison.

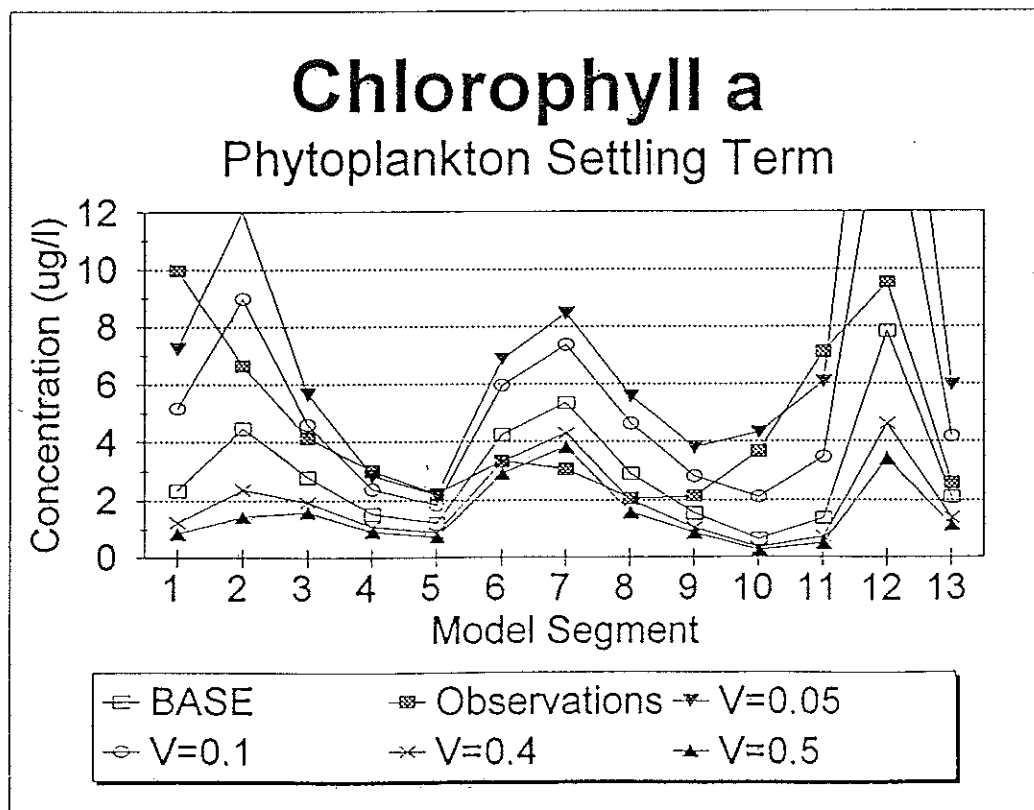
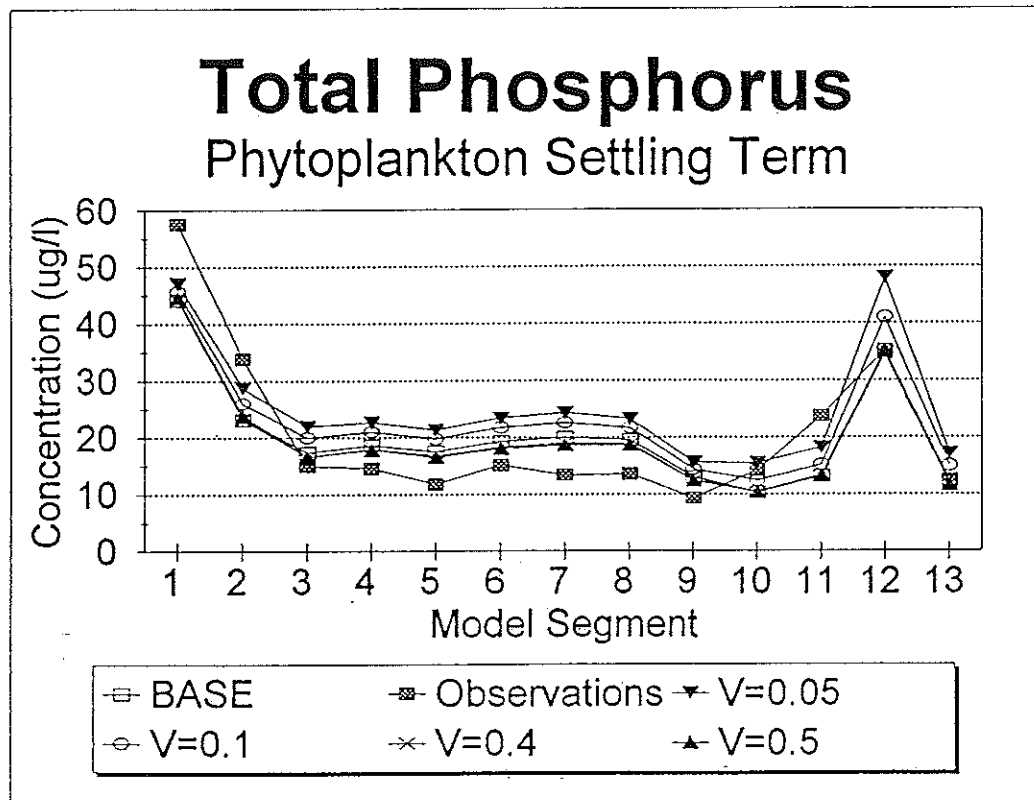


Figure 3.22 Effect on model-predicted concentrations of varying the phytoplankton settling rate from a base case of 0.25 to values of 0.05, 0.1, 0.4, or 0.5 m/day for (a) total phosphorus and (b) chlorophyll *a*. Mean annual observed concentrations and base case predictions are shown for comparison.

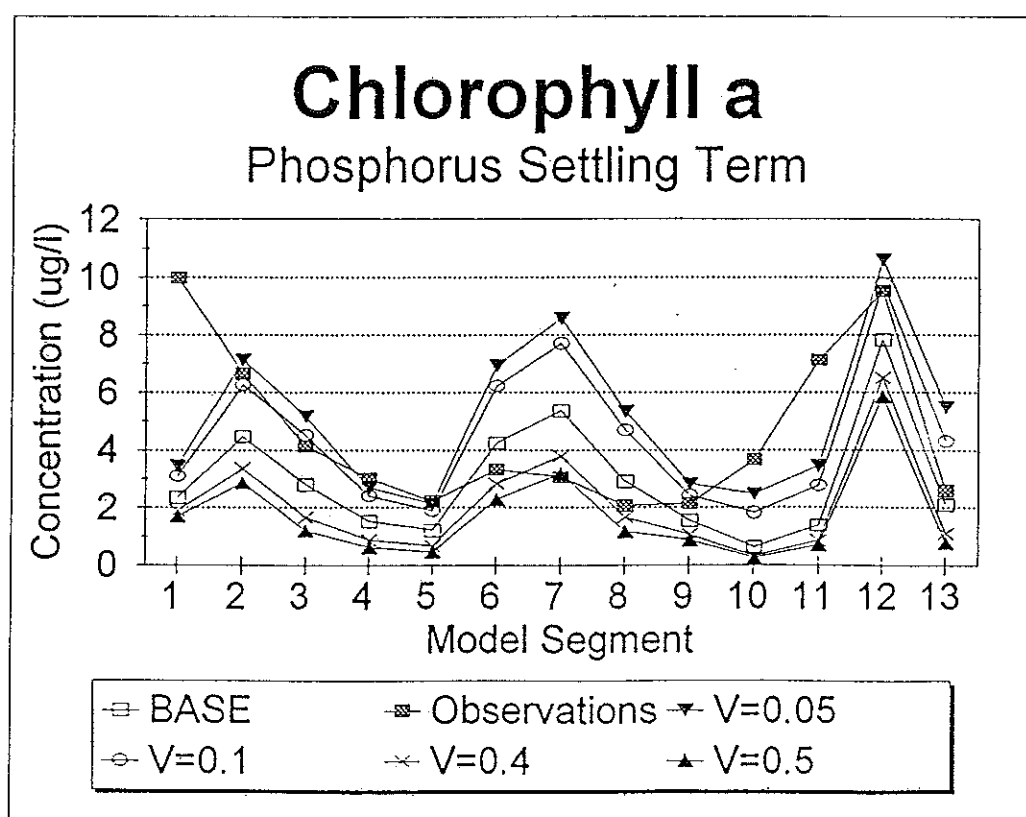
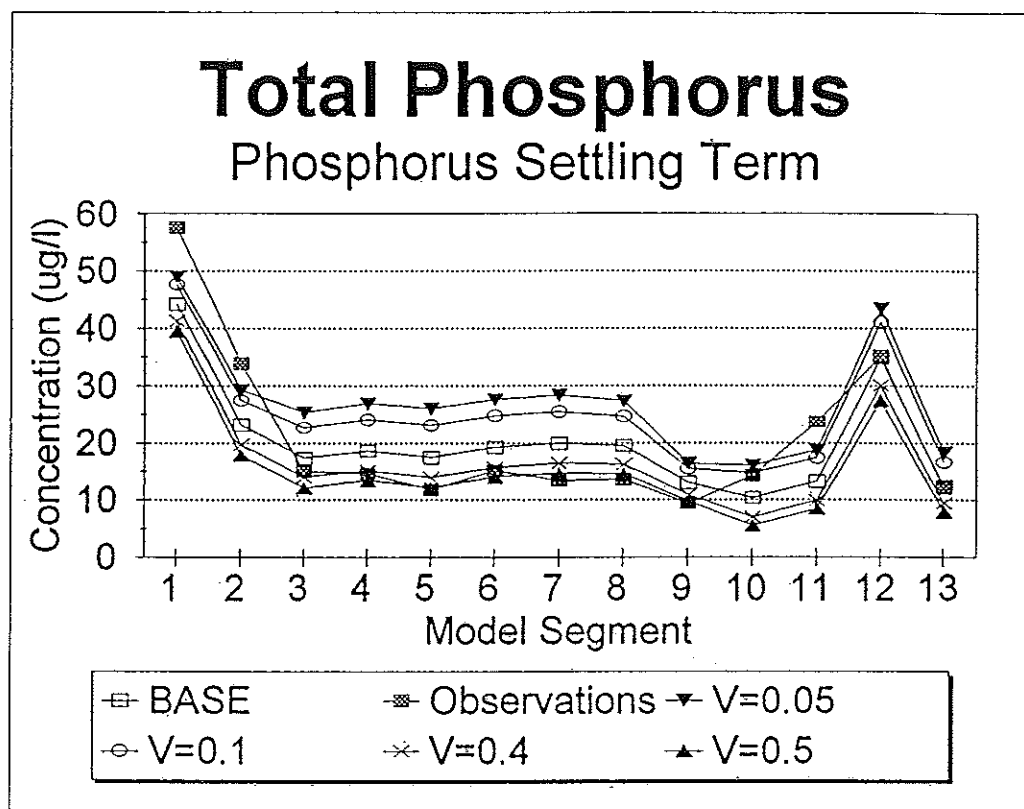


Figure 3.23 Effect on model-predicted concentrations of varying the phosphorus settling rate from a base case of 0.25 to values of 0.05, 0.1, 0.4, or 0.5 m/day for (a) total phosphorus and (b) chlorophyll *a*. Mean annual observed concentrations and base case predictions are shown for comparison.

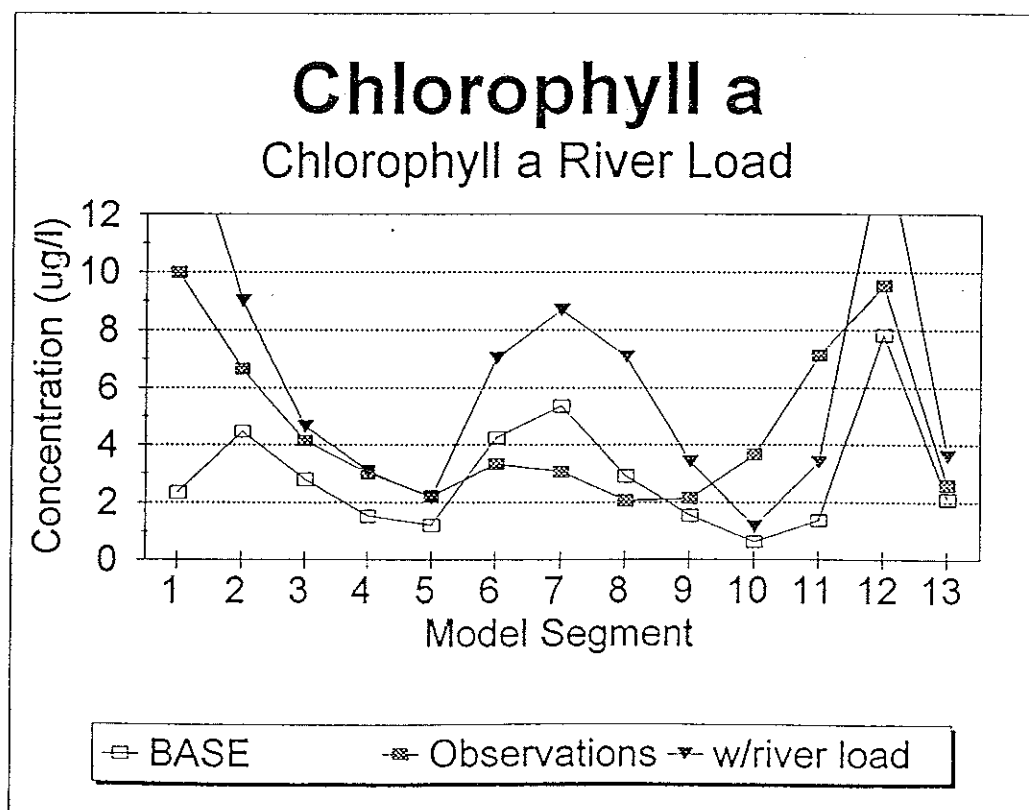
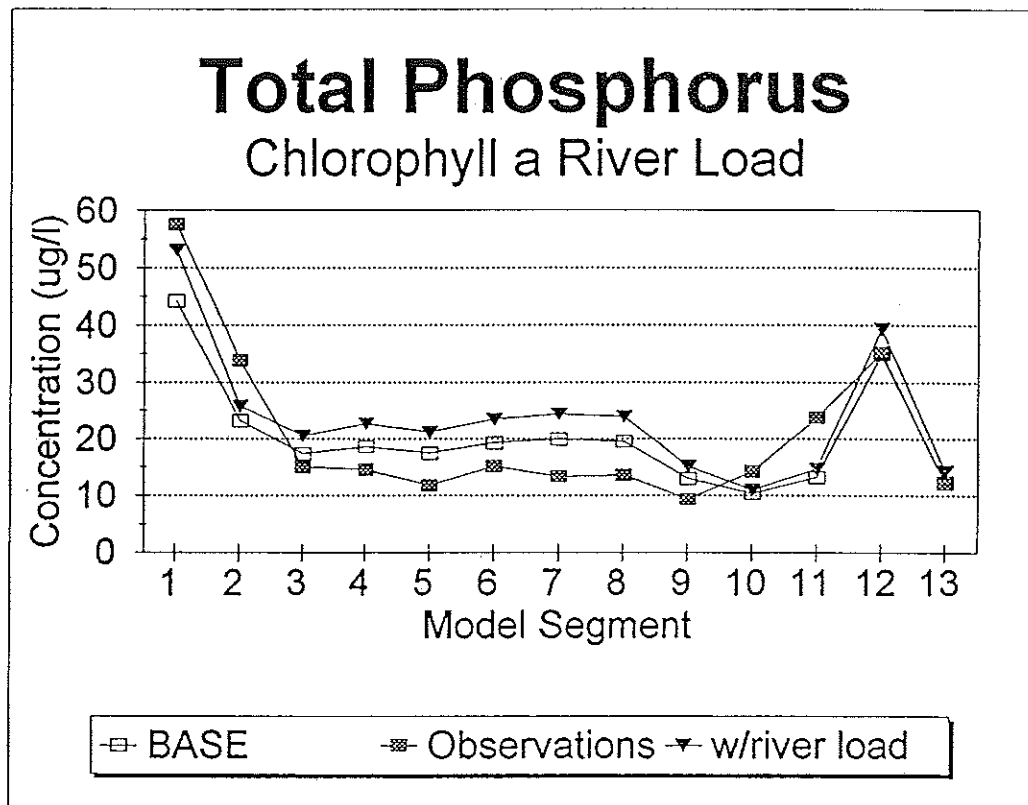


Figure 3.24 Effect on model-predicted concentrations of adding chlorophyll loads to river inputs based on their total phosphorus concentrations for (a) total phosphorus and (b) chlorophyll *a*. Mean annual observed concentrations and base case predictions are shown for comparison.

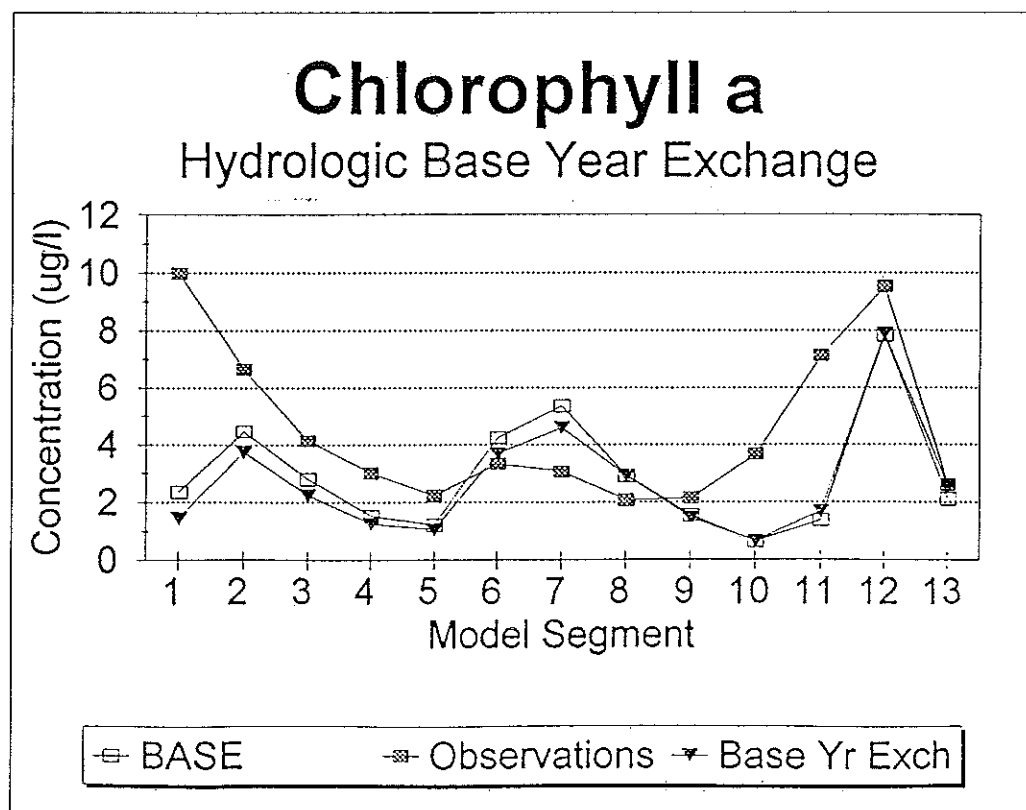
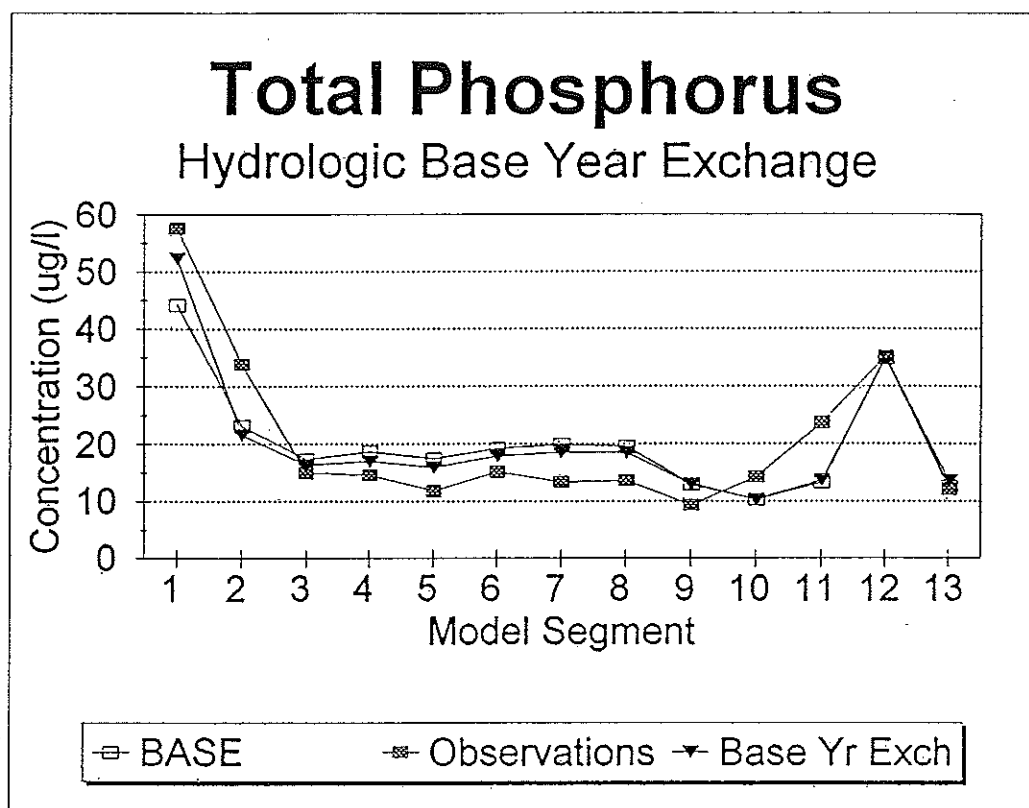


Figure 3.25 Effect on model-predicted concentrations using the hydrologic base year exchange values instead of the two year average for (a) total phosphorus and (b) chlorophyll *a*. Mean annual observed concentrations and base case predictions are shown for comparison.

calibration, it was apparent that the only way to get the measured value of chlorophyll *a* found in the rapidly-flushed segment 1 was to add it in the rivers. A best-fit value was iteratively determined to be 12 $\mu\text{g/L}$ chlorophyll *a* in the river to segment 1 only. Based on observations in VTDEC and NYSDEC (1993), the poor simulation of TP concentration in segment 11 was attributed to a non-equilibrium state in which sediments provide a net TP source in that segment. A value of 6.4 $\text{mg/m}^2/\text{day}$ provided a best fit of TP and chlorophyll *a* together. The results of the calibration process are shown in Figures 3.26a,b. TP values are still predicted to be somewhat low in segments 1, 2, 10, and 11 and very close or slightly high in the others. Chlorophyll *a* values are low in segments 3, 4, 5 and 10 while being very close or high in the others. Additional variations were run to examine the possibility of improving fit by manipulating phytoplankton respiration and exchange. These did not improve fit.

Several approaches to statistical evaluation of model fit to data are possible (McCutcheon et al., 1990). Two have been chosen here. The root mean square calculation (RMS) is evaluated as:

$$\left(\frac{\sum (C_D - C_M)^2}{n} \right)^{0.5}$$

where C_D is the measured value (data), C_M is the model-predicted value, and n is the number of measurements taken and compared. Relative error is evaluated as the absolute value of the difference between the mean measured value and the corresponding mean model prediction divided by the mean measured value. Relative error statistics provide measurements of model performance that are comparable between different variables because they are normalized to the value of each variable. Root mean square error was 5.33 $\mu\text{g/L}$ for TP and 1.27 $\mu\text{g/L}$ for Chlorophyll *a*. Mean relative error was 0.196 (i.e., ~20%) for TP and 0.308 for chlorophyll *a*. These are not what might be hoped for in a model calibration, but should be considered in the context of the sparsity of data to which to calibrate.

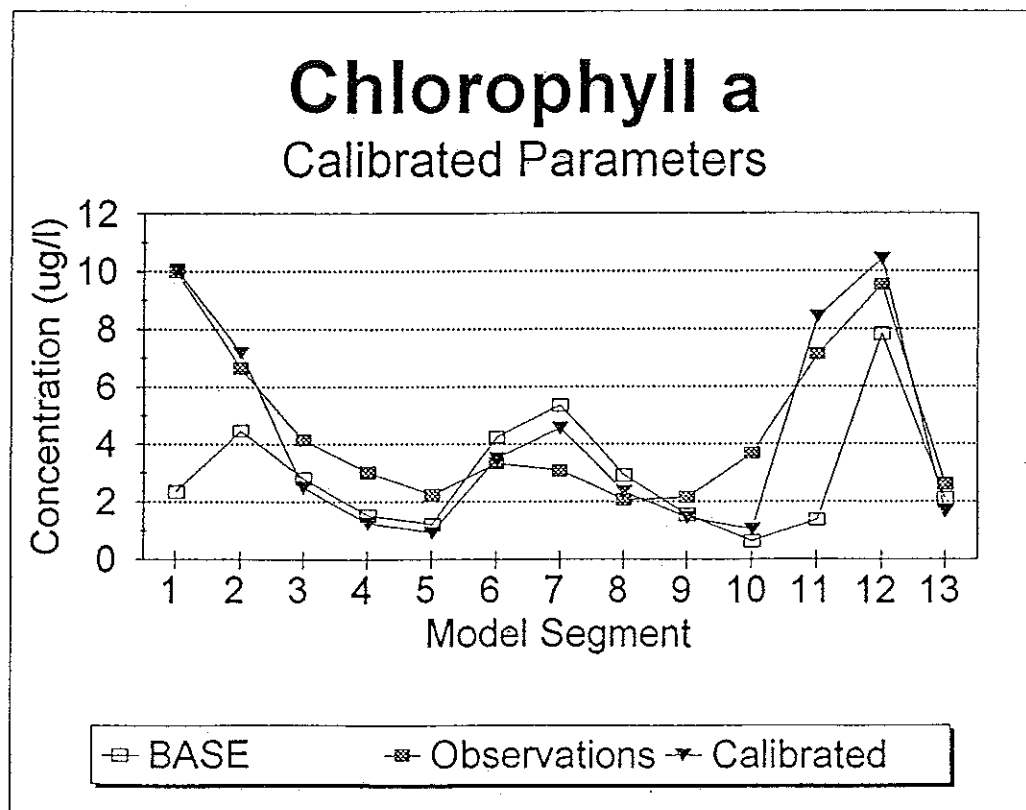
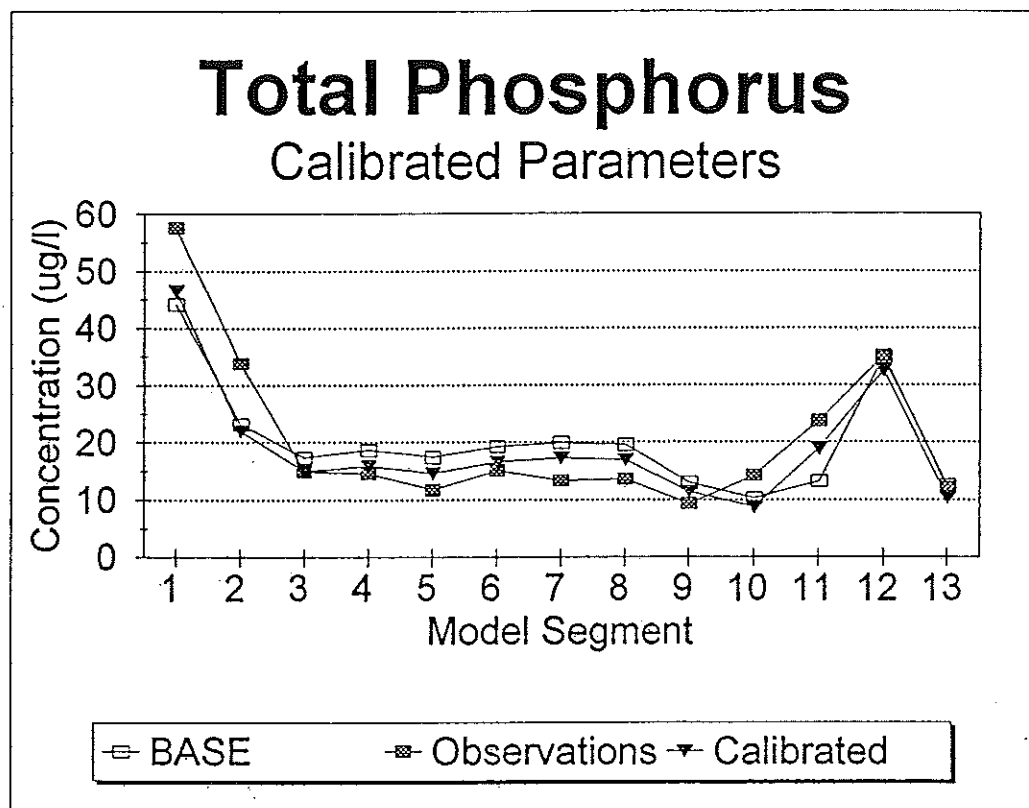


Figure 3.26 (a) Total phosphorus concentrations predicted by the model using the calibrated model parameters. Mean annual observed concentrations and base case predictions are shown for comparison. (b) Chlorophyll *a* concentrations predicted by the model using the calibrated model parameters. Mean annual observed concentrations and base case predictions are shown for comparison.

3.4 Discussion and Recommendations

The point has been made that a more detailed data set would have allowed a better calibration of the model. Clearly the data set collected should be driven by the ultimate use of the data set. One can easily propose a sampling program well beyond the means of almost any program or agency, so there will always be some selection among the variables that one might choose to measure. The spatial and temporal density of the data set that exists is excellent and cannot be faulted. There are a number of variables, however, that if measured would increase the quality of the model calibration process considerably. Adding orthophosphate and dissolved phosphorus measurements to the composite lake station data would help considerably. Tributary data should include Chlorophyll determinations. Certain *in situ* measurements such as productivity (light bottle-dark bottle with DO determination) for selected sites over several seasons could be very helpful. Similarly, knowledge of sediment oxygen demand and nutrient exchange rates would add considerably to the characterization of benthic processes. This could be amplified by measurements of surface and bottom concentrations at more stations in the lake. It is possible that more detail of phytoplankton processes could be achieved with more knowledge of its composition. Periodic counts of plankton from different areas of the lake with characterization of size and taxonomic composition would allow for a rational basis for segment-specific variation of processes such as nutrient limitation of growth and settling rates. Surely this would be an excellent masters degree project for some aspiring student in the area, and could tell us much about the lake's ecology. If it is desired to expand beyond the WASP dynamics, one could even justify modeling the whole food chain, a process that would require some background on zooplankton and fish ecology of the area as well. These processes are all part of a whole with each reflected and being reflected in the other, but we are not proposing here that it is needed for the goals at hand.

4. SUMMARY AND CONCLUSIONS

A hydrodynamic and water quality model system has been developed to simulate hydrodynamic circulation, transport and mixing processes in Lake Champlain and to simulate the spatial and temporal distribution and concentration of phosphorus and phytoplankton. The model system developed was divided into two focus areas, hydrodynamics and water quality (phosphorus), due to the great disparity in spatial and temporal scales at which relevant events occur in each.

To study the wind driven circulation in the lake with a particular focus on the simulation of large amplitude internal seiches, which are reported to occur in stratified conditions, a three dimensional, vertically averaged layer, finite difference hydrodynamic model was developed. The model developed was based on the lake hydrodynamic equations presented by Lynch (1986). Model calculations were compared to analytical solutions for two test cases including a two layer system in a rectangular channel open at one end, driven at the open boundary, and a wind driven, two layer system in a closed basin. Model predictions for both test cases produced good results indicating basic model development and coding integrity.

The hydrodynamic model was applied to the main basin of the lake to simulate the internal seiche. Model grids of three resolutions were initially investigated; a very coarse (2 km), a coarse (1 km) and a fine (0.5 km). The 2 km grid was rejected at the outset as unable to resolve enough detail. The 0.5 km resolution grid, although producing some enhanced detail, showed little improvement over the 1 km grid for internal seiche simulation.

A number of simulations were made which varied the depth of the thermocline and the density difference between the upper and lower layers and the results compared to the preliminary Middlebury College data from the summer of 1991. Model predicted currents were compared to observations at three mooring sites. Simulation times covered a one month period in August. A number of observations concerning the data and the predictions were made.

It is apparent from the simulations that wind is an important forcing function. The simulated currents responded strongly to the strong wind events. It is questionable how well the Burlington Airport wind record represents the lake surface, particularly for weak wind events. The model was capable, however, of simulating the observed internal seiche with the

appropriate ~4 day period. It became apparent that a shorter duration simulation, (of less than 3 internal seiche periods, 12 days) requires appropriate initial conditions to reproduce observed currents. In addition, for weak wind events it was difficult to synchronize the model predicted internal seiche with the observed oscillation without detailed initial conditions or a preceding strong wind event.

As a final note on the comparison of model calculations to the observations, it should be remembered that the field investigation that for the first time yielded extensive coverage in Lake Champlain is now in its second year and that the additional observations will be undoubtedly give us far more insight and understanding of the lake hydrodynamics. It is premature to make any judgement with respect to the field data that we have so far. The expected data report and analysis are essential for further studies.

Recommendations for future surveys on the lake environment include, verification of the wind field and additional wind stations, current measurements in Malletts and Missisquoi Bays and the northeast arm and simultaneous current measurements at each of the passages connecting the various basins comprising Lake Champlain. From a modeling perspective mass flux between layers and variable density within a layer should be investigated. In addition with the additional current measurements suggested above, better calibration of the model application to the other basins and interbasin flux issues could begin to be addressed.

For the second half of the study a three-dimensional multiply connected control volume water quality model was developed. Water quality terms focussed on the phosphorus cycle and related kinetics. An application was made to Lake Champlain and results compared to the data set collected and compiled by NYSDEC and VTDEC.

A comparison of mixing exchange calculations of the present model and those of the VTDEC model were made, for the two year average data set with consistent results. The method for determination of mixing exchange coefficients presented here make calculation relatively easy.

Hydrodynamic model calculated exchange coefficients were also compared to the data derived coefficients for the segment interfaces adjoining the Main Lake. Interestingly, the values were similar for most of the inter-segment exchanges although the hydrodynamics covered a single month and the data derived values were annual averages. The most notable exception was the Isle LaMotte-Main basin exchange which was substantially higher for the

most calculated value than for the data derived value. Annual variation in the circulation may account for much of the discrepancy. It is suggested that seasonal and, preferably, annual hydrodynamic data sets be generated from which to calculate the seasonal and/or annually averaged exchange coefficients.

Total phosphorus concentration predictions were made based on a "hydrologic base year" input data set and in-lake concentrations. A sensitivity study on ten parameters was performed. Based on these sensitivity runs a best-fit parameter set was iteratively chosen. Overall phosphorus predictions compared well with observations.

The data for calibration was sparse in some areas leaving room for additional calibration work in continuing studies. Additional information is needed in orthophosphate concentrations throughout the lake as well as the tributary flows. Similarly chlorophyll *a* concentrations and phytoplankton species and productivity data would be of interest. Finally, almost no data exists pertaining to the benthic processes.

Recommendations for future studies include comparisons and calibration of intersegment mixing exchange and transport with hydrodynamic model calculations. Additionally, transient phosphorus model simulations could be performed to investigate the seasonal variations and other cyclical responses in phosphorus concentration in the lake.

5. REFERENCES

- Ambrose, R.B., T. Wool and J.L. Martin, 1993. The water quality analysis simulation program, WASP5. Part A: Model documentation. Environmental Research Laboratory, Athens, Georgia.
- Beeton, A.M., 1958. Relationship between secchi disk readings and light penetration in Lake Huron, American Fisheries Society Trans. Volume 87, pp. 73-79.
- Chapra, S.C. and K.M. Reckhow, 1983. Engineering approaches for lake management, Volume 2: Mechanistic modeling. Butterworth Publishers, Woburn, MA.
- DiToro, D.M., D.J. O'Connor, and R.V. Thomann, 1971. A dynamic model of the phytoplankton population in the Sacramento San Joaquin Delta. Adv. Chem. Ser. 106, Am. Chem. Soc., Washington, DC, pp. 131-180.
- DiToro, D.M. and J.P. Connolly, 1980. Mathematical models of water quality in large lakes, Part 2: Lake Erie. EPA-600/3-80-065. pp. 90-101.
- Duffie, J.A. and W.A. Beckman, 1980. Solar engineering of thermal processes. John Wiley and Sons, NY.
- Henson, E.B. and G.K. Gruendling, 1977. The trophic status and phosphorus loadings of Lake Champlain, Ecological research series EPA - 600/3-77-106. US Environmental Protection Agency, Boston, Massachusetts and Corvallis, OR. 142 p.
- Lake Champlain Management Conference, 1993. Personal communication with the technical advisory committee physical processes subcommittee.
- Lynch, D.R. 1986. "Basic Hydrodynamic Equation for Lakes", in Physics-Based Modeling of Lakes, Reservoirs, and Impoundments (edited by W.G.Gray) American Society of Civil Engineers.
- Manley, T., 1993. Personal communication.
- McCutcheon, S.C., Z. Dongue, and S. Bird, 1990. Model calibration, validation and use. pp. 5-1 to 5-77 In Morton, J.L., R.B. Ambrose and S.C. McCutcheon (eds.) Technical Guidance Manual for performing waste load allocations, Book III: Estuaries, Part 2: Application of Estuarine Wasteload Allocation Models. US EPA Office of Water, Washington, DC.
- Myer, G.E. 1977. Currents of Northern Lake Champlain, Department of Earth Sciences, State University of New York, Plattsburg, New York.
- Myer, G.E. and G.K.Gruendling, 1979. Limnology of Lake Champlain: Lake Champlain Basin Study, SUNY at Plattsburg, 407p.

- Officer, C.B., 1980. Box models revisited. In: P. Hamilton and R.B. McDonald (eds.), *Estuaries and Wetland Processes*, Maine Science Series Volume II, Plenum Press, New York, pp. 65-114.
- Riley, G.A., H. Stommel, and D.F. Bumpus, 1949. Quantitative ecology of the plankton of the western north atlantic. *Bull. Bingham Oceanog. Coll.* 12(3):1-169.
- Roache, P.J., 1976. *Computational fluid dynamics*. Hermosa Publishers, Albuquerque, NM. Revised printing.
- Smith, R.A., 1980. The theoretical basis for estimating phytoplankton production and specific growth rate from chlorophyll, light and temperature data. *Ecological Modeling*. 10 pp. 243-264.
- Sverdrup, H.U., H.W. Johnson, and R.H. Fleming, 1942. *The oceans*, Prentice-Hall, Englewood Cliffs, NJ, 1087 pp.
- Swanson, J.C. and K. Jayko, 1988. A simplified estuarine box model of Narragansett Bay. Final Report prepared for the Narragansett Bay Project, Rhode Island Department of Environmental Management, Providence, RI.
- Thomann, R.V. and J.A. Mueller, 1987. *Principles of surface water quality modeling and control*. Harper and Row, New York.
- Turner, J.S., 1973. *Buoyancy effects in fluids*. Cambridge University Press, London and New York.
- Vermont Department of Conservation and New York State Department of Environmental Conservation, 1993. Lake Champlain diagnostic-feasibility study, Interim Progress Report, US Environmental Protection Agency, Region I, Boston, MA and Region II, New York, NY.
- Vermont Department of Conservation and New York State Department of Environmental Conservation, 1993. Lake Champlain diagnostic-feasibility study, Final Report, Part 1: A phosphorus budget, model and load allocation for Lake Champlain. US Environmental Protection Agency, Region I, Boston, MA and Region II, New York, NY.
- Wang, J.D. and J.J. Connor, 1975. *Mathematical Modeling of Near Coastal Circulation*, MIT Sea Grant Program, MITSG 75-13.

APPENDIX A

This File Name: \WQMAP\DATA\DATA_DEF\DATADEF.cde
Date: 31jan94
Author: Tatsu Isaji

filename : \WQMAP\LOC_DATA\location\GRIDS\gridname.cde

file_open : see \WQMAP\SOURCE\LAYER_HD\SRC_LYR\FLAGIN.FOR or
(EXAMPLE CODE TO READ)

purpose : This is the binary output grid file created by the
\WQMAP\SOURCE\LAYER_HD\SETUP program which converts a
2-d grid into one dimensional sequential grid.
This file stays as long as the grid specification
remain same.

written by: \WQMAP\SOURCE\LAYER_HD\SETUP

Variable Description:

block 1:imax,jmax,nseq,orglon,orglat,dlon,dlat		
imax	: grid dimension in east/west	! i*4
jmax	: grid dimension in north/south	! i*4
nseq	: total number of active grid cell	! i*4
orglon	: grid origin in longitude radian	! r*4
orglat	: grid origin in latitude radian	! r*4
dlon	: longitudinal grid resolution in radian	! r*4
dlat	: latitudinal grid resolution in radian	! r*4
block 2: nflg,index,indey,hc,hx,hy,sinv,cosv,tanv		
nflg	: grid flag	! i*2
index	: i cell index	! i*2
indey	: j cell index	! i*2
hc	: depth at center cell	! r*4
hx	: depth at u location	! r*4
hy	: depth at v location	! r*4
sinv	: longitudinal cell distance	! r*4
cosv	: latitudinal cell distance	! r*4
tanv	: spherical term	! r*4
block 3: iseq		
nflg	: cell sequential number	! i*2

-----{ EXAMPLE CODE TO READ}-----

\$declare

subroutine flagin

include 'layer.cmn'

c
c reads base grid in ??????.cde file

c integer nftn,n,i,j,readln

c-----
i = readln(nftn_inp, '.cde', 0) ! 0: found ' ', <>0 not

read(nftn_inp, *) path_name

file_name = path_name//name_grid//'.cde'

call unb_string(file_name, 120)

inquire(file=file_name, exist=there)

if(.not.there) then

write(*,*) ' file does not exists, program stops'

write(*,*) file_name


```

        stop
    else
        nftn = 9
        open(unit=nftn,file=file_name,status='old',
            form='unformatted')
        write(*, '('nftn_flg:',60a)') file_name
    endif

    read(nftn) imax,jmax,nseq,orglon,orglat,dlon,dlat

    if(imax .gt. maxi) goto 91
    if(jmax .gt. maxj) goto 91
    if(nseq .gt. mseq) goto 91
    imaxp = imax + 1
    jmaxp = jmax + 1

    read(nftn) (nflg(n),index(n),indey(n),hc(0,n),hx(0,n),hy(0,n),
        . sinv(n),cosv(n),tanv(n),n=1,nseq)
    read(nftn) ((iseq(i,j),i=0,imaxp),j=0,jmaxp)
    close(nftn)

    return

91 write(*, '(' [flagin] need to redimension,i,jmax,nseq=',3i5)')
    . imax,jmax,nseq
    close(nftn)
    stop
end

```

```

c ASA   File Name: o:\wqmap\source\viewtide\datadef.hmo
c ASA   Date: 1993/9/15
c ASA   Author: Daniel L. Mendelsohn
c ASA   Purpose: Definition file for WQMAP hydrodynamic data
c-----

```

The following is an example read of a WQMAP hydrodynamic (Hrun.hmo) data set. The data consists of model hydrodynamic model run description headers, followed by a time series of surface elevation and current vector fields. Data is stored for each computational cell as determined by an associated model grid (gridname.DGR).

The following variable definitions apply.

```

Hgrid    = grid name
Hrun      = name (prefix) of this file
Hloc      = WQMAP\loc_data\{location name}
Hext      = grid name extension ; DGR=boundary fitted, FGR=rectangular
IMAX      = number of grids in the x-dir
JMAX      =                y-dir
KMAX      =                z-dir
NSEQ      = number of sequential computational cells
NSTRT     = total number of model time steps at start of run
NSTOP     = total number of model time steps at end of run
DT        = time step (sec)
TPER      = period (for harmonic forcing, sec)
IYR_ST    = Start year - start date all I2
IMO_ST    = Start month
IDY_ST    = Start day
IHR_ST    = Start hour
IMI_ST    = Start minute
NST       = present time step
Year      = present year - all I2
Month     = month
Day       = day
Hour      = hour
Minute    = minute
I         = grid cell number in the east(I) - direction
J         = grid cell number in the north(J) - direction
Elevation = free surface elevation at cell I,J (m)
U(k)      = east(I) velocity vector component at cell I,J,K (m/s)
V(k)      = north(J) velocity vector component at cell I,J,K (m/s)
W(k)      = up(K) velocity vector component at cell I,J,K (m/s)
SIGMA_T   = sigma(T) (density) at cell I,J,K (Rho - 1000. kg/m^3)
NSPH      =: =0 cylindrical approx, =1 spherical approx
NADV      =: =0 no advection terms, =1 advection terms
NCOR      =: =0 no coriolis, =1 coriolis
NAVE      = step inc for variable time averaging
NBND      =: =0 manning, =1 linear(drag), =-1 quadratic(drag)
NSMTH     = time step for smoothing of elevation
NSMUV     = time step for smoothing of momentum
ASMTH     = fraction of smoothing - elevation, 1.0=no smooth
ASMUV     = fraction of smoothing - momentum, 0.0=max.
RKH       = horiz momentum diffusion coeff(m**2/s)
RKVA      = vert    ''      ''      ''      (m/s)
RKVB      = ''      ''      ''      ''      (m**2/s)
SKH       = horiz salt diffusion coeff(m**2/s)
SKVV      = vert    ''      ''      ''      (m**2/s)
CDBOT     = manning (n) or drag coeff (cf)
NTIDE     = : =0 no, =2 real tide, =3 real w/e-w slopes
NRIVR     = : =0 no river flows
NDENS     = density induced flow, =0 no, =1 diag, =2 prog
NWIND     = wind forcing, =0 no, =1 yes
RAIR      = air density (kg/m**3)
CDSRF     = air/water drag coeff
WINDU     = wind velocity x-dir (m/s)

```

WINDV = ' ' y-dir ' '

! File Open

! -----
OPEN(UNIT = NUNIT, ! Open direct access file
FILE = FILE_NAME,
ACCESS = 'DIRECT',
RECL = 16,
FORM = 'UNFORMATTED')

! Headers

! -----
READ(NWDATA,REC=1) Hgrid,Hrun ! 2A*8
READ(NWDATA,REC=2) Hloc,Hext ! 2A*8
READ(NWDATA,REC=3) IMAXH,JMAXH,KMAX,NSEQ ! 4I*2
READ(NWDATA,REC=4) NSTRT, NSTOP, DT, TPER ! I*4,I*4,R*4,R*4
READ(NWDATA,REC=5) NSPH,NADV,NCOR,NAVE,NBND,NSMTH,NSMUV ! 7I*2
READ(NWDATA,REC=6) ASMTH, ASMUV ! 2R*4
READ(NWDATA,REC=7) RKH, RKVA, RKVB ! 3R*4
READ(NWDATA,REC=8) SKH, SKVV, CDBOT ! 3R*4
READ(NWDATA,REC=9) NTIDE, NRIVR, NDENS, NWIND ! 4I*2
READ(NWDATA,REC=10) RAIR, CDSRF, WINDU, WINDV ! 4R*4
READ(NWDATA,REC=11) IYR_ST,IMO_ST,IDY_ST,IHR_ST,IMI_ST ! 5I*2

! Data Blocks

! -----
DO WHILE(.true.)
READ(NWDATA,REC=IREC,end=99) NST, Year, Month, Day, Hour, Minute
! I*4,5I*2
DO J=1,JMAX ! Read in domain from bottom to top
DO I=1,IMAX ! Read in 1 row at a time
if(Mflg(i,j) .eq. 0) cycle ! Check for land
IREC = IREC + 1
READ(NWDATA,REC=IREC,end=99) I,J,Elevation
DO K=1,KMAX
IREC = IREC + 1
READ(NWDATA,REC=IREC,err=99,end=99) U(k),V(k),W(k),SIGMA_T
END DO
END DO
END DO
END DO

This File Name: \WQMAP\DATA\DATA_DEF\DATADEF.hvl
Date: 31jan94
Author: Tatsu Isaji

filename : \WQMAP\LOC_DATA\location\hydro_out\runname.hvl

file_open: only required is FORM='UNFORMATTED'

purpose : This is an output file of the hydrodynamic model.
The file contains entire model parameters for user
specified time step interval.

written by: \WQMAP\SOURCE\LAYER_HD\HYDRO

Variable Description: see (EXAMPLE CODE TO READ)

```
-----{ EXAMPLE CODE TO READ}-----
      subroutine read_hvl(nftn)
      include 'viewhd.cmn'
c
c      reads hd output -- layered version --
c
      integer nftn
c-----
      integer nseq0,nst,n,k
      real      dt,cdf,pdepth,tme
c-----
      read(nftn) kmax,nseq0,dt,cdf,pdepth
c
c      kmax = maximum number of layers
c      nseq0 = maximum number of active cells
c      dt = model time step (seconds)
c      cdf = bottom friction
c      pdepth= depth code ( not unused)
c-----
c----- hd. output -----
      1 read(nftn,end=9,err=9) nst,tme,
         ((d2s(k,n),hc(k,n),k=0,kmax),n=1,nseq)
      read(nftn,err=9) ((u2s(k,n),v2s(k,n),k=0,kmax),n=1,nseq)
      goto 1
c
      9 return
      end
c
c      nst = model time step
c      tme = model time = dt*nst (seconds)
c      d2s(k,n) = surface location of k-th layer at n-th cell(m)
c      hc(k,n) = thickness of k-th layer at n-th cell(m)
c      u2s(k,n) = east/west velocity of k-th layer at n-th cell
c      v2s(k,n) = north/south velocity of k-th layer at n-th cell
```

this File Name: \WQMAP\DATA\DATA_DEF\LAYERIN.INP
Date: 1/27/94
Author: John McCue
Purpose: Layer model input file description.

Filename : \WQMAP\LOC_DATA\location\GRIDS\scenname.INP

File_open : OPEN(unit,file=scenname, status='unknown')

Purpose : This is the input file for the layer model.

Written by: \WQMAP\SOURCE\LAYERIN\LAYRSUBS.FOR; subroutine writeinputfile

General : This file contains all of the parameters necessary to run the layer model. This file is composed of data from many small forms and files. When the user saves the data, all of these files are read and the data are written to the scenname.INP file. When the user calls up an old case, the reverse happens.

Read by: \WQMAP\SOURCE\LAYERIN\LAYRSUBS.FOR; subroutine getoldcase

READ FORMATS: Most of the read statements have either * or '(a)' formats.

Consult subroutine getoldcase for the exact reads.

-----{ EXAMPLE FILE AS DESCRIBED ABOVE.}-----

```
run name -----
'jtest'
grid name -----
'LW1K'
.cde path -----
'c:\fdhm\setup\output'
opn path -----
'c:\fdhm\setup\output'
.out path -----
'c:\fdhm\output'
computational characteristics -----
      1
      1
      1.00000
      .99800
      1.00000
      .00000
      25.00000
      .00000
      43200.00000
      43200.00000
/o parameter -----
      3456
      288
      1
      1
      288
surface stress -----
      1
      5.00000
      90.00000
bottom stress -----
      1
      .00000
      1.00000
time series output -----
      3
      8          70
      15         54
      14         32
```

```

river inflow -----
      1
      6           2      5.00000
transport report -----
      6
      32          32          1      122
      54          54          1      122
      70          70          1      122
      1          21          70      70
      1          21          54      54
      1          21          32      32
putout -----
      345600.000000
tek10 -----
      1
coriolis term -----
      1
layer parameters -----
      2
      -20.00000      .00000
      -50.00000      1.00000

```

this File Name: \WQMAP\DATA\DATA_DEF\DATADEF.log

Date: 31jan94

Author: Tatsu Isaji

filename : \WQMAP\LOC_DATA\location\hydro_out\runame.log

Purpose : This is the ascii output of the hydrodynamic run.

Written by: \WQMAP\SOURCE\LAYER_HD\HYDRO

Variable Description:

The contents shows a general progress of simulation
and error messages.

This File Name: \WQMAP\DATA\DATA_DEF\DATADEF.LWD

Date: 31jan94

Author: Tatsu Isaji

filename : \WQMAP\LOC_DATA\location\GRIDS\gridname.LWD
The file name can be any name. The main input must spell out an exact name.

file_open : see \WQMAP\SOURCE\LAYER_HD\SRC_LYR\WINDIN.FOR or
{EXAMPLE CODE TO READ}

purpose : The file provides a time series of wind speed.
"WINDIN.FOR" assumes some characteristics of wind file, such as constant time step of wind observation.

written by: Third party, complying free format read

Variable Description:

line 1: title description (not used, but read)

line 2: iyr,imo,idy,ihr,ideg,iknt,wx1,wyl

iyr	: year	(not used)	! i*4
imo	: month	(not used)	! i*4
idy	: day	(not used)	! i*4
ihr	: hour	(not used)	! i*4
ideg	: wind direction	(not used)	! i*4
iknt	: wind speed	(not used)	! i*4
wx1	: east/west component of wind		! r*4
wyl	: north/south component of wind		! r*4

-----{ EXAMPLE data}-----

yr mo dy hr deg knt u v(m/sec)

91 8 1 0 170 7 -0.6 3.5

91 8 1 1 170 8 -0.7 4.1

91 8 1 2 100 4 -2.0 0.4

.
.
.
.

-----{ EXAMPLE CODE TO READ}-----

\$declare

subroutine windin
include 'layer.cmn'

c
c reads wind time series, constant in space
c

integer n,l,readln
integer iyr,imo,idy,ihr,ideg,iknt
real tstep,t1/0.0/,t2/-1.0/,wx0,wy0,wx1,wy1,wx2,wy2
real wind_dt/3600.0/ ! wind data time step
character wind_file*120
integer nftn/14/

c-----
if(readln(nftn_inp,'surf',1).eq.0) then
read(nftn_inp,*)
read(nftn_inp,*)
read(nftn_inp,*)
read(nftn_inp,*) wind_file
endif

open(nftn,file=wind_file,status='old')

read(nftn,*)

1 read(nftn,*,end=9) iyr,imo,idy,ihr,ideg,iknt,wx1,wyl
goto 1


```
9 close(nftn)
  stop
end
```

```
C*****
```

This File Name: \WQMAP\DATA\DATA_DEF\DATADEF.opn

Date: 31jan94

Author: Tatsu Isaji

filename : \WQMAP\LOC_DATA\location\GRIDS\gridname.opn

file_open: see \WQMAP\SOURCE\LAYER_HD\SRC_LYR\openbd.FOR or
(EXAMPLE CODE TO READ)

purpose : supplies open boundary conditions for hydrodynamic
simulation.

written by: \WQMAP\SOURCE\LAYER_HD\SETUP

Variable Description:

line 1:	not used but read	
line 2:	not used but read	
line 3:	ntide	: number of tidal constituents : I*4
line 4:	name_of_tide	: name of constituent (ex, M2) : a*2
line 5:	scale2	: amplitude value scaler : r*4
line 6:	shift2	: phase value scaler : r*4
line 7:	range	: depth adjustment parameter : r*4
line 8:	fmt	: format to read record following:a*40
line 9 . . .:	n,i,j,iflg,values	
	n	: sequential grid cell number : i*4
	i	: cell index : i*4
	j	: cell index : i*4
	iflg	: cell flag : i*4
	values	: surface elevation : i*4

-----{ EXAMPLE CODE TO READ}-----

\$declare

```
subroutine openbd
include 'layer.cmn'
integer*4 ipass
```

```
real    scale2,shift2,range,values
integer nftn,n,i,j,iflg,im,jm,ip,jp,n1,n2,k,readln
character ascii*4,fmt*40
data ncnt2/0/, ncnt3/0/, ncnt4/0/, ncnt5/0/, ncnt6/0/, ncnt7/0/
```

```
c----- read file-open.### for sea,u,v
if(readln(nftn_inp,'.opn',0).eq.0) read(nftn_inp,*) path_name
file_name = path_name//name_grid//'.opn'
call unb_string(file_name,120)
```

```
inquire(file=file_name,exist=there)
```

```
write(*,*) ' [openbd] open boundary conditions'
read(nftn,'(10x,10a4)')  ascii      ! year
read(nftn,'(10x,10a4)')  ascii      ! jday
read(nftn,'(10x,i10)')   ntide      ! ntide
read(nftn,'(10x,10a4)')  ascii      ! m2
read(nftn,'(10x,f10.0)') scale2     ! value scaler
read(nftn,'(10x,f10.0)') shift2     ! value scaler
read(nftn,'(10x,f10.0)') range      ! depth adjustment
read(nftn,'(10x,a40)')   fmt
```

```
write(*,*) '      ntide=',ntide
write(*,*) '      scale2=',scale2
write(*,*) '      shift2=',shift2
write(*,*) '      range =',range
write(*,*) '      n      i      j      iflg      values'
```

```
10 read(nftn,fmt,end=3) n,i,j,iflg,values
write(*,'(3x,4i5,f10.4)') n,i,j,iflg,values
goto 10
```

```
3 write(*,1004) ncnt2,ncnt3,ncnt4,ncnt5,ncnt6,ncnt7
1004 format(' nopen2-7=',6i5)
close(nftn)
```

```
return
end
```

```
-----{ EXAMPLE DATA }-----
```

```
iy      =      00
jday    =      1
ntide   =      1
tidal mode
scale   =      1.0
shift   =      0.0
range   =      0.0
format  =(i5,2i4,6x,i1,20f8.3)
660 12 122      4:2 00.000
```

This File Name: \WQMAP\DATA\DATA_DEF\DATADEF.tsr

Date: 31jan94

Author: Tatsu Isaji

filename : \WQMAP\LOC_DATA\location\hydro_out\runname.tsr

file_open: only required is FORM='UNFORMATTED'

purpose : This is an output file of the hydrodynamic model.
The file contains time series of model parameters for
user specified grid cells.

written by: \WQMAP\SOURCE\LAYER_HD\HYDRO

Variable Description: see {EXAMPLE CODE TO READ}

```
-----{ EXAMPLE CODE TO READ}-----
      subroutine datain1L(nftn)
      include 'histo.cmn'
c
c      reads hydrodynamic model time ser. output ( layered version)
c      one variable parameter for all stations
c
      integer nftn
c-----
      integer*2 nflg
      integer   l,nst,nst0,nseq,nl,k,m
      real      dt,tme,wx,wy,cd
c-----
      read(nftn,end=91) imax,jmax,kmax,nseq,dt,nloc

c      imax= i index limit
c      jmax= j
c      kmax= k(layers)
c      nseq= sequential limit
c      dt   = model time step (sec)
c      nloc= number of grid cells retained as time series

      read(nftn) (locs_read(l),l=1,nloc) ! grid sequential number
c-----
      do l=1,nloc
        read(nftn,err=8,end=8) nst,tme,nl,nflg,wx,wy,cd,
          .      (sea(k),hc(k),k=0,kmax),
          .      (ul(k),hx(k),xgravi(k),xcorio(k),xsurfs(k),
          .      xbotom(k),xadvect(k),xspher(k),xdense(k),k=0,kmax),
          .      (v1(k),hy(k),ygravi(k),ycorio(k),ysurfs(k),
          .      ybotom(k),yadvect(k),yspher(k),ydense(k),k=0,kmax)
      enddo

      8 return
      end

c      nst   = model time step
c      tme   = model time = nst*dt   (seconds)
c      nl    = grid sequential number for this write-record
c      nflg  = cell flag
c      wx    = wind stress in Newton/m**2, east/west
c      wy    = wind stress in Newton/m**2, north/south
c      cd    = bottom friction parameter(non dimensional)
c      sea(k)= top location of K-th layer(meters)
c      hc(k) = thickness of K-th layer(meters)
c      ul(k) = east/west velocity in K-th layer(meters/second)
c      hx(k) = thickness of K-th layer(meters) in u location
c      xgravi(k) = term balance of gravity (meters/second**2)
c      xcorio(k) = Coriolis
c      xsurfs(k) = surface stress
c      xbotom(k) = bottom stress
```

```

c      xadvec(k) =          advection
c      xspher(k) =          spherical
c      xdense(k) =          density
c      vl(k) = north/south velocity in K-th layer(meters/second)
c      hy(k) = thickness of K-th layer(meters) in v location
c      ygravi(k) = term balance of gravity (meters/second**2)
c      ycorio(k) =          Coriolis
c      ysurfs(k) =          surface stress
c      ybotom(k) =          bottom stress
c      yadvec(k) =          advection
c      yspher(k) =          spherical
c      ydense(k) =          density
c-----
```

APPENDIX B

c ASA File Name: c:\wqmap\data\data_def\datadef.bdf
: ASA Date: 1994/1/28
: ASA Author: Daniel L. Mendelsohn
: ASA Purpose: Box definition file for the box model.

Filename : \WQMAP\LOC_DATA\{any location}\BOX_IN\{scenario}.BDF

File_open : OPEN(unit, file=filename)

Purpose : File contains the box model system and segment (control volume) grid definition parameters. These define the morphometry of the control volumes, the interbox connections, the river input and output locations and the flow path through the system. The variables read from this file are:

- * NBOX = number of control volumes (segments)
- * NSIDES = max number of connections per segment
- * NRIVER = number of rivers
- * ONED = vertical structure flag: T=1-D , F=2-D
- * ALPHA = ratio of river flow between upper and lower boxes
- * ADJ = adjacent grid on each of NSIDES sides of each box, in order 1-->NSIDES. A negative number is an adjacent open boundary (tracer, conc specified). The total number of connections, sides + rivers, cannot exceed NSIDES.
- * DEL = specifies direction of river flow on each of NSIDES sides of box (as described above).
0 = flow out of box
1 = flow into box
9 = closed face
- * FRCFLOW = fraction (0-1) of flow into box leaving across each face. Always 1 unless flow exits from 2 sides of box.
- * AREA = x-sectional area between upper and lower boxes (m^2)
- * VOLUP = volume of upper box (m^3)
- * VOLLOW = volume of lower box (m^3)
- * NU = ratio of mixing exchange to net circulation on each face of box (default is 1)

Written by: \WQMAP\RUNBOX.EXE

Read by : \WQMAP\PHOSPHOR.EXE
* VOLUP VOLLOW = volume of upper and lower boxes

General : This file can be created and edited through the WQMAP interface under RUNMODEL - WATER QUALITY. The {scenario} file name prefix must be the same as the accompanying control parameter, load and tracer files. The four files make the input set necessary to run the box model.

Associated files are:

- | | | |
|----|----------------|---------------------------------|
| 1. | {scenario}.CTF | : simulation control parameters |
| 2. | {scenario}.LOD | : flow and load file |
| 3. | {scenario}.TRA | : tracer conc and load file |

format : The format used for reading the file is as follows:

----- FORTRAN read statements -----

```
900 FORMAT(10X,F10.0)
901 FORMAT(10X,I10)
902 FORMAT(19X,L1)
```

```
READ(6,901) NBOX
READ(6,901) NSIDES
READ(6,901) NRIVER
READ(6,902) ONED
READ(6,900) ALPHA
READ(6,*)
```

! Read headers

```

DO N = 1,NBOX                                ! adjacent cell definition
  READ(6,*) NB, (ADJ(I,NB), I=1,NSIDES)
END DO
READ(6,*)
DO N = 1,NBOX                                ! flow direction
  READ(6,*) NB, (DEL(I,NB), I=1,NSIDES)
END DO
READ(6,*)
DO N = 1,NBOX                                ! flow fraction at face
  READ(6,*) NB, (FRCFLOW(I,NB), I=1,NSIDES)
END DO
READ(6,*)
DO N = 1,NBOX                                ! area, upper, lower volume
  READ(6,*) NB, AREA(NB), VOLUP(NB), VOLLOW(NB)
END DO
READ(6,*)
DO N=1,NBOX                                ! NU estuarine parameter
  READ(6,*) NB, (NU(I,N), I=1,NSIDES)
END DO

```

----- Example Data -----

The following example file is:

C:\WQMAP\LOC_DATA\CHMPLAIN\BOX_IN\PH_BASE.BDF

```

NBOX      =      13      ! NUMBER OF CONTROL VOLUMES (SEGMENTS)
NSIDES    =      8      ! MAX NUMBER OF CONNECTIONS PER SEGMENT
NRIVER    =      14      ! NUMBER OF RIVERS
ONED      =      T      ! VERTICAL STRUCTURE FLAG: T=1-D , F=2-D
ALPHA     =      1.00000 ! FRACTION OF RIVER FLOW IN SURFACE LAYER

BOX #      ADJ
1  2  -1   0   0   0   0   0   0
2  1   3  -2   0   0   0   0   0
3  2   4  -3   0   0   0   0   0
4  3   5  -4   0   0   0   0   0
5  4   8   7   6  13   9  -5   0
6  5  -6   0   0   0   0   0   0
7  5  -7   0   0   0   0   0   0
8  5  -8   0   0   0   0   0   0
9  5  10  -9   0   0   0   0   0
10 9  11  12  13 -10   0   0   0
11 10 -11   0   0   0   0   0   0
12 10 -12   0   0   0   0   0   0
13 5  10 -13 -14   0   0   0   0

BOX #      DEL
1  0   1   9   9   9   9   9   9
2  1   0   1   9   9   9   9   9
3  1   0   1   9   9   9   9   9
4  1   0   1   9   9   9   9   9
5  1   1   1   1   0   1   1   9
6  0   1   9   9   9   9   9   9
7  0   1   9   9   9   9   9   9
8  0   1   9   9   9   9   9   9
9  0   0   1   9   9   9   9   9
10 1   1   1   0   1   9   9   9
11 0   1   9   9   9   9   9   9
12 0   1   9   9   9   9   9   9
13 1   1   1   0   9   9   9   9

BOX #      FRCFLOW
1  1.00  1.00  1.00  1.00  1.00  1.00  1.00  1.00
2  1.00  1.00  1.00  1.00  1.00  1.00  1.00  1.00
3  1.00  1.00  1.00  1.00  1.00  1.00  1.00  1.00
4  1.00  1.00  1.00  1.00  1.00  1.00  1.00  1.00
5  1.00  1.00  1.00  1.00  1.00  1.00  1.00  1.00
6  1.00  1.00  1.00  1.00  1.00  1.00  1.00  1.00

```


[illegible]

c ASA File Name: c:\wqmap\data\data_def\datadef.ctf
c ASA Date: 1994/1/28
c ASA Author: Daniel L. Mendelsohn
c ASA Purpose: Control parameter input file for the box model.

filename : \WQMAP\LOC_DATA\{any location}\BOX_IN\{scenario}.CTF

file_open : OPEN(unit, file=filename)

purpose : File contains the control volume model runtime control parameters and the phosphorus kinetics constants and coefficients.

written by: \WQMAP\RUNBOX.EXE

read by : \WQMAP\PHOSPHOR.EXE

general : This file can be created and edited through the WQMAP interface under RUNMODEL - WATER QUALITY. The {scenario} file name prefix must be the same as the accompanying box definition, load and tracer files. The four files make the input set necessary to run the box model.
Associated files are:
1. {scenario}.BDF : box definition file
2. {scenario}.LOD : flow and load file
3. {scenario}.TRA : tracer conc and load file

format : The format used for reading the file is as follows:

----- FORTRAN read statements -----

900 FORMAT(10X,F10.0)
901 FORMAT(10X,I10)

line #	format	variable
1	READ(5,*)	
2	READ(5,'(A30)')	DESCRIPTION1
3	READ(5,'(A30)')	DESCRIPTION2
4	READ(5,'(A30)')	DESCRIPTION3
5	READ(5,'(12X,A8)')	GRID
6	READ(5,'(12X,A8)')	TRACER
7	READ(5,*)	
8	READ(5,901)	ISTEADY
9	READ(5,901)	ISED
10	READ(5,901)	IEXC
11	READ(5,901)	NSTMAX
12	READ(5,900)	DT
13	READ(5,900)	SOR
14	READ(5,900)	CONV
15	READ(5,901)	ITERMAX
16	READ(5,*)	
17	READ(5,900)	BLOSS
18	READ(5,900)	EXPLOSS
19	READ(5,900)	WSINK(1)
20	READ(5,900)	EVSED
21	READ(5,*)	
22	READ(5,900)	PCRB
23	READ(5,900)	FOP
24	READ(5,900)	K58C
25	READ(5,900)	K58T
26	READ(5,900)	KOPDC
27	READ(5,900)	KOPDT
28	READ(5,900)	TFPO4
29	READ(5,900)	WSINK(2)
30	READ(5,900)	WSINK(3)

```

31      READ(5,*)
32      READ(5,900)      IPHYTO
33      READ(5,900)      KPZDC
34      READ(5,900)      KPZDT
35      READ(5,900)      K1C
36      READ(5,900)      K1T
37      READ(5,900)      KMPG1
38      READ(5,900)      K1RC
39      READ(5,900)      K1RT
40      READ(5,900)      K1D
41      READ(5,900)      K1G
42      READ(5,900)      ZOO
43      READ(5,900)      KMPHYT
44      READ(5,900)      LGHTSW
45      READ(5,900)      IS1
46      READ(5,900)      XKC
47      READ(5,900)      PHIMX
48      READ(5,900)      CCHL
49      READ(5,900)      KE(1)
50      READ(5,900)      ITOT
51      READ(5,900)      FDAY
52      READ(5,900)      WSINK(4)

```

----- Example Data -----

The following example file is:

C:\WQMAP\LOC_DATA\CHMPLAIN\BOX_IN\PH_BASE.CTF

```

***** DESCRIPTION AND FILENAMES *****
Phytoplankton calibration      ! Simulation description
Hydrologic 'base' year data    ! 3-30 character lines
1-D simulation, with settling !
GRIDNAME = VTNEW1              ! .BGR box file name (for plotting)
TRACER = PH_BASE               ! .TRA tracer data file name
***** SIMULATION CONTROL *****
ISTEADY = 0                    ! solution type; 0=steady state,1=transient
ISED = 1                      ! sediment interaction; 0=sink,1=opo4 flux param,2
IEXC = 1                      ! mixing exchange calc flag. 0=calculate,1=read
NSTMAX = 1000                 ! max. number of time steps
DT = 7200.                    ! time step
SOR = 0.020                   ! successive Over-relaxation Parameter
CONV = 0.00001                ! convergence criteria
ITERMAX = 4000                ! max. number of iterations allowed for convergenc
***** TRACER AND GENERAL CONSTANTS *****
BLOSS = 0.0                   ! Flux loss rate (mass/vol) (tracer constituent)
EXPLOSS = 0.0                 ! Exponential decay const. (1/day) (tracer constit
WSINK(1) = 0.0                 ! Settling velocity (m/day) (tracer constituent)
EVSED = 2.0E-4                ! Sediment diffusive exchange (m^2/day) (for ISED=
***** PHOSPHOROUS RELATED CONSTANTS *****
PCRB = 0.025                  ! phosphorous to carbon ratio, (mg P/mg C)
FOP = 0.50                    ! frac phyt phos recycled to org phos default=1
K58C = 0.22                   ! mineralization rate of dissolved organic phospho
K58T = 1.08                    ! temperature coeff. for K58C. default=1
KOPDC = 0.0004                ! decomposition rate of organic phos. in the sedim
KOPDT = 1.08                  ! temperature coeff. for KOPDC. default=1
TFPO4 = 1.00                  ! normalized phosphate flux from bed, (unitless):
WSINK(2) = 0.25                ! Settling velocity (m/day) POP
WSINK(3) = 0.25                ! Settling velocity (m/day) PIP
***** PHYTOPLANKTON RELATED CONSTANTS *****
IPHYTO = 1.0                  ! 0=simplified kinetics,1=full kinetics
KPZDC = 0.02                  ! decomp rate const for sediment phyt @20C, (1/day)
KPZDT = 1.08                  ! temperature coeff. for KPZDC. default=1
K1C = 2.000                   ! saturation growth rate for phytoplankton, (1/day)
K1T = 1.068                   ! temperature coeff. for K1C. default=1
KMPG1 = 0.001                 ! phosphorous half saturation constant for phytopl

```

K1RC	=	0.125	!	endogenous respiration rate of phytoplankton at
K1RT	=	1.045	!	temperature coeff. for K1RC. default=1
K1D	=	0.02	!	non-predatory phytoplankton death rate, (1/day)
K1G	=	0.00	!	grazing rate on phytoplankton per unit zooplankton
ZOO	=	0.00	!	herbivorous zooplankton population, (mg C/L): ZOO
KMPHYT	=	1.00	!	half saturation constant for phytoplankton, (mg C/L)
LGHTSW	=	1.00	!	light form switch. 1=DiToro, 2=Smith's(USGS)
IS1	=	300.00	!	saturation light intensity for phytoplankton, (u
XKC	=	0.017	!	chlorophyll extinction coeff, (used only when LG
PHIMX	=	720.00	!	maximum quantum yield constant, (used only when
CCHL	=	35.00	!	carbon to chlorophyll ratio, (used only when LG
KE	=	1.00	!	light extinction coefficient(unitless or 1/m) de
ITOT	=	312.01	!	total daily solar radiation, Langleys
FDAY	=	0.50	!	fraction of day with sufficient light for phyto
WSINK(4)	=	0.25	!	Settling velocity (m/day)

c ASA File Name: p:\wqmap\data\data_def\datadef.dbr
c ASA Date: 1994/3/24
c ASA Author: Daniel L Mendelsohn
c ASA Purpose: Phosphorus model concentration output data.

filename : \WQMAP\LOC_DATA\{any location}\BOX_OUT\{scenario}.DBR

file_open : OPEN(unit, file=filename)

purpose : File contains the model calculated concentration data for the four constituents; tracer, total organic and inorganic phosphorus, phytoplankton and chlorophyll a. It also contains hydraulic detention time and mass conservation check data for the conservative constituent.

* Conservative constituent concentration is in mg/l
* TOP, TIP, phyt and Chl a concentration are in ug/l

written by: \WQMAP\PHOS_DT.EXE

read by : \WQMAP\VIEWBOX.EXE

general : This file can be viewed through the WQMAP interface under MODEL OUTPUT - WATER QUALITY. The {scenario} file name prefix is the same as the accompanying box definition, control and tracer files used to define the simulation.

Associated files are:

- | | |
|-------------------|-----------------------|
| 1. {scenario}.BDF | : box definition file |
| 2. {scenario}.CNC | : simulation log file |
| 3. {scenario}.DXC | : exchange output |

Format : The format used for reading the file is as follows:

----- FORTRAN read statements -----

```
read(112, fmt='(12x,a8)') GRID boxname      ! .BGR file name: plotting
read(112, fmt='(12x,a8)') TRACER             ! header line 2
read(112, '(10x,I10)') NBOX                   ! line 3
read(112, '(10x,I10)') NSIDES                 ! line 4
read(112, '(10x,I10)') NRIVER                 ! line 5
read(112, '(10x,I10)') NCONST                ! line 6 Number of constituents
read(112,*)                                  ! header line
do nb = 1,nbox                               ! upper:tracer, TOP, TIP, TP, PHYT
  read(112,*) N, (valuesU(nct,N),nct=1,nconst)
enddo
read(112,*)                                  ! header line
do nb = 1,nbox                               ! lower:tracer, TOP, TIP, TP, PHYT
  read(112,*) N, (valuesL(nct,N),nct=1,nconst)
enddo
read(112,*)                                  ! header line
do nb = 1,nbox                               ! sediment:tracer, TOP, TIP, TP, PHYT
  read(112,*) N, (valuesS(nct,N),nct=1,nconst)
enddo
read(112,*)                                  ! header line
do nb = 1,nbox                               ! hydraulic detention
  read(112,*) N, valuesU(6,N)
enddo
read(112,*)                                  ! header line
do nb = 1,nbox                               ! conservative mass balance - upper
  read(112,*) N, valuesCu(N)
enddo
read(112,*)                                  ! header line
do nb = 1,nbox                               ! conservative mass balance - lower
  read(112,*) N, valuesCl(N)
enddo
```

close(112)

----- Example Data -----

The following example file is:

C:\WQMAP\LOC_DATA\CHMPLAIN\BOX_OUT\PH_BASE.DBR

GRIDNAME = VTNEW1
TRACER = PH_BASE
NBOX = 13
NSIDES = 8
NRIVER = 14
NCONST = 4

BOX# UPPER CONCENTRATION, CONSTITUENTS 1=>NCONST

1	1.26295E+01	3.45301E+01	1.20074E+01	4.65374E+01	3.52359E+02
2	1.44816E+01	1.74582E+01	4.54537E+00	2.20036E+01	2.51597E+02
3	1.14422E+01	1.15644E+01	3.38376E+00	1.49481E+01	8.68820E+01
4	1.09271E+01	1.15002E+01	4.45452E+00	1.59547E+01	4.36661E+01
5	1.08175E+01	1.07159E+01	3.90809E+00	1.46240E+01	3.25386E+01
6	1.10604E+01	1.24698E+01	4.07991E+00	1.65497E+01	1.22147E+02
7	1.09668E+01	1.28609E+01	4.44147E+00	1.73024E+01	1.59109E+02
8	1.04195E+01	1.22106E+01	4.72229E+00	1.69328E+01	8.17566E+01
9	9.51791E+00	1.01407E+01	1.26623E+00	1.14069E+01	5.05920E+01
10	9.34721E+00	7.91968E+00	8.36193E-01	8.75587E+00	3.55283E+01
11	1.00804E+01	1.28551E+01	6.04140E+00	1.88965E+01	2.94853E+02
12	7.81090E+00	2.72496E+01	5.33487E+00	3.25845E+01	3.64234E+02
13	1.04752E+01	9.04388E+00	1.28857E+00	1.03324E+01	5.74864E+01

BOX# LOWER CONCENTRATION, CONSTITUENTS 1=>NCONST

1	0.00000E+00	4.37500E-25	4.37500E-25	8.75000E-25	3.50000E-23
2	0.00000E+00	4.37500E-25	4.37500E-25	8.75000E-25	3.50000E-23
3	0.00000E+00	4.37500E-25	4.37500E-25	8.75000E-25	3.50000E-23
4	0.00000E+00	4.37500E-25	4.37500E-25	8.75000E-25	3.50000E-23
5	0.00000E+00	4.37500E-25	4.37500E-25	8.75000E-25	3.50000E-23
6	0.00000E+00	4.37500E-25	4.37500E-25	8.75000E-25	3.50000E-23
7	0.00000E+00	4.37500E-25	4.37500E-25	8.75000E-25	3.50000E-23
8	0.00000E+00	4.37500E-25	4.37500E-25	8.75000E-25	3.50000E-23
9	0.00000E+00	4.37500E-25	4.37500E-25	8.75000E-25	3.50000E-23
10	0.00000E+00	4.37500E-25	4.37500E-25	8.75000E-25	3.50000E-23
11	0.00000E+00	4.37500E-25	4.37500E-25	8.75000E-25	3.50000E-23
12	0.00000E+00	4.37500E-25	4.37500E-25	8.75000E-25	3.50000E-23
13	0.00000E+00	4.37500E-25	4.37500E-25	8.75000E-25	3.50000E-23

BOX# SEDIMENT CONCENTRATION, CONSTITUENTS 1=>NCONST

1	0.00000E+00	0.00000E+00	0.00000E+00	0.00000E+00	0.00000E+00
2	0.00000E+00	0.00000E+00	0.00000E+00	0.00000E+00	0.00000E+00
3	0.00000E+00	0.00000E+00	0.00000E+00	0.00000E+00	0.00000E+00
4	0.00000E+00	0.00000E+00	0.00000E+00	0.00000E+00	0.00000E+00
5	0.00000E+00	0.00000E+00	0.00000E+00	0.00000E+00	0.00000E+00
6	0.00000E+00	0.00000E+00	0.00000E+00	0.00000E+00	0.00000E+00
7	0.00000E+00	0.00000E+00	0.00000E+00	0.00000E+00	0.00000E+00
8	0.00000E+00	0.00000E+00	0.00000E+00	0.00000E+00	0.00000E+00
9	0.00000E+00	0.00000E+00	0.00000E+00	0.00000E+00	0.00000E+00
10	0.00000E+00	0.00000E+00	0.00000E+00	0.00000E+00	0.00000E+00
11	0.00000E+00	0.00000E+00	0.00000E+00	0.00000E+00	0.00000E+00
12	0.00000E+00	0.00000E+00	0.00000E+00	0.00000E+00	0.00000E+00
13	0.00000E+00	0.00000E+00	0.00000E+00	0.00000E+00	0.00000E+00

BOX# HYDRAULIC DETENTION TIME - DAYS

1	.00
2	.00
3	.00
4	.00
5	.00
6	.00
7	.00
8	.00
9	.00

10 .00
11 .00
12 .00
13 .00

BOX# CONSERVATION CHECK, UPPER LAYER

1 2.24777E-01
2 1.03035E+00
3 1.00073E+01
4 4.18261E+01
5 4.63446E+01
6 2.92375E+00
7 1.83259E+00
8 5.29790E+00
9 8.84170E-02
10 9.68439E-01
11 3.66907E-01
12 3.32819E-02
13 6.74844E+00

BOX# CONSERVATION CHECK, LOWER LAYER

1 0.00000E+00
2 0.00000E+00
3 0.00000E+00
4 0.00000E+00
5 0.00000E+00
6 0.00000E+00
7 0.00000E+00
8 0.00000E+00
9 0.00000E+00
10 0.00000E+00
11 0.00000E+00
12 0.00000E+00
13 0.00000E+00

GLOBAL CONSERVATION CHECK (%), CONSTITUENTS

3.5632

c ASA File Name: p:\wqmap\data\data_def\datadef.dxc
c ASA Date: 1994/3/24
c ASA Author: Daniel L Mendelsohn
c ASA Purpose: Phosphorus model exchange coefficient data.

filename : \WQMAP\LOC_DATA\{any location}\BOX_OUT\{scenario}.DXC

file_open : OPEN(unit, file=filename)

purpose : File contains model calculated exchange coefficients.
Also contains inter-box net river flow rate balance
calculations. This file can also be used to enter exchange
coefficients, calculated elsewhere, for use in the phosphorus
model.

The data blocks are as follows.

1. Mixing exchange coefficients - upper layer
2. Mixing exchange coefficients - lower layer
3. Net circulation - upper layer
4. Net circulation - lower layer
5. Vertical net circulation and exchange

written by: \WQMAP\PHOS_DT.EXE

read by : \WQMAP\PHOS_DT.EXE

general : The format of the data blocks is integrally linked with
the *.BDF file. Each connection (face) of a segment to
a river or another segment, as defined by the ADJ array given
in the associated *.BDF file, has an associated exchange
coefficient, river flow etc. The values are tabulated in order
for face 1 to NSIDES of each segment for segment 1 to NBOX
respectively.

Associated files are:

- | | | |
|----|----------------|-----------------------|
| 1. | {scenario}.BDF | : box definition file |
| 2. | {scenario}.CNC | : simulation log file |
| 3. | {scenario}.DXC | : exchange output |

format : The format used for reading the file is as follows:

----- FORTRAN read statements -----

```
DO N=1,5
  READ(111,*,END=11)
END DO

READ(111,'(10X,A8)') GRID
READ(111,'(10X,A8)') TRACER
READ(111,'(10X,I10)') NBOX
READ(111,'(10X,I10)') NSIDES
READ(111,'(10X,I10)') NRIVER
READ(111,'(10X,F10.0)') LSRATE
READ(111,*,)
DO N = 1,NBOX
  READ(111,*,) NB, ( EUP(NS,NB), NS=1,NSIDES)
END DO
READ(111,*,)
DO N = 1,NBOX
  READ(111,*,) NB, ( ELOW(NS,NB), NS=1,NSIDES)
END DO
READ(111,*,)
DO N = 1,NBOX
  READ(111,*,) NB, ( QUP(NS,NB), NS=1,NSIDES)
END DO
READ(111,*,)
```



```

DO N = 1,NBOX
  READ(111,*,) NB, ( QLOW(NS,NB), NS=1,NSIDES)
END DO
READ(111,*,)
DO N = 1,NBOX
  READ(111,*) NB, QV(NB), EV(NB)
END DO
READ(111,*,)
DO N = 1,NBOX
  READ(111,*,) NB, (RIVER(NS,N),NS=1,NSIDES)
END DO

```

----- Example Data -----

The following example file is:

C:\WQMAP\LOC_DATA\CHMPLAIN\BOX_OUT\PH_BASE.dxc

```

GRIDNAME = VTNEW1
TRACER = CHL_CALI
NBOX = 13
NSIDES = 8
NRIVER = 14
LSRATE = 7.992E-02

```

BOX# UPPER EXCHANGE (M3/SEC) : SIDES 1->NSIDES

1	21.95	.00	.00	.00	.00	.00	.00
2	21.95	42.68	.00	.00	.00	.00	.00
3	42.68	470.76	.00	.00	.00	.00	.00
4	470.76	1693.49	.00	.00	.00	.00	.00
5	1693.49	282.82	97.83	156.08	100.11	4.72	.00
6	156.08	.00	.00	.00	.00	.00	.00
7	97.83	.00	.00	.00	.00	.00	.00
8	282.82	.00	.00	.00	.00	.00	.00
9	4.72	.00	.00	.00	.00	.00	.00
10	.00	59.20	5.37	32.25	.00	.00	.00
11	59.20	.00	.00	.00	.00	.00	.00
12	5.37	.00	.00	.00	.00	.00	.00
13	100.11	32.25	.00	.00	.00	.00	.00

BOX# LOWER EXCHANGE (M3/SEC) : SIDES 1->NSIDES

1	.00	.00	.00	.00	.00	.00	.00
2	.00	.00	.00	.00	.00	.00	.00
3	.00	.00	.00	.00	.00	.00	.00
4	.00	.00	.00	.00	.00	.00	.00
5	.00	.00	.00	.00	.00	.00	.00
6	.00	.00	.00	.00	.00	.00	.00
7	.00	.00	.00	.00	.00	.00	.00
8	.00	.00	.00	.00	.00	.00	.00
9	.00	.00	.00	.00	.00	.00	.00
10	.00	.00	.00	.00	.00	.00	.00
11	.00	.00	.00	.00	.00	.00	.00
12	.00	.00	.00	.00	.00	.00	.00
13	.00	.00	.00	.00	.00	.00	.00

BOX# UPPER NET FLOW (M3/SEC) : SIDES 1->NSIDES

1	.00	.00	.00	.00	.00	.00	.00
2	.00	.00	.00	.00	.00	.00	.00
3	.00	.00	.00	.00	.00	.00	.00
4	.00	.00	.00	.00	.00	.00	.00
5	.00	.00	.00	.00	.00	.00	.00
6	.00	.00	.00	.00	.00	.00	.00
7	.00	.00	.00	.00	.00	.00	.00
8	.00	.00	.00	.00	.00	.00	.00
9	.00	.00	.00	.00	.00	.00	.00
10	.00	.00	.00	.00	.00	.00	.00
11	.00	.00	.00	.00	.00	.00	.00
12	.00	.00	.00	.00	.00	.00	.00
13	.00	.00	.00	.00	.00	.00	.00

BOX#	LOWER NET FLOW (M3/SEC) : SIDES 1->NSIDES							
1	.00	.00	.00	.00	.00	.00	.00	.00
2	.00	.00	.00	.00	.00	.00	.00	.00
3	.00	.00	.00	.00	.00	.00	.00	.00
4	.00	.00	.00	.00	.00	.00	.00	.00
5	.00	.00	.00	.00	.00	.00	.00	.00
6	.00	.00	.00	.00	.00	.00	.00	.00
7	.00	.00	.00	.00	.00	.00	.00	.00
8	.00	.00	.00	.00	.00	.00	.00	.00
9	.00	.00	.00	.00	.00	.00	.00	.00
10	.00	.00	.00	.00	.00	.00	.00	.00
11	.00	.00	.00	.00	.00	.00	.00	.00
12	.00	.00	.00	.00	.00	.00	.00	.00
13	.00	.00	.00	.00	.00	.00	.00	.00

BOX#	VERTICAL NET , EXCHANGE (M3/SEC)	
------	----------------------------------	--

1	.00	.00
2	.00	.00
3	.00	.00
4	.00	.00
5	.00	.00
6	.00	.00
7	.00	.00
8	.00	.00
9	.00	.00
10	.00	.00
11	.00	.00
12	.00	.00
13	.00	.00

BOX#	CALCULATED RIVER FLOW, N=1->NSIDES							
------	------------------------------------	--	--	--	--	--	--	--

1	34.56	34.56	.00	.00	.00	.00	.00	.00
2	34.56	54.07	19.51	.00	.00	.00	.00	.00
3	54.07	58.09	4.02	.00	.00	.00	.00	.00
4	58.09	110.03	51.94	.00	.00	.00	.00	.00
5	110.03	30.44	.21	2.40	289.29	38.36	107.84	
6	2.40	2.40	.00	.00	.00	.00	.00	.00
7	.21	.21	.00	.00	.00	.00	.00	.00
8	30.44	30.44	.00	.00	.00	.00	.00	.00
9	38.36	9.59	47.95	.00	.00	.00	.00	.00
10	9.59	1.93	63.74	76.93	1.68	.00	.00	.00
11	1.93	1.93	.00	.00	.00	.00	.00	.00
12	63.74	63.74	.00	.00	.00	.00	.00	.00
13	289.29	76.93	14.46	380.76	.00	.00	.00	.00

ASA File Name: c:\wqmap\data\data_def\datadef.lod
ASA Date: 1994/1/28
ASA Author: Daniel L. Mendelsohn
ASA Purpose: River flow, load and segment specific parameter
data file for the box model.

filename : \WQMAP\LOC_DATA\{any location}\BOX_IN\{scenario}.LOD

file_open : OPEN(unit, file=filename)

purpose : File contains the direct loading input, by segment, for
the four constituents; tracer, total organic and inorganic
phosphorus and phytoplankton (as chlorophyll a). It also
contains the river flow rates and constituent concentrations
for the river flow (an optional method for load input).

- * Load data are input in g/l
- * The fraction of load in the upper box is also input
- * The lower box (2-D cases) gets (1-f) of the load
- * Flow rates are input in m³/s
- * Flow divided between upper and lower based on ALPHA (in .BDF)
- * Constituent 1 river concentration is input in mg/l
- * TOP, TIP and phyt river concentration are input in ug/l
- * Upper and lower concentrations are given

Finally, the file contains the segment specific phosphorus
cycle kinetics parameters:

TMPSG = temperature (C)
KESG = extinction coefficient (1/m)
FPO4 = avg phosphate sediment flux, for ISED=1, (mg/m²-day)
F_DIP = fraction dissolved phosphorus (-)
ZOOSG = zooplankton population (mgC/l), see ZOO in *.CTF file
ITOTLIM = segment specific percent shading (-)
DEPTHSED = sediment depth (M)
PHYT = phyto. initial conc. as chlorophyll a (ug/l)

written by: \WQMAP\RUNBOX.EXE

read by : \WQMAP\PHOSPHOR.EXE

general : This file can be created and edited through the WQMAP
interface under RUNMODEL - WATER QUALITY. The {scenario}
file name prefix must be the same as the accompanying
box definition, control and tracer files. The four files make
the input set necessary to run the box model.

Associated files are:

- | | | |
|----|----------------|-----------------------------------|
| 1. | {scenario}.BDF | : box definition file |
| 2. | {scenario}.CTF | : simulation control and kinetics |
| 3. | {scenario}.TRA | : tracer conc and load file |

format : The format used for reading the file is as follows:

----- FORTRAN read statements -----

01 FORMAT(10X,I10)

Read in Direct Loading Data

```
READ(7,901) NCONST
READ(7,*)          ! Read header
DO N=1,NBOX          ! #, load (g/s) , upper fraction
  READ(7,*) NB, (W(NCS), FRAC(NCS), NCS=1,NCONST)
```

```

DO NCS=1,NCONST
  WUP (NCS,N) = W(NCS) * FRAC(NCS)      ! (flux x FRAC) into upper
  WLOW(NCS,N) = W(NCS) * (1.0 - FRAC(NCS)) ! lower layer
END DO
END DO

```

```

C
C Read in River Data
C -----
  READ(7,*)      ! Read header
  DO N=1,NRIVER  ! flow rate (m^3/s); conc (ug/l)
    READ(7,*) NO, BCFLOW(N),      ! #, flow rate
    (COPNUP(NCS,N), COPNLO(NCS,N),NCS=1,NCONST) ! upper,lower
  END DO      ! concentration

```

```

C Define box specific parameters
C -----
  READ(7,*)      ! Read header
  DO N=1,NBOX
    READ(7,*) NB, TMPSG(N), KESG(N),      FPO4(N),      F_DIP(N),
    !      ZOOSG(N), ITOTLIM(N), DEPTHSED(N), CONUP(4,N)
  END DO

```

----- Example Data -----

The following example file is:

C:\WQMAP\LOC_DATA\CHMPLAIN\BOX_IN\PH_BASE.LOD

```

NCONST =          4          : NUMBER OF CONSTITUENTS
BOX#  LOAD(1)  FRAC(1): TOP LOAD  TOP FRAC: TIP LOAD  TIP FRAC: PHYT LOAD  PHYT
1  291.8664    1.000  1.361365    1.000  0.420579    1.000    .0001    1
2  428.7481    1.000  0.242495    1.000  0.293661    1.000    .0000    1
3  31.18246    1.000  0.090007    1.000  0.068382    1.000    .0000    1.
4  404.6087    1.000  2.086901    1.000  1.776024    1.000    .0000    1.
5  920.5904    1.000  3.239172    1.000  0.779381    1.000    .0000    1
6  61.46753    1.000  0.202655    1.000  0.300002    1.000    .0000    1
7  18.66438    1.000  0.098221    1.000  0.273354    1.000    .0000    1.
8  169.8567    1.000  0.658466    1.000  0.631211    1.000    .0000    1.
9  347.0732    1.000  0.76076    1.000  0.285219    1.000    .0000    1
10 22.78349    1.000  0.070971    1.000  0.02882    1.000    .0000    1
11 58.16337    1.000  0.138771    1.000  0.123669    1.000    .0000    1.
12 415.0717    1.000  3.997309    1.000  1.273557    1.000    .0000    1
13 132.8914    1.000  0.536384    1.000  0.328231    1.000    .0000    1
RIV#  FLOW  CONC(1U)  CONC(1L)  TOP (U)  TOP (L)  TIP (U)  TIP (L)  CHLA
1  26.31088  .00000  .00000  .00000  .00000  .00000  .00000  1.00
2  14.40576  .00000  .00000  .00000  .00000  .00000  .00000  .0
3  2.810439  .00000  .00000  .00000  .00000  .00000  .00000  .0
4  40.4506   .00000  .00000  .00000  .00000  .00000  .00000  .00
5  84.87443  .00000  .00000  .00000  .00000  .00000  .00000  .00
6  1.864536  .00000  .00000  .00000  .00000  .00000  .00000  .0
7  0.202943  .00000  .00000  .00000  .00000  .00000  .00000  .0
8  26.59437  .00000  .00000  .00000  .00000  .00000  .00000  .00
9  37.10046  .00000  .00000  .00000  .00000  .00000  .00000  .00
10 1.300101  .00000  .00000  .00000  .00000  .00000  .00000  .0
11 1.427575  .00000  .00000  .00000  .00000  .00000  .00000  0.0
12 54.19203  .00000  .00000  .00000  .00000  .00000  .00000  .00
13 12.46366  .00000  .00000  .00000  .00000  .00000  .00000  .0
14 -99.0     .00000  .00000  .00000  .00000  .00000  .00000  .0
BOX#  TMPSG  KESG  FPO4  F_DIP  ZOOSG  ITOTLIM  DEPTHSED(M)  PHY
1  14.5    4.00  0.0   0.8    1.0    1.0      0.5          0.0
2  14.5    1.27  0.0   0.8    1.0    1.0      0.5          0.
3  14.5    0.29  0.0   0.8    1.0    1.0      0.5          0.
4  14.5    0.23  0.0   0.8    1.0    1.0      0.5          0.0
5  14.5    0.20  0.0   0.8    1.0    1.0      0.5          0.0
6  14.5    0.21  0.0   0.8    1.0    1.0      0.5          0.
7  14.5    0.19  0.0   0.8    1.0    1.0      0.5          0.

```

8	14.5	0.28	0.0	0.8	1.0	1.0	0.5	0.0
9	14.5	0.21	0.0	0.8	1.0	1.0	0.5	0.0
10	14.5	0.19	0.0	0.8	1.0	1.0	0.5	0.0
11	14.5	0.41	0.0	0.8	1.0	1.0	0.5	0.0
12	14.5	0.71	0.0	0.8	1.0	1.0	0.5	0.0
13	14.5	0.23	0.0	0.8	1.0	1.0	0.5	0.0

c ASA File Name: c:\wqmap\data\data_def\datadef.tra
c ASA Date: 1994/1/28
c ASA Author: Daniel L. Mendelsohn
c ASA Purpose: River flow, load and segment specific parameter
data file for the box model.

filename : \WQMAP\LOC_DATA\{any location}\BOX_IN\{scenario}.TRA

file_open : OPEN(unit, file=filename)

purpose : File contains the tracer data set for calculation of the mixing exchange coefficients. Tracer concentration must be given for each segment, upper and lower for 2-D, as well as the direct tracer load to that segment. The river flow rates are read from the {scenario}.LOD file.

* In-situ tracer concentration is input in mg/l
* Load data are input in g/l

written by: \WQMAP\RUNBOX.EXE

read by : \WQMAP\PHOSPHOR.EXE

general : This file can be created and edited through the WQMAP interface under RUNMODEL - WATER QUALITY. The {scenario} file name prefix must be the same as the accompanying box definition, control and tracer files. The four files make the input set necessary to run the box model.
Associated files are:
1. {scenario}.BDF : box definition file
2. {scenario}.CTF : simulation control and kinetics
2. {scenario}.LOD : flow and load file

format : The format used for reading the file is as follows:

```
----- FORTRAN read statements -----  
C  
C Tracer Data - upper/lower concentration, river load  
C -----  
C Define each Box  
C -----  
C READ(8,*) ! Read header  
C DO N=1,NBOX ! upper, lower, load, fraction upper  
C READ(8,*) NB, SUP(N), SLOW(N), W(1), FRAC(1)  
C SOPNUP(N) = W(1) * FRAC(1)  
C SOPNLO(N) = W(1) * (1.0 - FRAC(1))  
C END DO
```

----- Example Data -----

The following example file is:

C:\WQMAP\LOC_DATA\CHMPLAIN\BOX_IN\PH_BASE.TRA

BOX#	TRA(U)	TRA(L)	TRA LOAD	FRAC(U/L)
1	11.62	11.62	291.8664	1.0
2	13.47	13.47	428.7481	1.0
3	11.18	11.18	31.18246	1.0
4	10.72	10.72	404.6087	1.0
5	10.61	10.61	920.5904	1.0
6	10.89	10.89	61.46753	1.0
7	10.78	10.78	18.66438	1.0
8	10.18	10.18	169.8567	1.0
9	9.43	9.43	347.0732	1.0
10	9.29	9.29	22.78349	1.0
11	10.20	10.20	58.16337	1.0

1
2
3
4
5
6
7
8
9
10
11
12
13
14
15
16
17
18
19
20
21
22
23
24
25
26
27
28
29
30
31
32
33
34
35
36
37
38
39
40
41
42
43
44
45
46
47
48
49
50
51
52
53
54
55
56
57
58
59
60
61
62
63
64
65
66
67
68
69
70
71
72
73
74
75
76
77
78
79
80
81
82
83
84
85
86
87
88
89
90
91
92
93
94
95
96
97
98
99
100

12	7.78	7.78	415.0717	1.0
13	10.33	10.33	132.8914	1.0

APPENDIX C

[illegible]

This File Name: \WQMAP\DATA\DATA_DEF\DATADEF.FGR

Date: 14jun93

Author: Daniel L. Mendelsohn

Purpose: Rectangular finite difference grid. Direct access,
binary output file format.

filename : \WQMAP\LOC_DATA\location\GRIDS\gridname.FGR

file_open : OPEN(unit = unit_number
file = 'gridname.fgr',
access = 'direct',
recl = 6
form = 'unformatted')

purpose : This is the direct access binary output grid file created
by the MAKEGRID program module of WQMAP. It can be read and
edited by MAKEGRID and displayed by any WQMAP module through
the data button (F8).

written by: \WQMAP\SOURCE\MAKEGRID\GRIDFILE.FOR; subroutine write_fgr.

general : This file contains a computational description (IMAX,JMAX and
computational flags) of the grid as well as a geographical
(lon,lat,depth) description. Cells are rectangular in lon-lat
not necessarily in distance.

Variable Description:

line 1:	Imax,Jmax : Grid dimensions	! 2(i*2)
line 2:	NSEQ : Total number of computational cells.	! i*4
line 3:	DLON : Grid cell width in degrees longitude	! r*4
line 4:	DLAT : Grid cell height in degrees latitude	! r*4
line 5:	OLON : Grid origin (lower left) longitude	! r*4
line 6:	OLAT : Grid origin (lower left) latitude	! r*4
line 7:	Iflg,Depth: Cell flag and depth arrays.	! i*2,r*4

: Describes the computational use of the cell. The flag
: and depth data in a particular record are linked
: linked to a grid cell by its position, (record number) in
: the direct access file and the indicial, [I,J] notation. The
: record number of a cell is calculated as
:
: $Irec = (J - 1) * Imax + I + 6$
:
: The definition of the cell flags are as follows:
:
: Iflg: 0 = Land point.
: 1 = Water point.
: 2 = Open boundary point.
: 3 = River boundary point.

.....
line Imax*Jmax+6 : End of the Iflg and depth arrays.

-----{ EXAMPLE CODE TO WRITE GRID.}-----

C*****

```
Subroutine Write_FGR(file_name)
include 'makegrid.cmn'
```

```
character*80 file_name
integer*4 irec
```

```
nftn = 10
open( unit = 10,
. file = file_name,
. access = 'direct',
. recl = 6,
. form = 'unformatted' )
```

```

write(nftn,rec=1) imax,jmax      ! 2(i*2)
write(nftn,rec=2) nseq          ! i*4
write(nftn,rec=3) dlon          ! r*4
write(nftn,rec=4) dlat          ! r*4
write(nftn,rec=5) olon          ! r*4
write(nftn,rec=6) olat          ! r*4
irec = 6

do j=1,jmax
  do i=1,imax
    irec = irec + 1
    write(nftn,rec=irec) iflg(i,j), depflg(i,j)      ! i*2,r*4
  end do
end do

close(nftn)

return
end

```

-----{ EXAMPLE FILE AS DESCRIBED ABOVE. }-----

Rec#	Data	
1:	28 86	: Imax,Jmax
2:	862	: Nseq
3:	0.02	: DLON
4:	0.01	: DLAT
5:	-71.2534	: OLON
6:	41.2534	: OLAT
7:	0 0.0	: Iflg,Depth at cell [1,1]
8:	0 0.0	: Iflg,Depth at cell [2,1]
9:	0 0.0	: Iflg,Depth at cell [3,1]
10:	2 12.0	: Iflg,Depth at cell [4,1]
11:	2 14.0	: Iflg,Depth at cell [5,1]
....
2413:	0 0.0	: Iflg,Depth at cell [27,86]
2414:	0 0.0	: Iflg,Depth at cell [28,86]

This File Name: \WQMAP\DATA\DATA_DEF\DATADEF.GDD
 Date: 14jun93
 Author: Daniel L. Mendelsohn
 Purpose: Rectangular finite difference gridded data.
 Direct access, binary output file format.

filename : \WQMAP\LOC_DATA\{any location}\DATA\{filename.GDD}

file_open : OPEN(unit = unit_number ,
 file = 'filename.GDD',
 access = 'direct' ,
 recl = 6
 form = 'unformatted')

purpose : This is the direct access binary output gridded data file.
 It can be displayed by any WQMAP module through the data
 button (F8) - GRIDDED DATA.

written by: Any gridding program.

general : This file contains gridded data on a rectangular grid
 (IMAX,JMAX and computational flags) as a geographical
 (lon,lat,depth) description. Cells are rectangular in lon-lat
 not necessarily in distance.

Variable Description:

line 1:	Imax,Jmax : Grid dimensions	! 2(i*2)
line 2:	NSEQ : Total number of computational cells.	! i*4
line 3:	DLON : Grid cell width in degrees longitude	! r*4
line 4:	DLAT : Grid cell height in degrees latitude	! r*4
line 5:	OLON : Grid origin (lower left) longitude	! r*4
line 6:	OLAT : Grid origin (lower left) latitude	! r*4
line 7:	Iflg,Data: Cell flag and depth arrays.	! i*2,r*4

: Describes the computational use of the cell. The flag
 : and data in a particular record are linked
 : to a grid cell by its position, (record number) in
 : the direct access file and the indicial, [I,J] notation. The
 : record number of a cell is calculated as
 :
 : Irec = (J - 1) * Imax + I + 6
 :
 : The definition of the cell flags are as follows:
 : Iflg: 0 = Land point.
 : 1 = Water point.

....
 line Imax*Jmax+6 : End of the Iflg and data arrays.

-----{ EXAMPLE CODE TO WRITE GRID.}-----
 C*****

```
Subroutine Write_GDD(file_name)
include 'makegrid.cmn'
```

```
character*80 file_name
integer*4 irec
```

```
nftn = 10
open( unit = 10,
.     file = file_name,
.     access = 'direct',
.     recl = 6,
.     form = 'unformatted' )
```

```
write(nftn,rec=1) imax,jmax      ! 2(i*2)
write(nftn,rec=2) nseq          ! i*4
write(nftn,rec=3) dlون         ! r*4
```

```

write(nftn,rec=4) dlat      ! r*4
write(nftn,rec=5) olon     ! r*4
write(nftn,rec=6) olat     ! r*4
irec = 6

do j=1,jmax
  do i=1,imax
    irec = irec + 1
    write(nftn,rec=irec) iflg(i,j), depflg(i,j)      ! i*2,r*4
  end do
end do

close(nftn)

return
end

```

```

-----{ EXAMPLE FILE AS DESCRIBED ABOVE. }-----
Rec# Data
-----
1: 28 86      : Imax,Jmax
2: 862        : Nseq
3: 0.02       : DLON
4: 0.01       : DLAT
5: -71.2534   : OLON
6: 41.2534    : OLAT
7: 0 0.0      : Iflg,Data at cell [1,1]
8: 0 0.0      : Iflg,Data at cell [2,1]
9: 1 11.0     : Iflg,Data at cell [3,1]
10: 1 12.0    : Iflg,Data at cell [4,1]
11: 1 14.0    : Iflg,Data at cell [5,1]
....
2413: 1 17.0   : Iflg,Data at cell [27,86]
2414: 0 0.0    : Iflg,Data at cell [28,86]

```

c ASA File Name: \wqmap\data\data_def\datadef.grx
c ASA Date: 1993/3/3
c ASA Author: John McCue
c ASA Purpose: Definition file for the multiple graph file (.GRX)

filename : \{project}\{any path}\filename.GRX

file_open : OPEN(unit, file=filename)

purpose : File holding the data for a multiple graph.

written by: This file can be written by any routine. The important thing is
to write it in the format described below.

general : There is a call in one of the gis overlays
called viewgrflink. The full syntax is:
CALL VIEWGRFLINK(grxfilename)

----- Example Data -----

X Title

Y Title

Number of Y's

Y1 Legend

Y2 Legend

Y3 Legend

Y4 Legend

	.			
	.			
	.			
X	Y1	Y2	Y3	Y4
.
.
.
.

This File Name: \WOSM\DATA\DATA_DEF\DATADEF.KEY
Date: May 1993
Author: Chris Galagan
Purpose: Defines the KEY file format.

TITLE 1 (80 character string)
TITLE 2 (80 character string)
TITLE 3 (80 character string)
Key Name 1 (80 character string)
Color 1 Pattern 1 Backcolor 1 (3 free format integers)
Key Name 2
Color 2 Pattern 2 Backcolor 2
Key Name 3
Color 3 Pattern 3 Backcolor 3

This file Name: \WOSM\DATA\DATA_DEF\DATADEF.TIE
 Date: May 1993
 Author: Chris Galagan
 Purpose: defines the TIE import/export file format.

purpose: The TIE file format was developed by ASA to facilitate import and export of GIS data.

Written by: external, MAPTOOLS, or from GIS command 'EXPORT LAYER'.

***** Data definition for TIE file *****

line no.	content	format	comments
1	ID number	(i5)	
2	name	(c20)	
3	description	(c20)	
4	"POINT"		object type
	"LINE"		"
	"POLYLINE"		"
	"POLYGON"		"
5	color width height	(3i3)	point object
	color width height	(3i3)	line object
	color width height	(3i3)	polyline object
	pcolor bcolor pattern	(3i3)	polygon object
6	icon name (ie "RECTANGLE")		points only
7	layer number	(i2)	values 1-50
8	attribute(1)	(c40)	(attrs attached
9	attribute(2)	"	to objects)
10	attribute(3)	"	
11	attribute(4)	"	
12	attribute(5)	"	
13	attribute(6)	"	
14	link file name	(c40)	PCX,grf,txt,grx,mlf
15	real number	(real*4)	
16	number of vertices	(i4)	
17	x y	(2f14.6)	coords in decimal degrees. West lons negative, south lats negative.


```
filename : \{project}\loc_data\{location}\data\filename.XYZ
```

Purpose : File holding data for viewing or gridding in EDITBFCG.

General : It is a simple ASCII format lon,lat,z-value file with arbitrarily spaced data used for gridding (.GDD) or viewing in the GIS database. The data can be either comma or space delimited.

-117.196	32.67956	22
-117.192	32.67913	27
-117.186	32.67935	25
-117.183	32.67902	20
-117.171	32.6788	17
-117.169	32.67865	16
-117.163	32.67915	10
-117.154	32.67889	7
-117.148	32.67897	12
-117.143	32.67863	11
-117.139	32.67839	28
-117.134	32.67828	36
-117.118	32.60075	1.0
-117.12	32.60275	1.0
-117.118	32.60336	3.5
-117.122	32.60451	2.5
-117.12	32.60511	2.5
-117.118	32.60512	1.5
-117.124	32.60746	1.0

The image shows three vertical columns of dots. The first column has 10 dots, the second has 10 dots, and the third has 10 dots. This represents the number 100 in base 10, base 2, and base 3 respectively.